

NORTHEAST UTILITIES



THE CONNECTICUT LIGHT AND POWER COMPANY
WESTERN MASSACHUSETTS ELECTRIC COMPANY
HOLYOKE WATER POWER COMPANY
NORTHEAST UTILITIES SERVICE COMPANY
NORTHEAST NUCLEAR ENERGY COMPANY

General Offices • Selden Street, Berlin, Connecticut

P.O. BOX 270
HARTFORD, CONNECTICUT 06141-0270
(203) 665-5000

September 19, 1984

Docket No. 50-423
A04078

Director of Nuclear Reactor Regulation
Mr. B. J. Youngblood, Chief
Licensing Branch No. 1
Division of Licensing
U.S. Nuclear Regulatory Commission
Washington, D.C. 20555

Reference: (1) B. J. Youngblood letter to W. G. Council, Request for
Additional Information for Millstone Nuclear Power Station,
Unit 3, dated May 25, 1984.

Dear Mr. Youngblood:

Millstone Nuclear Power Station, Unit No. 3
Response to Requests for Additional Information


Attached are Northeast Nuclear Energy Company's (NNECO) responses to the
requests for additional information forwarded in Reference (1).

If there are any questions related to this information, please contact our
licensing representative directly.

Very truly yours,

NORTHEAST NUCLEAR ENERGY COMPANY
et. al.

BY NORTHEAST NUCLEAR ENERGY COMPANY
Their Agent


W. G. Council
Senior Vice President

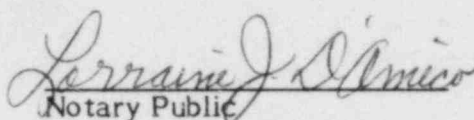
8410120212 840919
PDR ADOCK 05000423
F PDR

*Asentur
Card Diet*

*Boo1
1/40 oversize
Drawings*

STATE OF CONNECTICUT)
) ss. Berlin
COUNTY OF HARTFORD)

Then personally appeared before me W. G. Counsil, who being duly sworn, did state that he is Senior Vice President of Northeast Nuclear Energy Company, an Applicant herein, that he is authorized to execute and file the foregoing information in the name and on behalf of the Applicants herein and that the statements contained in said information are true and correct to the best of his knowledge and belief.


Notary Public

My Commission Expires March 31, 1988

NRC Letter May 25, 1984

Question 210.47

during the review of the classification of the Feedwater System, Figure 10.4-6 Sheet 2 of 2, it was found that the following 3 lines have been incorrectly classified Safety Class 3. These lines should be classified Safety Class 2. The line numbers are:

3 FWA-004-139-3 (A-)

3 FWA-004-140-3 (B-)

3 FWA-004-141-3 (C-)

It is requested that the applicant revise Figure 10.4-6, Sheet 2 of 2 in a future FSAR amendment.

Response:

Refer to revised FSAR Figure 10.4-6, Sheet 2 of 2.

DOCUMENT/ PAGE PULLED

ANO. 8410120212

NO. OF PAGES 1

REASON:

☐ PAGE ILLEGIBLE

☐ HARD COPY FILED AT: PDR CF
OTHER _____

☐ BETTER COPY REQUESTED ON ____/____/____

☒ PAGE TOO LARGE TO FILM.

☒ HARD COPY FILED AT: PDR CF
OTHER _____

☐ FILMED ON APERTURE CARD NO. 8410120212-01

Question 810.1

- 1.) Provide further information as to how individuals without automobiles will be evacuated during an emergency.

Response

The nature of the environment within the 10 mile emergency planning zone of the Millstone Nuclear Station is primarily rural to suburban. Even cities such as New London are primarily suburban in nature. For this reason, public transportation is not a key method of transportation utilized by residents or transients. The private automobile is by far the primary mode of transportation. For this reason the number of individuals without automobiles requiring transportation in an emergency is not an issue. The evacuability study performed by Storch Engineers and submitted by Northeast Utilities dealt primarily with a conservative method of assigning passenger loading to private automobiles. The utilization of buses for school children was included in the report. Individuals with ambulatory problems are required to register with their local civil preparedness offices. In the event of an evacuation, special transportation will be arranged by the civil preparedness office for these individuals.

- 2.) Provide an estimate of the confirmation time(s) to verify that an evacuation has been completed.

Response

The estimation of confirmation times to verify that an evacuation has been completed are as follows.

8 minutes for two miles
33 minutes for five miles
163 minutes for ten miles

This information was taken from FEMA-REP3-Dynamic Evacuation Analyses; Independent Assessments of Evacuation Time from the Plume Exposure Pathway EPZs of 12 Nuclear Power Stations.

Question 492.7

Q.492.4 mentioned Seabrook rather than Millstone 3 (page 4 of response to Q.492.4). We therefore do not have confidence that you performed the required review of the Westinghouse standard response on flow measurement to assure that it applies to your plant. In order to provide this assurance, please answer the following questions.

- (1) The instrumentation uncertainties cited are the generic bounding values for Westinghouse instrumentation. Plant-specific instrumentation uncertainties exceeding the bounding values cited in the Westinghouse response should be identified and used for the plant-specific analysis. Identify any instrumentation which deviates from the Westinghouse instrumentation and provide the uncertainty value pertinent to this instrumentation and measurement arrangement with comparison to the Westinghouse generic value. The bases or sources for the uncertainty value should also be provided. The sources can be from purchase specifications, manufacturing specifications, calibration data provided by instrumentation vendor or obtained on site, published industry standard or other justifiable bases.
- (2) For the RCS flow measurement, the Westinghouse generic response states: "It is assumed for this error analysis, that this flow measurement is performed within seven days of calibrating the measurement instrumentation, therefore, drift effects are not included (except where necessary due to sensor location)." Does your plant operating procedure have provisions that require the RCS flow measurement be performed within seven days of calibrating the measurement instrumentation? If not, what are the drift uncertainty values associated with each component such as a P Cell, local meter, RTD, thermocouple, process rack and sensors? What is the effect on the overall flow measurement uncertainty?
- (3) The Westinghouse report states: "It is also assumed that the calorimetric flow measurement is performed at the beginning of a cycle, so no allowance has been made for feedwater venturi crud buildup;" and "If venturi fouling is detected by the plant, the venturi should be cleaned, prior to performance of the measurement. If the venturi is not cleaned, the effect of the fouling on the determination of the feedwater flow, and thus, the steam generator power and RCS flow, should be measured and treated as a bias, i.e., the error due to venturi fouling should be added to the statistical summation of the rest of the measurement errors."
 - (a) How do you assure that the venturi is clean at the beginning of a cycle? Is the venturi cleaned at the beginning of every cycle?
 - (b) How do you detect the venturi fouling and to what extent of uncertainty can you detect fouling?
 - (c) Describe the design provisions and procedures to clean the venturi if fouling is detected.
 - (d) How do you determine the error on feedwater flow measurement due to the fouling effect if the venturi is not cleaned or if the venturi fouling is not detected?

- (e) If the venturi is not cleaned prior to the calorimetric flow measurement because no fouling is detected, an error component should be added. The magnitude of the error component should depend on the minimum detectable value of fouling.

Response:

1. NNECO is currently in the process of evaluating the uncertainties associated with the instrumentation used in the Reactor Coolant System Flow Measurement. The results of this evaluation will be forwarded when complete.
2. As part of the instrument uncertainty analysis the effects of drift will be studied. If an instrument is not calibrated within seven (7) days of performing the flow measurement the effects of drift will be added to the overall flow measurement uncertainty.
3.
 - A. Prior to initial plant startup, main feedflow venturis were installed clean. In addition, the section of feedwater piping with the venturis will be flushed prior to initial plant startup. At the beginning of subsequent fuel cycles venturis will be inspected. If venturi fouling is discovered during inspection the venturis will be cleaned.
 - B. Venturi fouling is detected using the performance monitoring program. Plant performance data is collected automatically daily and trended on a monthly basis. The plant parameters specifically reviewed for determination of venturi fouling are - electrical output, feedwater flow, main stream flow, and first stage turbine pressure. The base relationship of these parameters will be established during start-up testing and the first month of operation by review of the collected performance monitoring data. During this period the venturi will be presumed to be clean. During the monthly performance review the trended daily data for the mean electrical output mean stream flow and mean turbine first stage bowl pressure will be compared to the mean feedwater flow. If the trend of the monthly review indicates that the relationship has deviated, corrective action will be taken before performing the next precision heat balance RCS flow measurement. The corrective action will involve inspecting and cleaning the venturi.
 - C. During the first refueling outage, inspection ports will be added upstream and downstream of the venturis. Cleaning will be done by hydrolasing when required.
 - D. The effect of fouling as a result of crud buildup is not taken into account in the feedwater flow measurement. The venturi fouling term is a bias that will result in a higher measured feedwater flow, and, in turn a higher RCS flow than actual measured value. Therefore, if the feedwater venturi is not cleaned, the effect of the fouling on the determination of the feedwater flow and thus the steam generator power and RCS flow is such that all values will be treated in a conservative manner. A visual inspection of the feedwater flow venturi will be done during each refueling outage to detect any buildup of fouling. The feedwater flow venturis will be cleaned as deemed necessary after the inspections. This will correct any deviations caused by feedwater flow venturi fouling.

- E. Prior to the start of each cycle the venturis will be inspected and cleaned if necessary. Because venturis will be verified clean at the beginning of each cycle it will be unnecessary to add an error component due to fouling on the RCS Flow Measurement.

NRC Letter: May 25, 1984

Question No. 210.46

The staff review of the FSAR Section 3.9.3 finds that asymmetric LOCA load effects resulting from postulated ruptures in the primary coolant loop have not been addressed. An acceptable basis for evaluating the asymmetric LOCA loadings is provided in NUREG-0609, "Asymmetric Blowdown Loads on PWR Primary Systems," which addressed the resolution of Generic Task Action Plan A-2. We require that you provide in the FSAR a discussion to specifically address the consideration of asymmetric LOCA loads with respect to satisfying the guidelines in NUREG-0609.

Response:

Please refer to FSAR Section 3.9.N.1.4.3. Additional information regarding evaluation of asymmetric loading effects due to postulated ruptures in the primary coolant loop is contained in the response to NRC Question 480.37.

NRC Letter: May 25, 1984 1.7

Question No. Q480.37

1.9

In the unlikely event of a pipe rupture inside a major component subcompartment, the initial blowdown transient would lead to nonuniform pressure loadings on both the structure and the enclosed component(s). To ensure the integrity of these design features, we request that you provide the following information for each subcompartment analyzed:

- a. Provide the peak and transient loadings on the major components used to establish the adequacy of the supports design. This should include the load forcing functions [e.g., $f(t)$, $f_x(t)$, $f_y(t)$] and transient moments [e.g., $M(t)$, $M_x(t)$, $M_y(t)$], as resolved about a specific, identified coordinate system. 1.12 1.13 1.14 1.15
- b. Provide the projected area used to calculate these loads and identify the location of the area projections on plan and section drawings in the selected coordinate system. This information should be presented in such a manner that confirmatory evaluations of the loads and moments can be made. 1.17 1.18 1.19 1.20 1.21 1.22 1.23 1.24 1.25
- c. For each compartment, provide a table of blowdown mass flow rate and energy release rate as a function of time for the break which was used for the component supports evaluation. 1.26 1.27
- d. Describe and justify the nodalization sensitivity study performed for the major component supports evaluation, where transient forces and moments acting on the components are of concern. 1.28 1.29
- e. Discuss the manner in which movable obstructions to vent flow (such as insulation, ducting, plugs, and seals) were treated. Provide analytical and experimental justification that vent areas will not be partially or completely plugged by displaced objects. Discuss how insulation for piping and components was considered in determining volumes and vent areas. 1.30 1.31 1.32 1.33 1.34
- f. Provide justification for the initial atmospheric conditions assumed in the analysis. An acceptable approach would be to assume air at maximum allowable temperature, minimum absolute pressure, and minimum relative humidity. 1.35 1.36 1.37

Response:

1.40

The following subcompartments were analyzed for postulated pipe rupture events:

- Reactor Pressure Vessel (RPV) Cavity 1.41 1.43
- Steam Generator (SG) Cubicle 1.44

The pressurizer cubicle also was analyzed, but will be submitted after completion of a reanalysis due to as-built modifications to this cubicle.

The peak and transient loadings (Item a) and the projected area (Item b) used to calculate these loads are provided in the following discussion, followed by specific responses to Items c through f of Q480.37.

Items a and b:

• [Reactor Nozzle Guillotine

Configuration

Figures Q480.37-1 and Q480.37-2 show the reactor cavity geometry for the postulated break at the inlet nozzle from Reactor Coolant Loop 2 (Cubicle B). The global coordinate system is defined as follows:

Origin - on containment centerline and 17 feet-6 inches below reactor nozzle centerlines
X - horizontal, south 80.4° west
Y - horizontal, south 9.6° east
Z - vertical upward

The local coordinate system is chosen, as shown in these figures, so that local x points from the RPV centerline away from the broken nozzle. Therefore, vertical forces will be aligned with local z (= global Z), horizontal forces will be aligned with local x, and overturning moments will be about the local y axis. Other loading components due to the slight asymmetry of the RPV nozzle layout are ignored.

The nodal volumes for the asymmetric pressurization analysis, shown on Figures Q480.37-1 and Q480.37-2, also are assumed to be symmetric about the x-z plane. (See FSAR Figure 6.2-23 for overall nodal arrangement.)

Projected Areas

Figures Q480.37-3 through Q480.37-5 show the projected areas over which the asymmetric pressures act on the RPV, the neutron shield tank (NST), and the primary shield wall (PSW). The projected areas (square inches) are shown as arrows, each of which represents the force (pounds) due to a unit (psi) pressure rise in the particular nodal volume. Because of the radiation shielding just below the RPV nozzles, ambient pressure is assumed below elevation 14 feet-2 inches (NST top).

Figure Q480.37-3 is divided into two parts to show the elevation ranges (A) above and (B) below the RPV nozzle centerlines. Due to symmetry, it is understood that each projected area shown includes its mirror image across the x-z plane and there is no net y-force or net moment about the z axis; therefore, each force can be applied as if in the x-z plane. Consequently, moment arms about the z axis are not shown.

MNPS-3 FSAR

The projected areas on the x-y (horizontal) plane are shown in plan view on Figure Q480.37-4. Most of these vertical forces are directed downward on the NST, RPV dome, and control rod drive mechanism (CRDM) shroud. The exception is the upward force on the flange where the RPV and dome are bolted together. The symmetry assumption cited above for horizontal forces also is made for the vertical forces. In Figure Q480.37-4, projected areas of Nodes 1 through 6 are shown for each side and must be added before being applied in the x-z plane.

Figure Q480.37-5 shows both horizontal and vertical forces in an elevation view (x-z plane section). The effective elevations of the horizontal forces in Nodes 1, 3, and 6 also apply to Nodes 2, 4, and 5, respectively.

Figure Q480.37-6 shows plan and elevation views of the refueling cavity and lower internals storage area. Although the pressure increases and pressure differences in these regions are small relative to those in the reactor cavity, the projected areas and moment arms are large, so their contributions to loads on the concrete walls and PSW (and through the grout to the NST) cannot be ignored. It is noted that all horizontal forces below elevation 24 feet-6 inches mutually cancel, therefore, they were not considered.

Jet Impingement Effects

A disk-type jet is postulated to issue from the guillotine break and impinge on exposed areas of the PSW and NST. Jet effects are confined to nodal volumes 1 and 3 (Figure Q480.37-4) in which the calculated pressures are already high. Conservatively, the higher of the calculated jet-impingement pressure or the calculated asymmetric pressure rise, was applied on any area.

Over the target area of the PSW inner wall, the calculated average jet pressure was relatively low, due to both the distances and the shallow impingement angles, so the calculated asymmetric pressure rise was applied. Conversely, over the NST top target area, which is very close to the nozzle and is nearly normal to the jet, impingement pressures prevailed. Therefore, a calculated target area of 2,540 square inches (Figure Q480.37-4) was deducted from the combined projected areas of Volume 1. The pressurization force (over the target area only) was replaced by the calculated downward component of jet impingement force (207,400 pounds) with a rise time equal to the assumed break-opening time (1 millisec). The centroid of the target area was 117.42 inches from the RPV centerline. Transient pressure forces were applied as usual over the remaining areas.

Force and Moment Histories

The net loads due to combined pressurization and jet impingement were calculated as functions of time. The projected areas and moment arms (Figures Q480.37-3 through Q480.37-6) and the pressure histories (Figures Q480.37-7 through Q480.37-10) were input to Stone & Webster Program No. ME-171 (ASYMPR) (see FSAR Appendix 3A.2.13). The results

MNPS-3 FSAR

are shown in Figures Q480.37-11 through Q480.37-13 for the RPV and Figures Q480.37-14 through Q480.37-16 for the PSW. The loads on the NST top are distributed among these curves on the basis of the anticipated load path. Specifically, NST vertical force is lumped with the RPV because the nozzle supports are very stiff vertically, while the grout has no vertical stiffness. Conversely, NST overturning moment is lumped with the PSW because the PSW and grout are much stiffer than the NST and nozzle supports to horizontal and bending loads.

• Steam Generator Cubicle

Configuration

FSAR Figures 6.2-19 through 6.2-22 show the SG Cubicle A (Loop 1) geometry and subcompartment nodalization for asymmetric pressurization (refer to FSAR Section 6.2.1.2). The global coordinate system, defined under Reactor Nozzle Guillotine for the reactor cavity, is used throughout this discussion. In this system, Cubicle A lies in the -X, +Y quadrant. Cubicle B, modeled for certain postulated breaks, is obtained by reflection of Cubicle A across the Y-Z plane plus minor changes.

Projected Areas

Figures Q480.37-17 through Q480.37-19 show the projected surface areas of the SG and reactor coolant pump (RCP) within the elevation ranges shown on Figure Q480.37-20. Each projection on the global system is indicated by an arrow with the associated force for a unit pressure rise. Since each force element is normal to the local surface, moments about the vertical centerlines vanish. Overturning moments are generated by both horizontal and vertical force components.

Postulated Breaks and Resultant Loads

Asymmetric pressure calculations were made for several break locations (Figure Q480.37-21 and FSAR Table 3.9B-15) within the SG cubicle. The analyzed breaks are listed in Table Q480.37-1, along with a summary of the peak loads resulting on the SG and RCP. Break 7 (SG Intrados Split), having the largest postulated opening area, clearly dominates most (9 of 10) listed load components. The sole exception is vertical force on the RCP, which is largest during Break 8. Breaks 4 and 8 also lift the SG nearly as forcefully as does Break 7.

Pressurization for a feedwater line guillotine was also calculated (FSAR Figure 3.6-10, Cubicle B, Break Location 4 or 5). Full lateral separation of pipe ends was assumed. Moments on the SG for the FW line guillotine were resolved about the upper support elevation, since the generated forces are basically confined to this region. For all other breaks, moments were resolved about the intersection of the inlet and outlet nozzle centerlines (see Table Q480.37-1 for elevations).

MNPS-3 FSAR

Based on these comparisons, time history loads (Figures Q480.37-22 4.16 through Q480.37-43) are shown only for Breaks 7, 4, and FWL. The signs 4.19 of each load component are for Cubicle B.

Item c: 4.21

Refer to revised FSAR Section 6.2.1.2 for the mass and energy release 4.22 tables used for the component supports evaluation. 4.23

Item d: 4.26

Subcompartment nodalization is described and justified in the response 4.27 to NRC Question 480.9. The justification given in this response applies 4.29 to all subcompartment analyses performed for the major component supports evaluation. The pressurizer subcompartment is presently being 4.31 reanalyzed for consistency with the guidelines of the Subcompartment Analysis Procedures (NUREG/CR-1199). Results will be submitted in a 4.33 future FSAR amendment.

Item e: 4.35

Refer to revised FSAR Section 6.2.1.2 for a discussion of the manner in 4.36 which movable obstructions to vent flow are treated. 4.37

Item f: 4.40

The initial containment temperature was selected at the maximum 4.41 allowable 120°F, and the initial air partial pressure was selected at 4.43 the minimum allowable, 9.0 psia. The initial relative humidity was 4.45 taken at 50 percent. This is the expected minimum during normal 4.46 operation. However, in extreme conditions, the humidity may go as low 4.47 as 10 percent. The sensitivity of the calculated subcompartment 4.48 pressure differential to the initial relative humidity was determined for the spray line break in the pressurizer cubicle. The pressure 4.50 differential increased by less than 0.2 psi (approximately 3 percent) when the humidity was decreased from 50 percent to 10 percent. This 4.53 difference in cubicle pressure differential is not significant; therefore, the assumption of 50 percent relative humidity is acceptable. 4.54

In addition, the Subcompartment Analysis Procedures (NNREG/CR-1199) are 4.55 in general support of the above conclusion regarding sensitivity to 4.56 relative humidity.

TABLE Q480.37-1

PEAK ASYMMETRIC LOADS

Steam Generator (at elevation 24 ft-5.1 in.)

| Break | Flow Area (in. ²) | Forces (kip) | | | Moments (in.-kip) | | M_z | |
|------------------|-------------------------------------|--------------|-------|-------|----------------------|-----------------------|-------|------|
| | | F_x | F_y | F_z | M_x | M_y | | |
| 11 | 196.6 | 137 | 51 | 79 | 6,742 | 17,207 | 0 | 1.19 |
| 9 | 196.6 | 63 | 30 | 62 | 6,806 | 9,537 | 0 | 1.21 |
| 7 | 707 | 301 | 174 | 292 | 16,457 | 34,798 | 0 | 1.23 |
| 3 | 196.6 | 116 | 71 | 69 | 8,262 | 17,136 | 0 | 1.25 |
| FW | 478 | 191 | 79 | 59 | 7,354 ⁽²⁾ | 17,808 ⁽²⁾ | 0 | 1.27 |
| 4 | 500 | 98 | 99 | 273 | 12,001 | 29,557 | 0 | 1.29 |
| 8 ⁽¹⁾ | 500 | 67 | 63 | 272 | 11,884 | 28,692 | 0 | 1.31 |

Coolant Pump (at elevation 17 ft-6 in.)

| Break | Flow Area (in. ²) | Forces (kip) | | | Moments (in.-kip) | | M_z | |
|-------|-------------------------------------|--------------|-------|-------|-------------------|-------|-------|------|
| | | F_x | F_y | F_z | M_x | M_y | | |
| 11 | 196.6 | 55 | 50 | 5 | 3,617 | 4,661 | 0 | 1.39 |
| 9 | 196.6 ⁽³⁾ | 48 | 29 | 13 | 1,125 | 3,004 | 0 | 1.41 |
| 7 | 707 | 91 | 79 | 14 | 6,056 | 8,198 | 0 | 1.43 |
| 3 | 196.6 ⁽³⁾ | 35 | 36 | 5 | 2,775 | 3,028 | 0 | 1.45 |
| FW | 478 | 4 | 2 | 2 | 258 | 570 | 0 | 1.47 |
| 4 | 500 | 23 | 35 | 13 | 2,359 | 1,639 | 0 | 1.49 |
| 8 | 500 ⁽³⁾ | 19 | 36 | 24 | 1,385 | 1,113 | 0 | 1.51 |

NOTES:

1. Loop closure weld, formerly Break 12.

2. Resolved at elevation 49 feet-8.5 inches.

3. Conservative (high) value based on another nearby break.

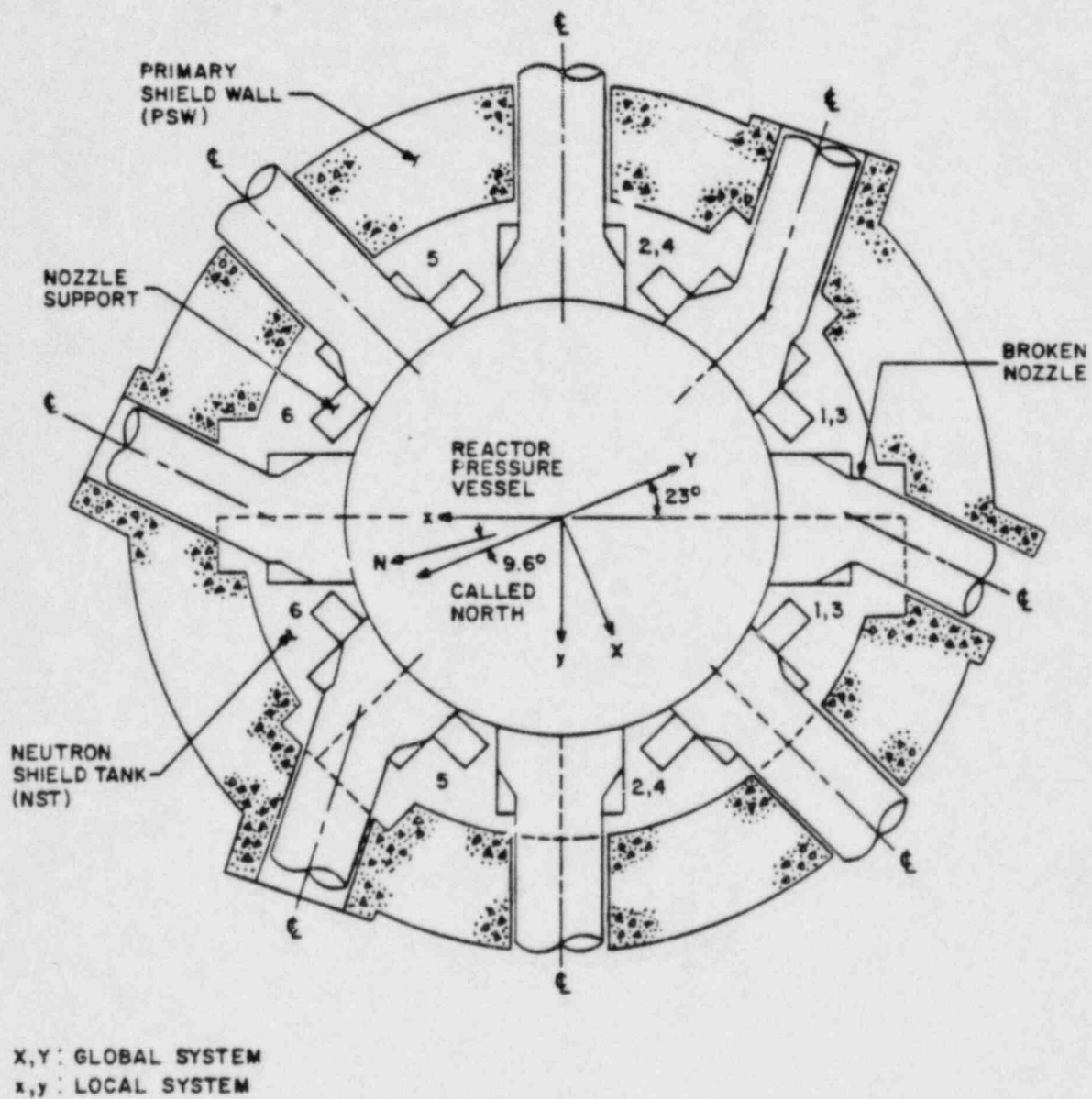


FIGURE Q480.37-1
 UPPER REACTOR CAVITY
 NODAL ARRANGEMENT
 MILLSTONE NUCLEAR POWER STATION
 UNIT 3
 FINAL SAFETY ANALYSIS REPORT

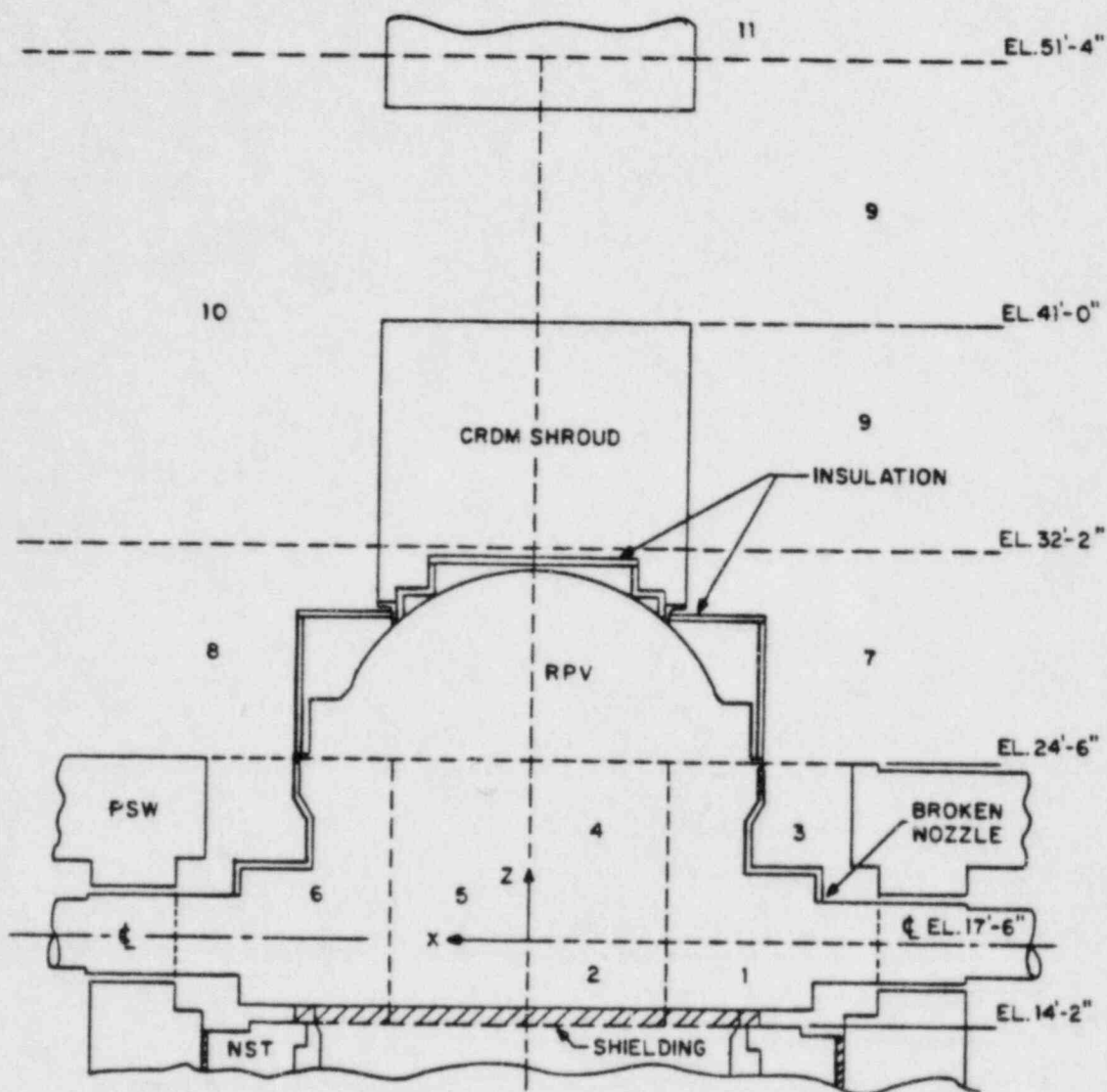
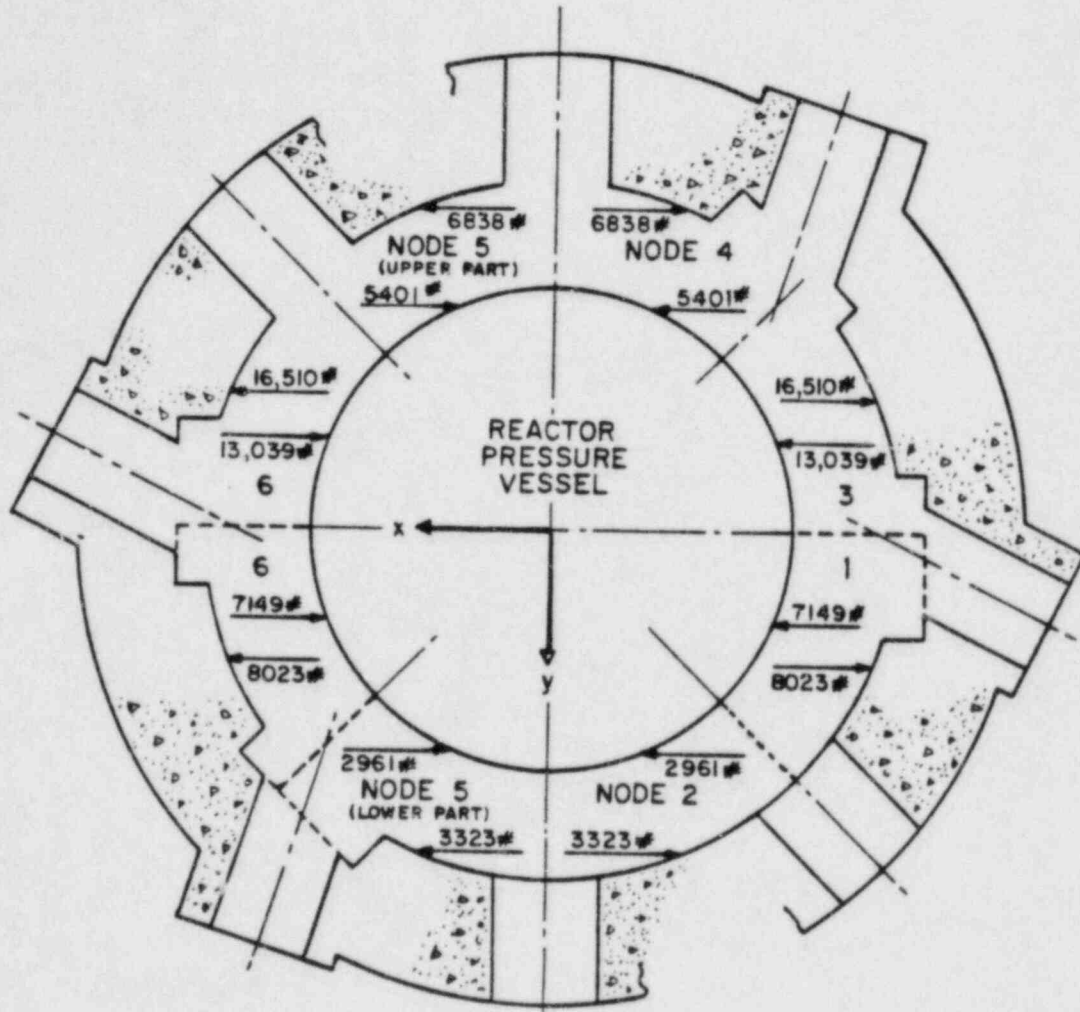


FIGURE Q480.37-2
ELEVATION VIEW OF NODAL
ARRANGEMENT IN UPPER REACTOR
CAVITY AND CRDM HOUSING
MILLSTONE NUCLEAR POWER STATION
UNIT 3
FINAL SAFETY ANALYSIS REPORT

(A) BETWEEN ELEVATIONS 17'-6" AND 24'-6"

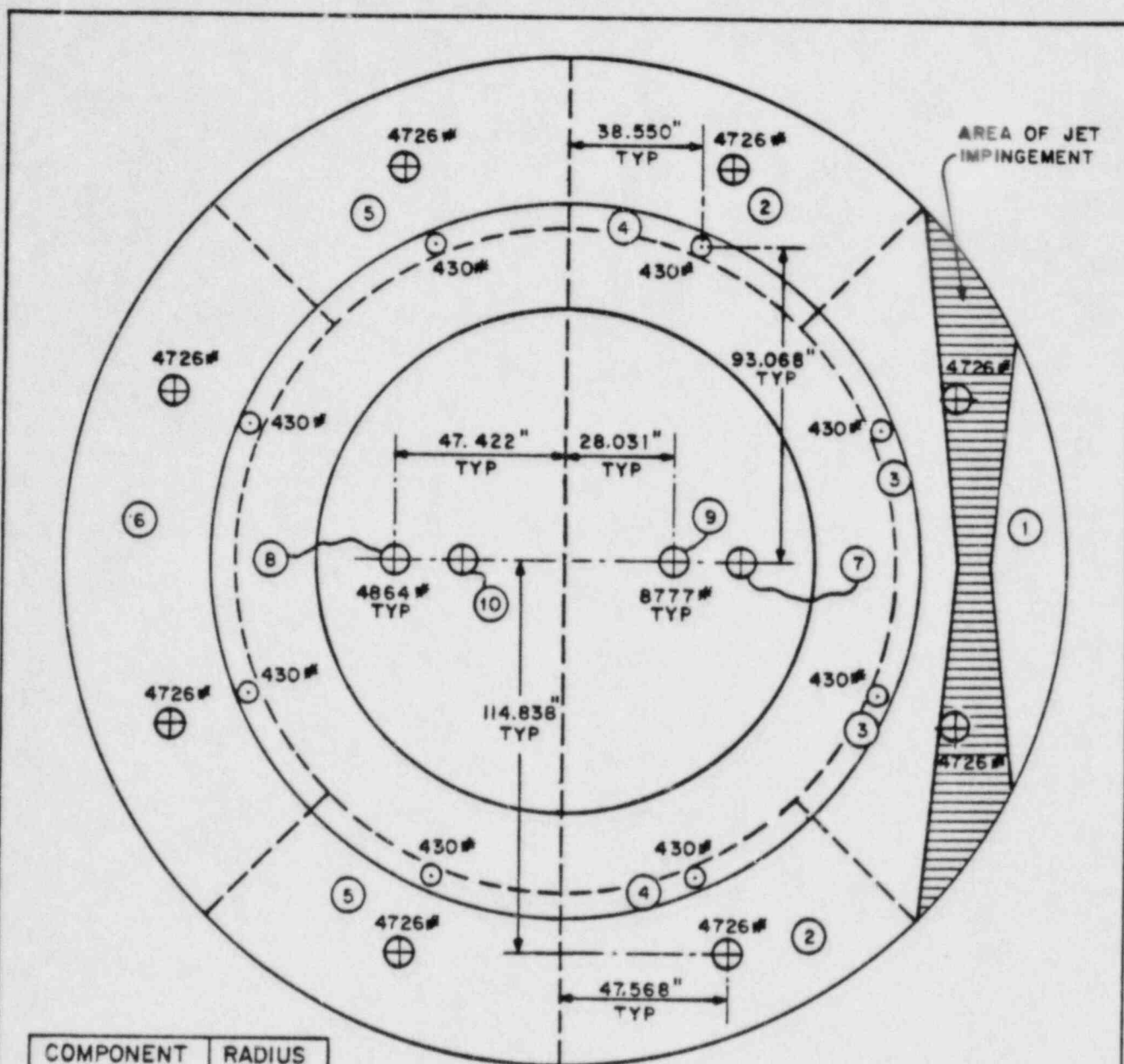


(B) BETWEEN ELEVATIONS 14'-2" AND 17'-6"

NOTE

INCLUDES PIPING INSIDE PSW BUT
EXCLUDES PSW PENETRATIONS

FIGURE Q480.37-3
HORIZONTAL FORCES ON RPV AND
PSW DUE TO UNIT PRESSURES
MILLSTONE NUCLEAR POWER STATION
UNIT 3
FINAL SAFETY ANALYSIS REPORT



| COMPONENT | RADIUS |
|-------------|----------|
| CRDM | 74.75" |
| RPV FLANGE | 106.00"* |
| RPV SHELL | 100.70"* |
| NST + GROUT | 150.00" |

* INCLUDES INSULATION

LEGEND

- = NODE NUMBER
- ⊙ = UPWARD FORCE
- ⊕ = DOWNWARD FORCE

FIGURE Q480.37-4
VERTICAL FORCES ON CRDM,
RPV, AND NST DUE TO UNIT
PRESSURES IN ADJACENT NODES
MILLSTONE NUCLEAR POWER STATION
UNIT 3
FINAL SAFETY ANALYSIS REPORT

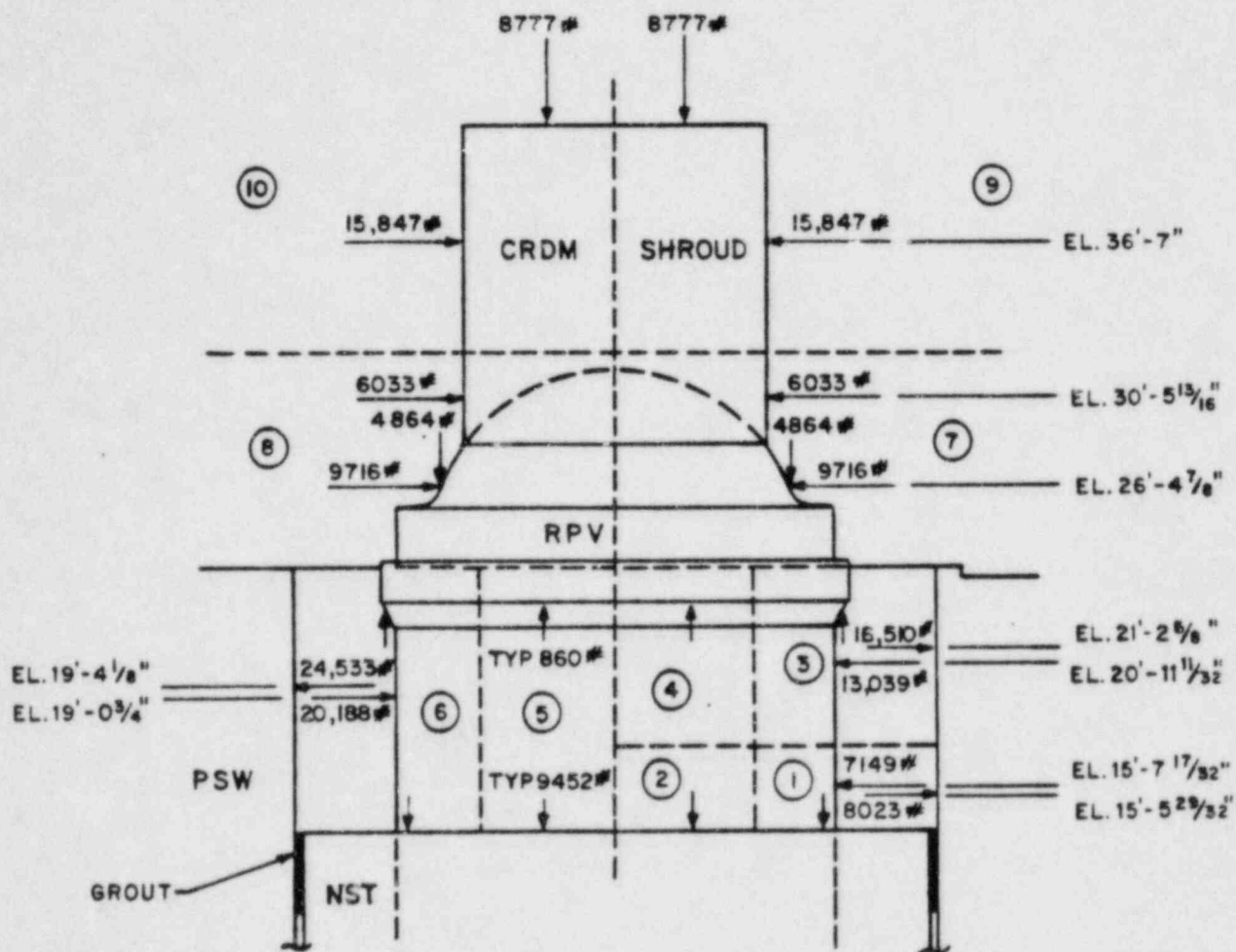


FIGURE Q480.37-5
ELEVATION VIEW OF RPV AND
VICINITY SHOWING FORCES
DUE TO UNIT PRESSURES
MILLSTONE NUCLEAR POWER STATION
UNIT 3
FINAL SAFETY ANALYSIS REPORT

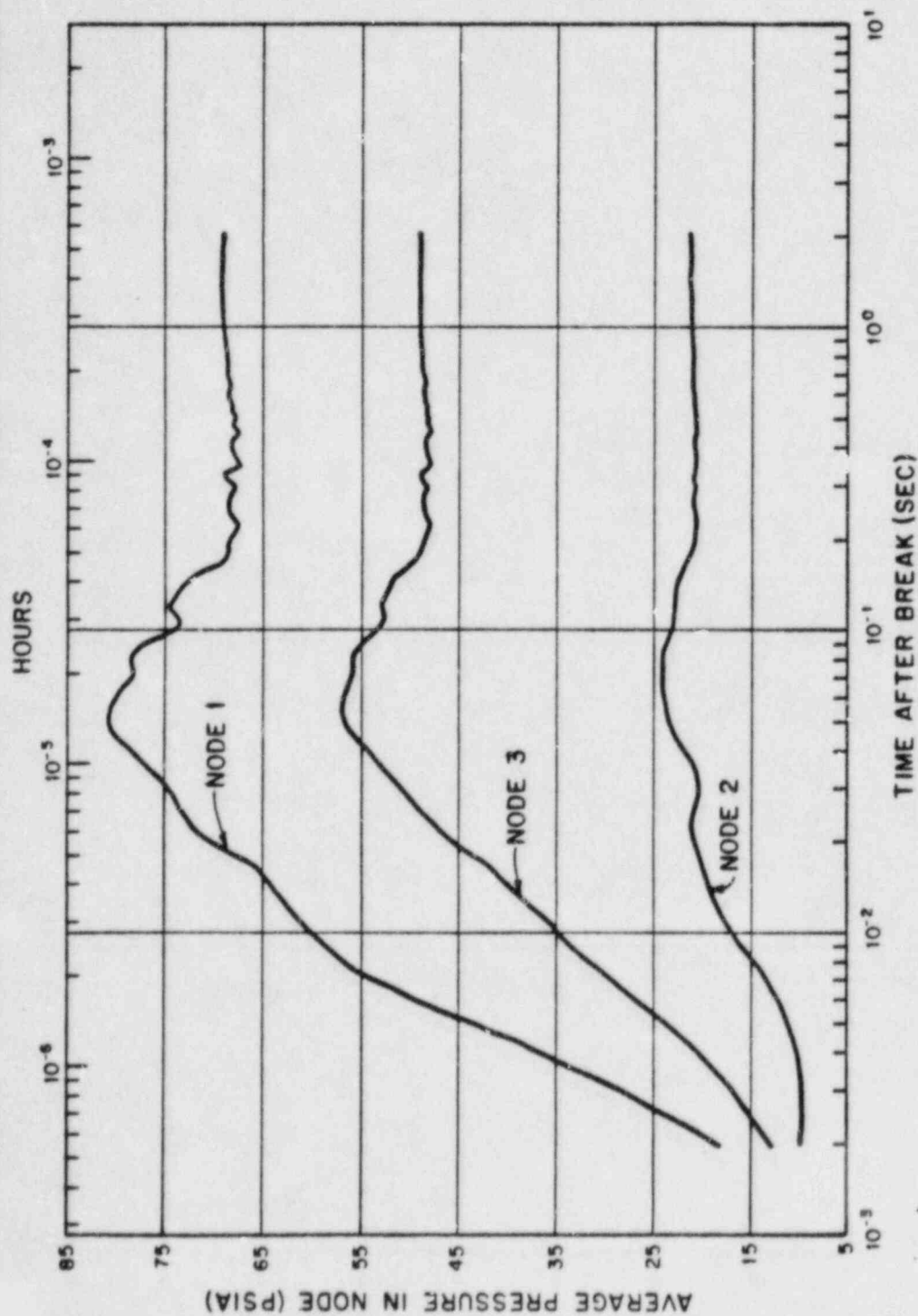


FIGURE Q480.37-7
REACTOR CAVITY PRESSURE TRANSIENTS
NODE NUMBERS 1,2,3
COLD LEG 100 SQ. IN. BREAK
MILLSTONE NUCLEAR POWER STATION
UNIT 3
FINAL SAFETY ANALYSIS REPORT

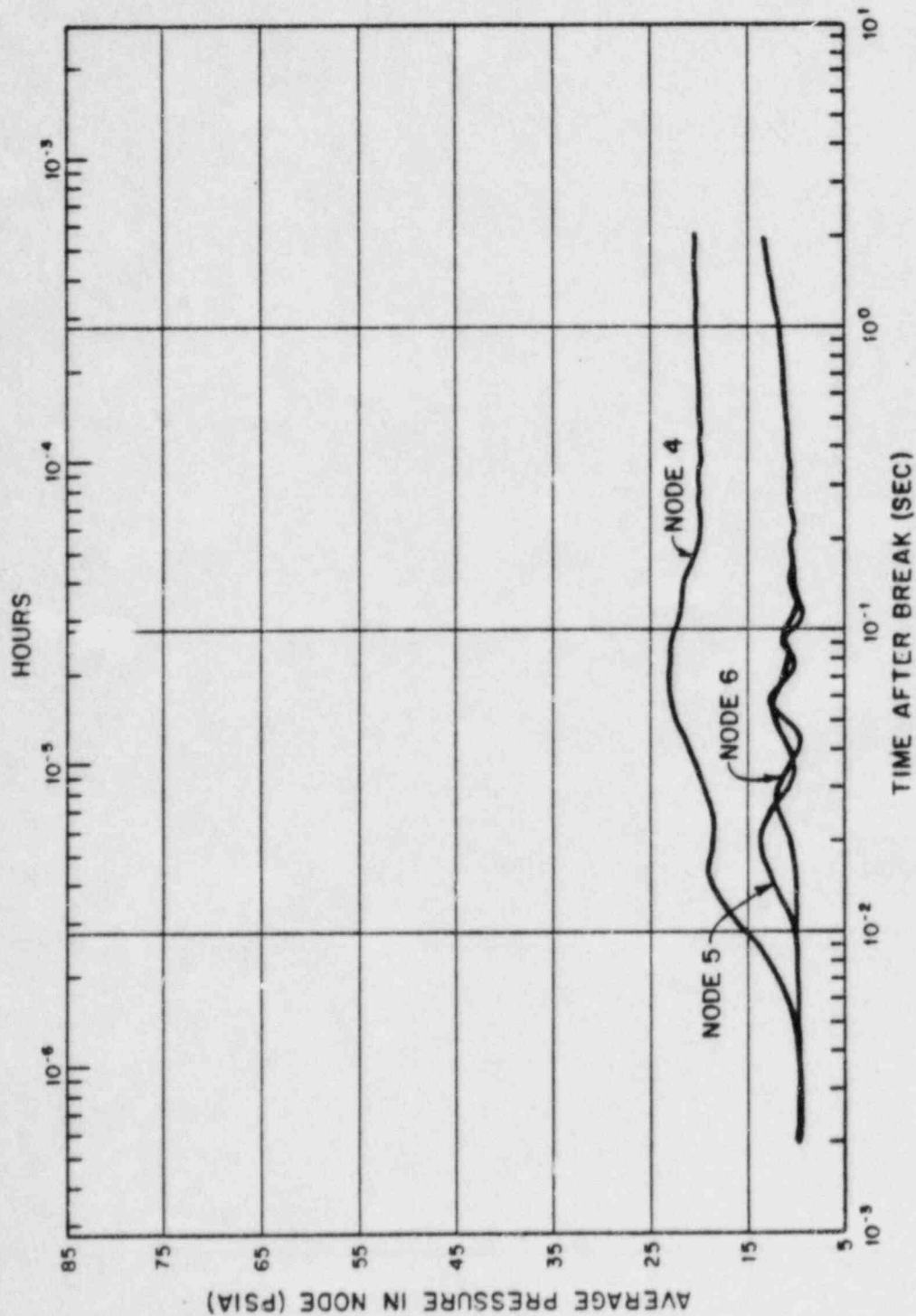


FIGURE Q480.37-8
REACTOR CAVITY PRESSURE TRANSIENTS
NODE NUMBERS 4,5,6
COLD LEG 100 SQ. IN. BREAK
MILLSTONE NUCLEAR POWER STATION
UNIT 3
FINAL SAFETY ANALYSIS REPORT

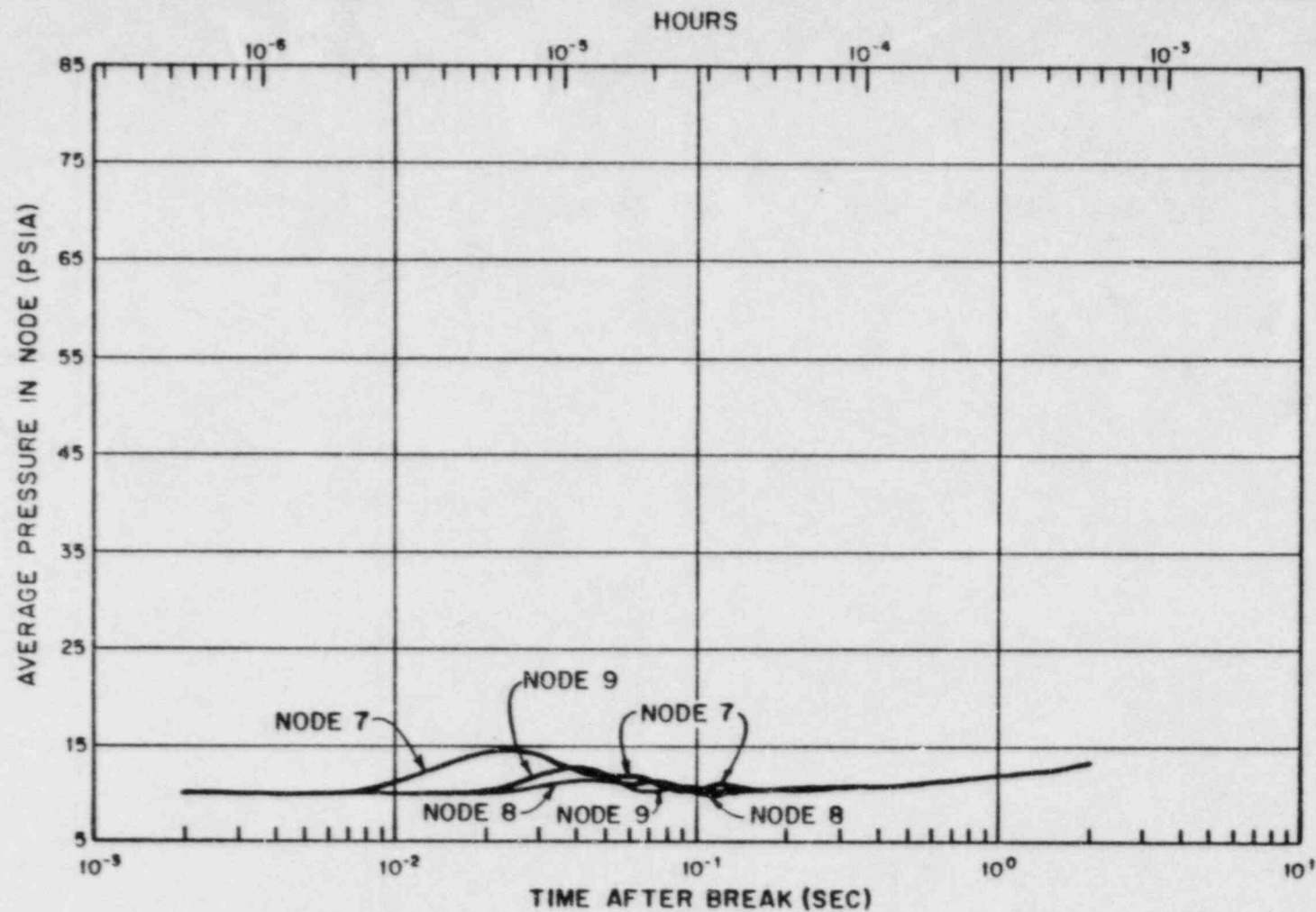


FIGURE Q480.37-9
REACTOR CAVITY PRESSURE TRANSIENTS
NODE NUMBERS 7,8,9
COLD LEG 100 SQ. IN. BREAK
MILLSTONE NUCLEAR POWER STATION
UNIT 3
FINAL SAFETY ANALYSIS REPORT

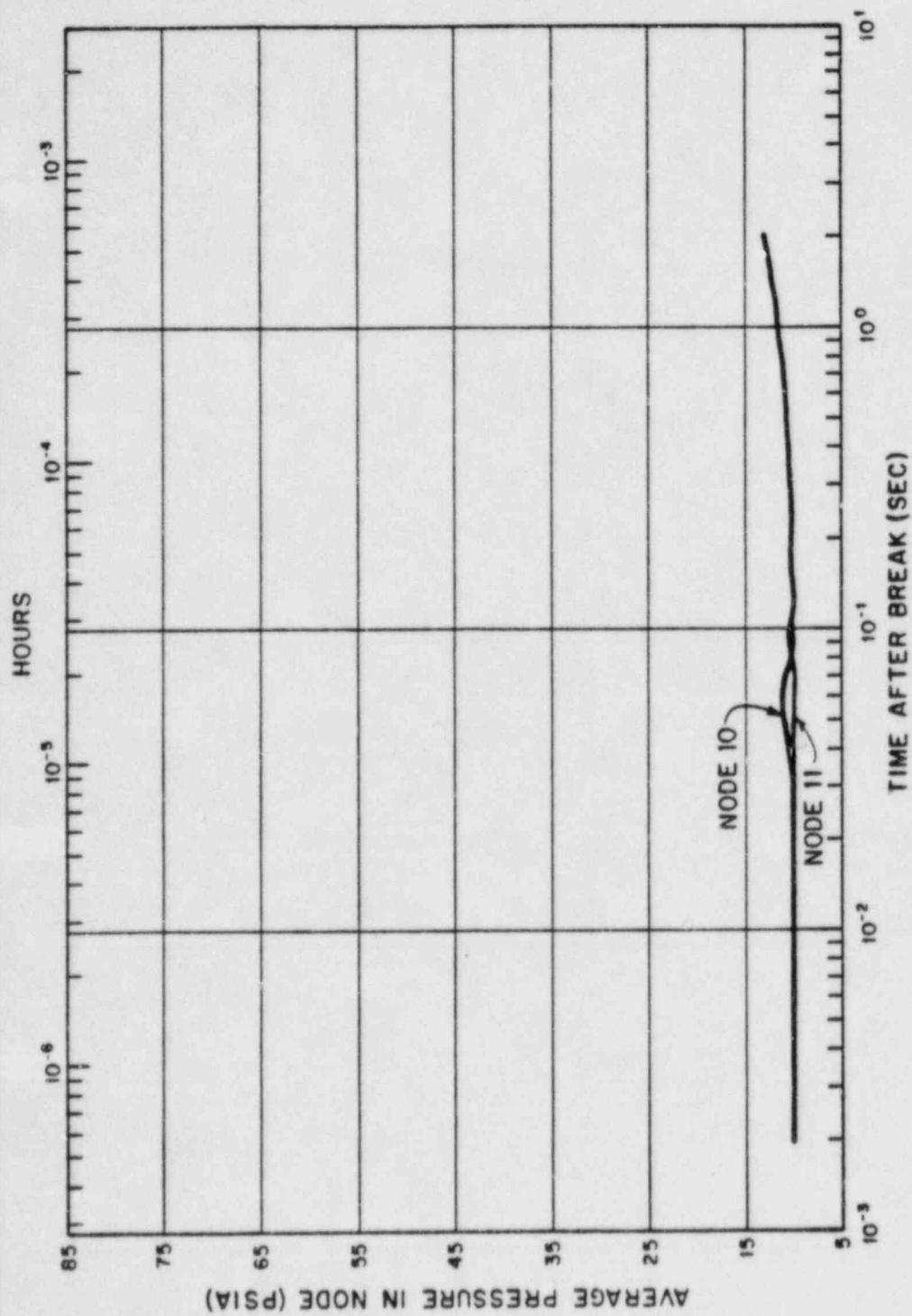


FIGURE Q480.37-10
 REACTOR CAVITY PRESSURE TRANSIENTS
 NODE NUMBERS 10, 11
 COLD LEG 100 SQ. IN. BREAK
 MILLSTONE NUCLEAR POWER STATION
 UNIT 3
 FINAL SAFETY ANALYSIS REPORT

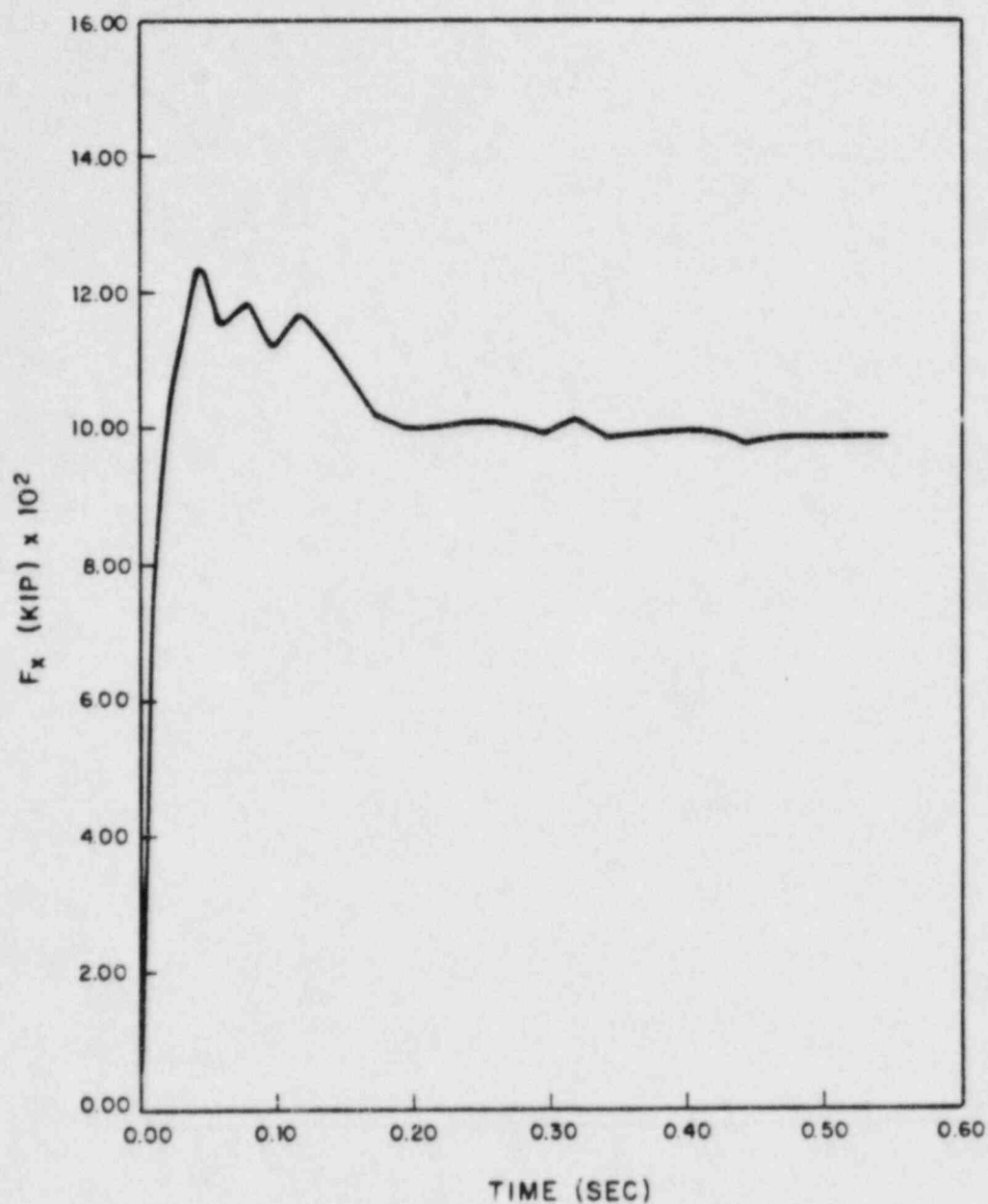


FIGURE Q480.37-11
HORIZONTAL FORCE ON RPV
AWAY FROM BREAK
MILLSTONE NUCLEAR POWER STATION
UNIT 3
FINAL SAFETY ANALYSIS REPORT

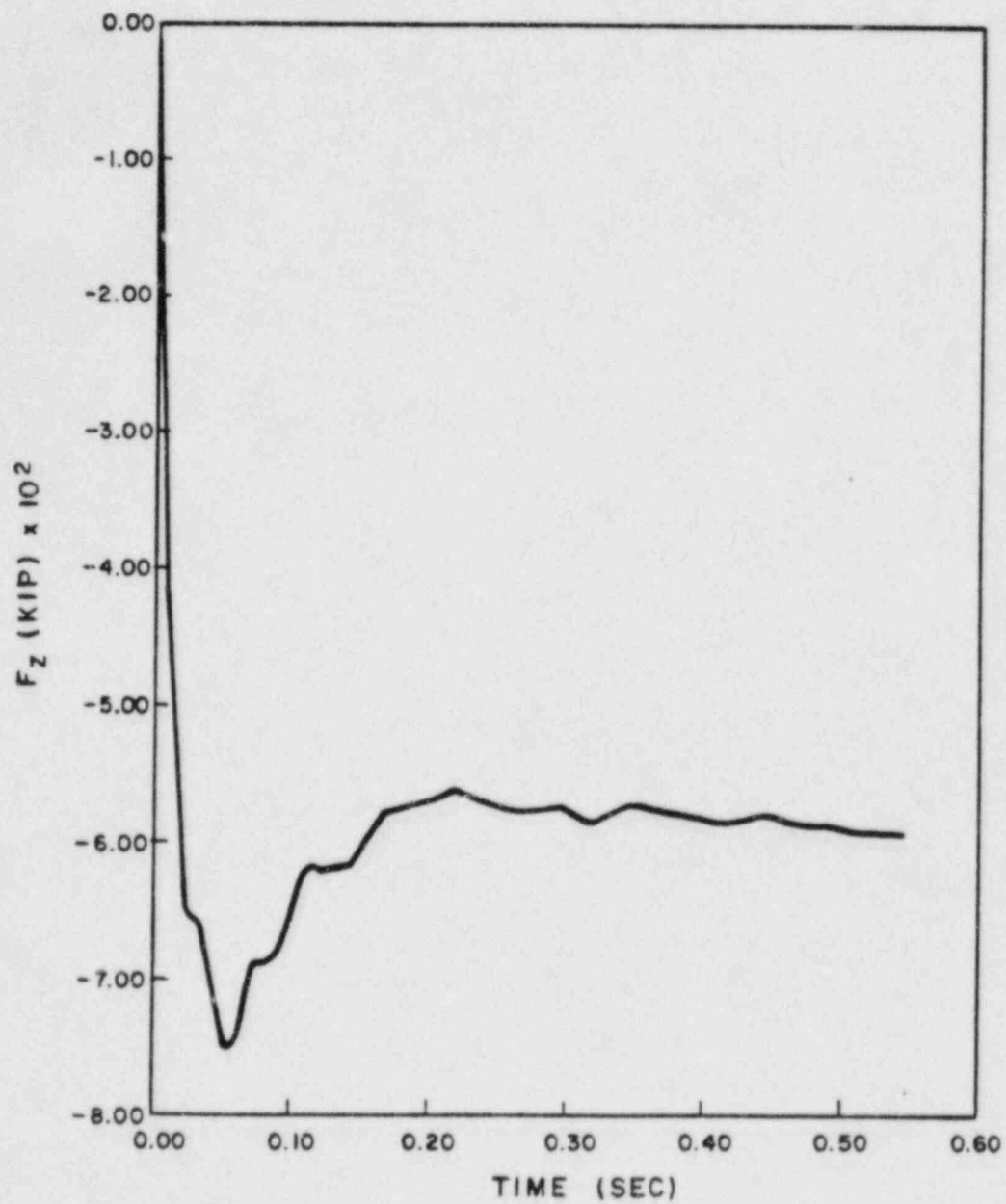


FIGURE Q480.37-12
VERTICAL UPWARD FORCE ON
RPV AND TOP OF NST
MILLSTONE NUCLEAR POWER STATION
UNIT 3
FINAL SAFETY ANALYSIS REPORT

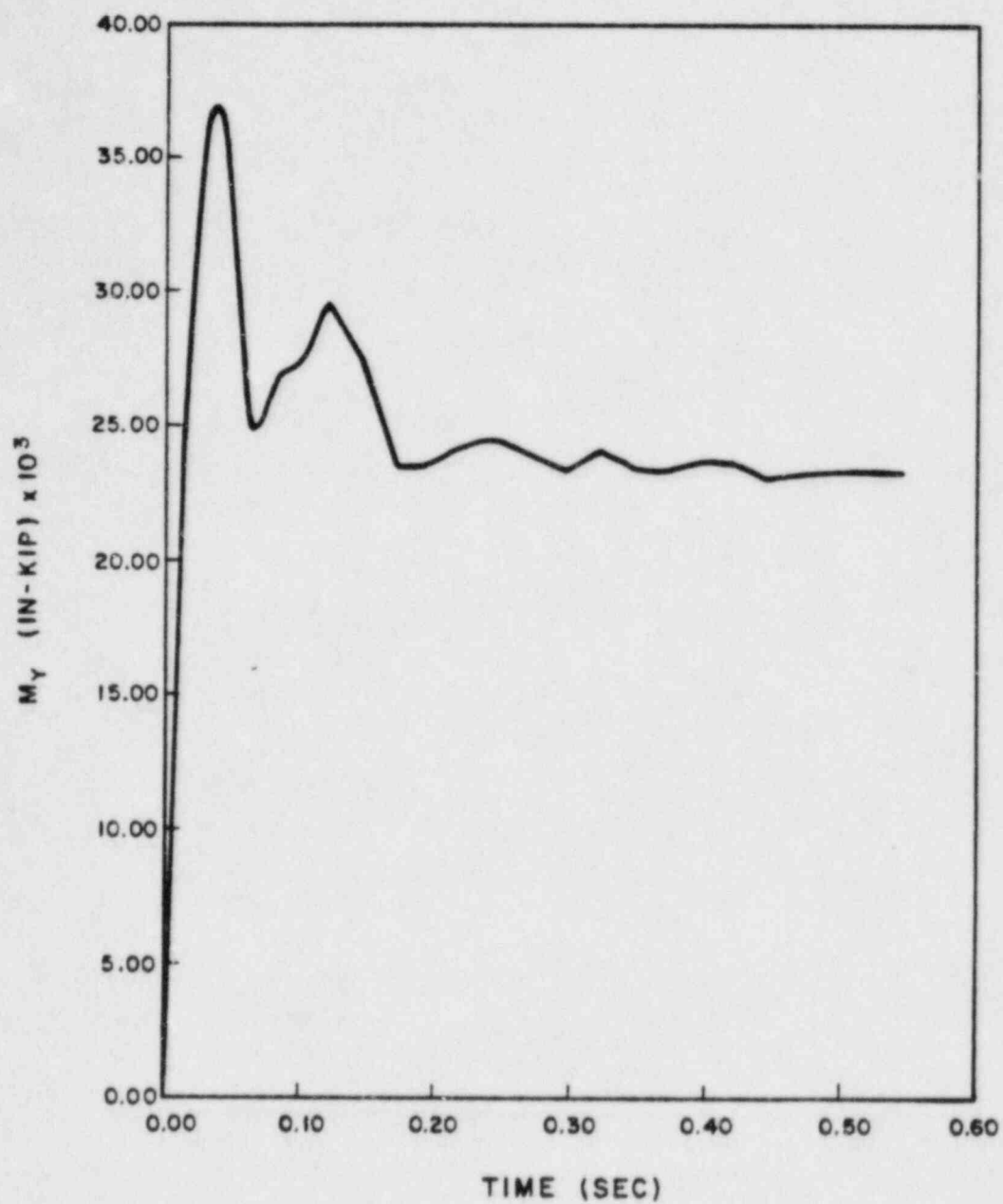


FIGURE Q480.37-13
OVERTURNING MOMENT ON
RPV AT ELEVATION 17'-6"
MILLSTONE NUCLEAR POWER STATION
UNIT 3
FINAL SAFETY ANALYSIS REPORT

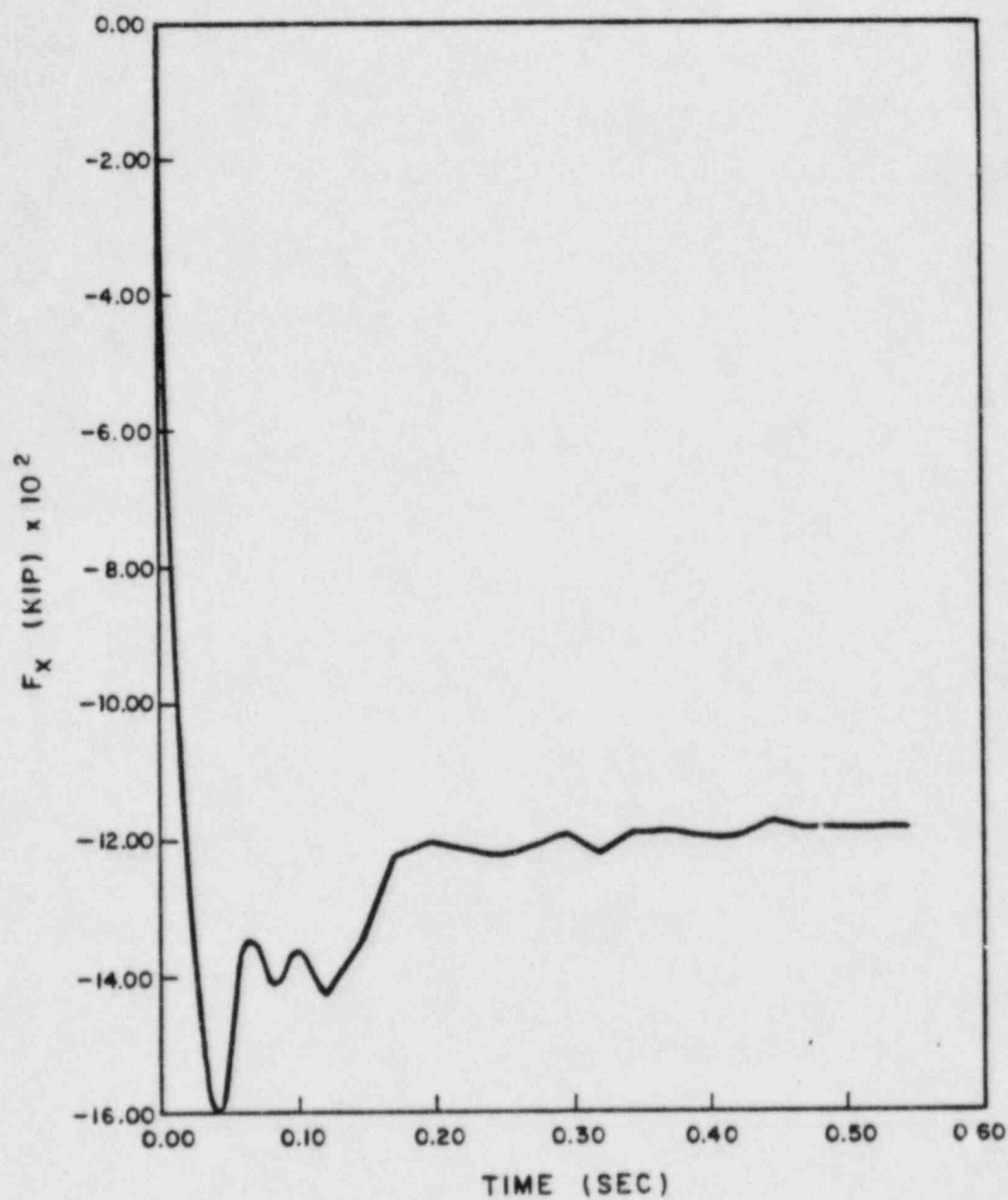


FIGURE Q480.37-14
HORIZONTAL FORCE ON PSW/
NST AWAY FROM BREAK
MILLSTONE NUCLEAR POWER STATION
UNIT 3
FINAL SAFETY ANALYSIS REPORT

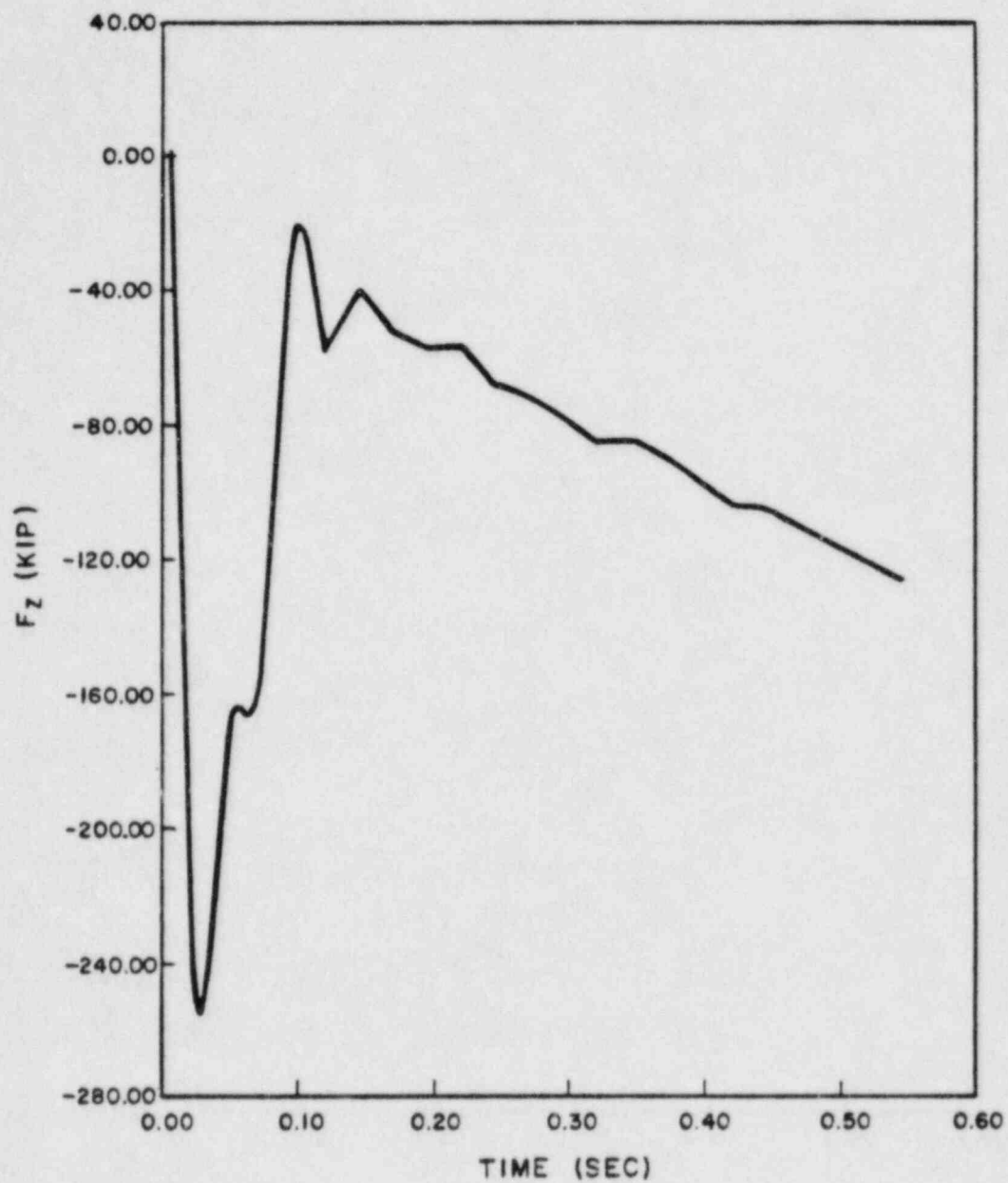


FIGURE Q480.37-15
VERTICAL UPWARD FORCE ON PSW
MILLSTONE NUCLEAR POWER STATION
UNIT 3
FINAL SAFETY ANALYSIS REPORT

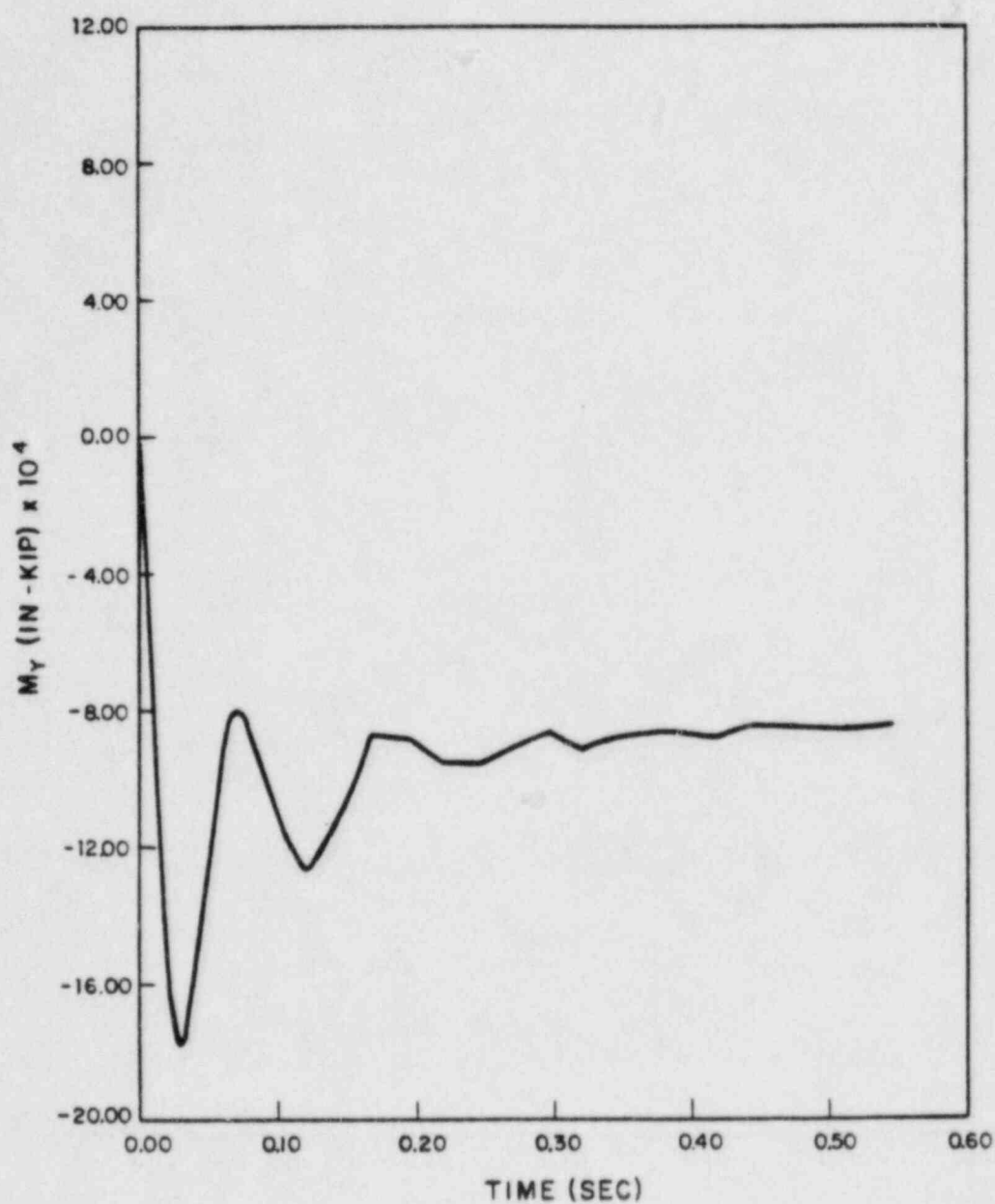


FIGURE Q 480.37-16
OVERTURNING MOMENT ON
PSW/NST AT ELEVATION 17'-6"
MILLSTONE NUCLEAR POWER STATION
UNIT 3
FINAL SAFETY ANALYSIS REPORT

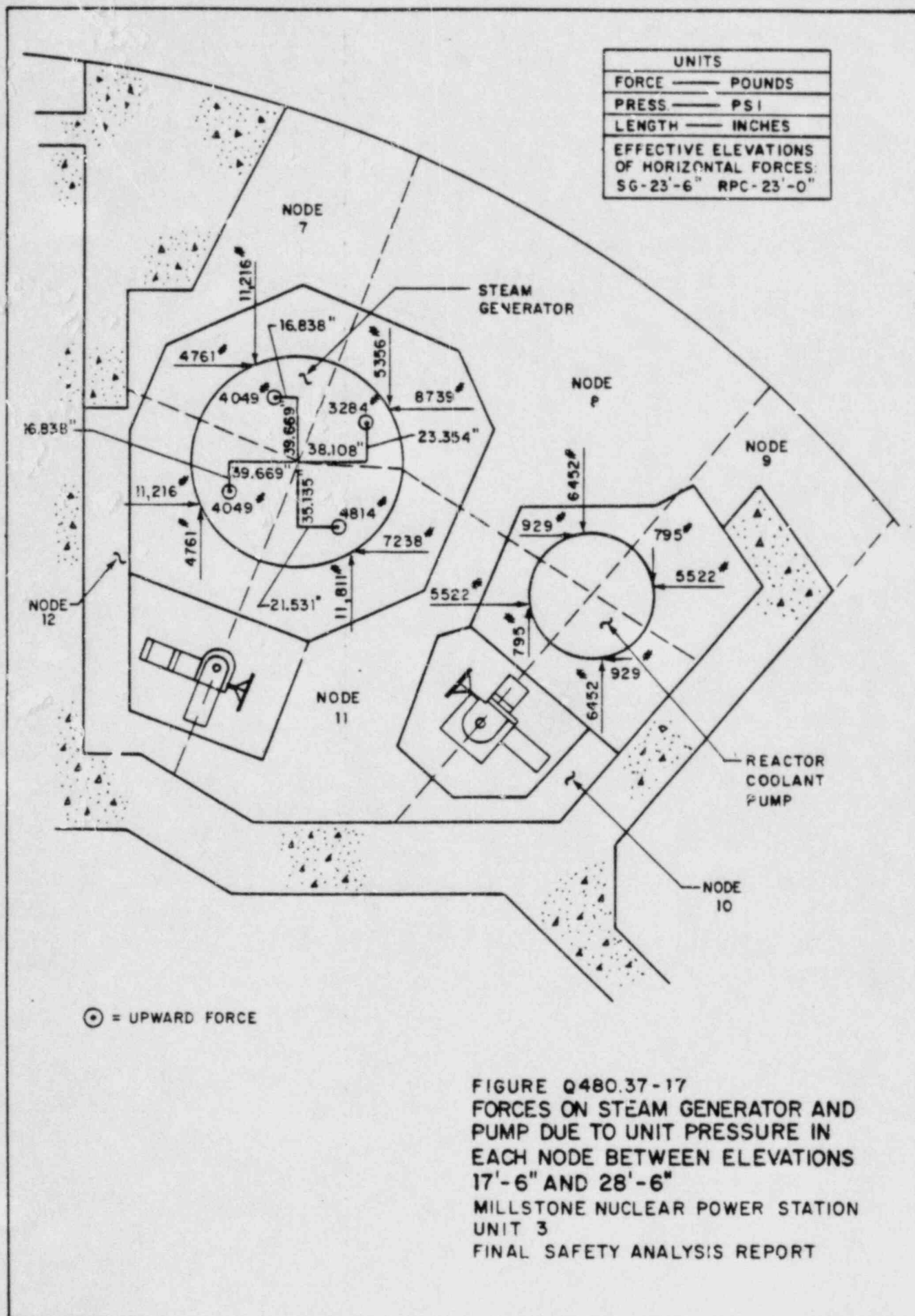
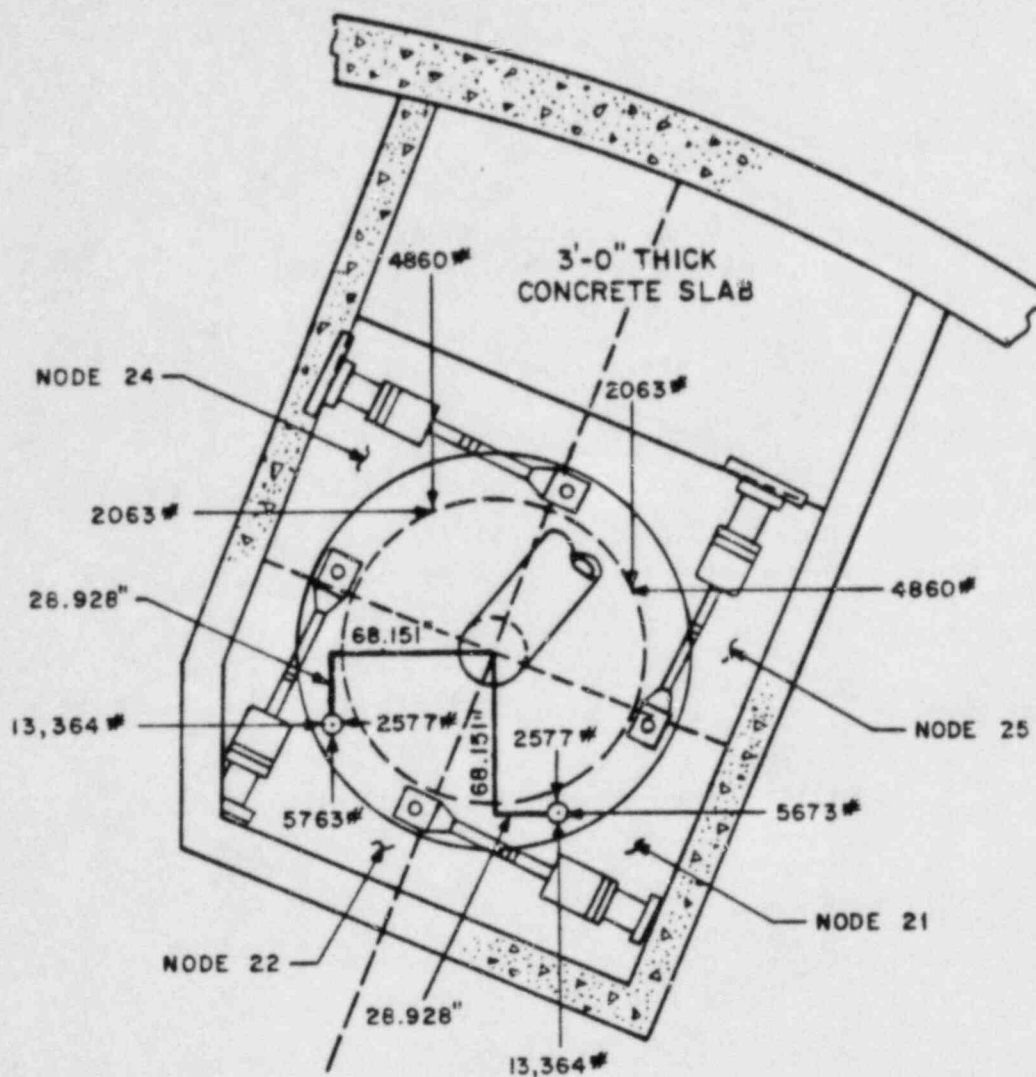


FIGURE Q480.37-17
 FORCES ON STEAM GENERATOR AND
 PUMP DUE TO UNIT PRESSURE IN
 EACH NODE BETWEEN ELEVATIONS
 17'-6" AND 28'-6"
 MILLSTONE NUCLEAR POWER STATION
 UNIT 3
 FINAL SAFETY ANALYSIS REPORT

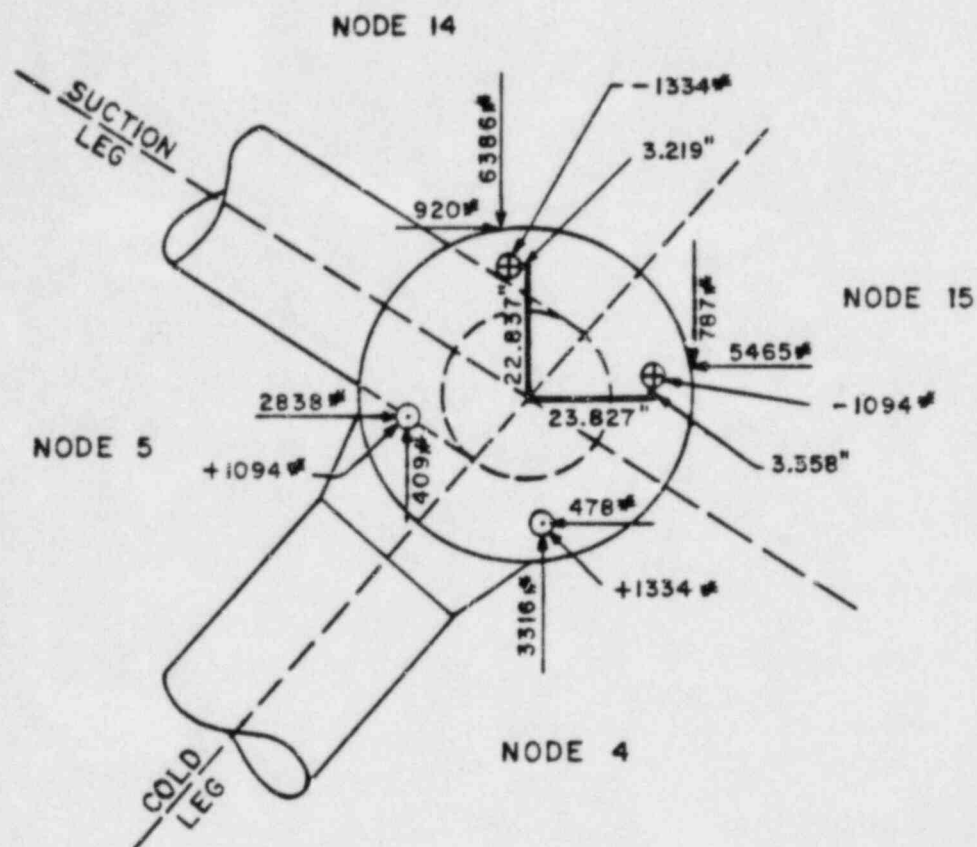


| NOT SHOWN | |
|-----------|----------|
| NODE | OPPOSITE |
| 19 | 21 |
| 20 | 22 |
| 26 | 24 |
| 27 | 25 |

| EFFECTIVE ELEVATIONS OF HORIZONTAL FORCES | |
|--|----------------|
| NODES | ELEV |
| 19 - 22 | 57' - 1 13/16" |
| 24 - 27 | 49' - 10" |

⊙ = UPWARD FORCE

FIGURE Q480.37-18
FORCES ON STEAM GENERATOR
DUE TO UNIT PRESSURES
BETWEEN ELEVATIONS 51'-4"
& 61'-4" (NODES 19-22) OR
48'-4" & 51'-4" (NODES 24-27)
MILLSTONE NUCLEAR POWER STATION
UNIT 3
FINAL SAFETY ANALYSIS REPORT

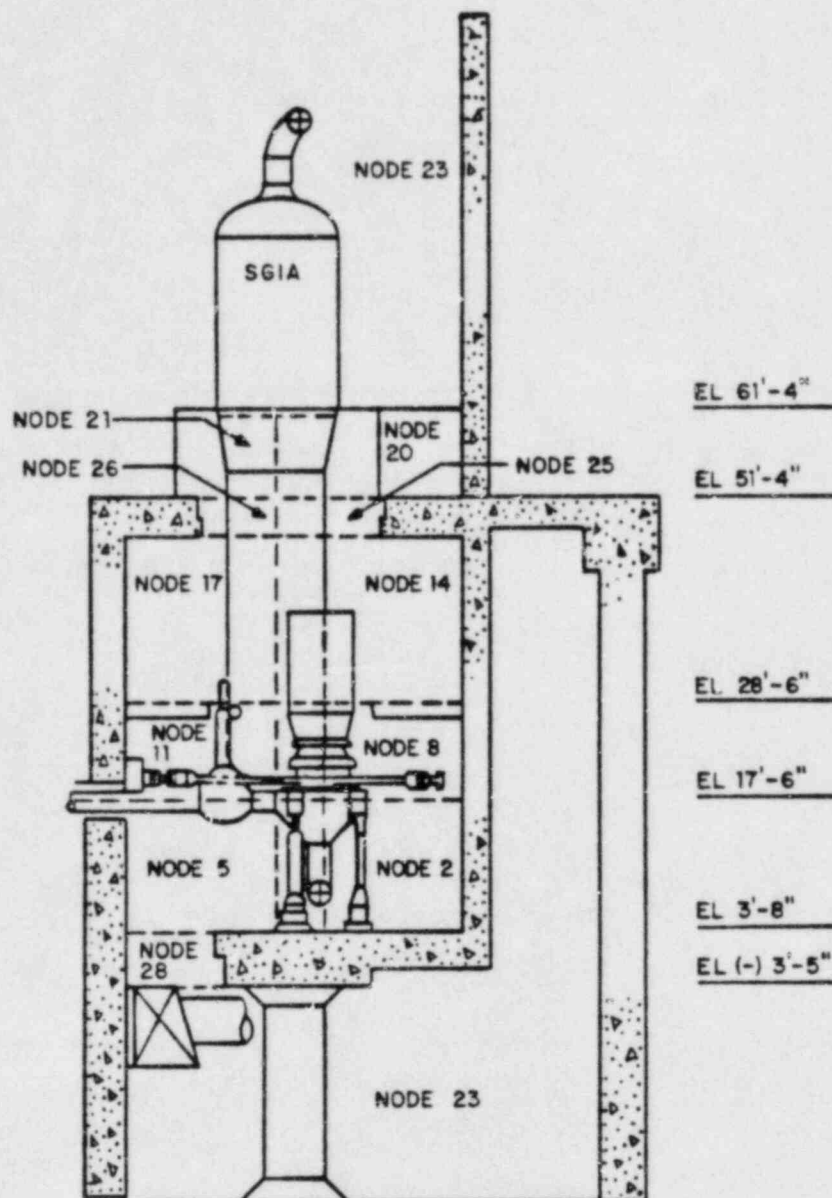


| NOT SHOWN | |
|-----------|----------|
| NODE | OPPOSITE |
| 2 | 4 |
| 3 | 5 |
| 16 | 14 |
| 17 | 15 |

| EFFECTIVE ELEVATIONS OF HORIZONTAL FORCES | |
|--|--------------|
| NODES | ELEV |
| 2 - 5 | 14' - 7" |
| 14 - 17 | 33' - 9 3/8" |

⊙ : UPWARD FORCE
 ⊕ : DOWNWARD FORCE

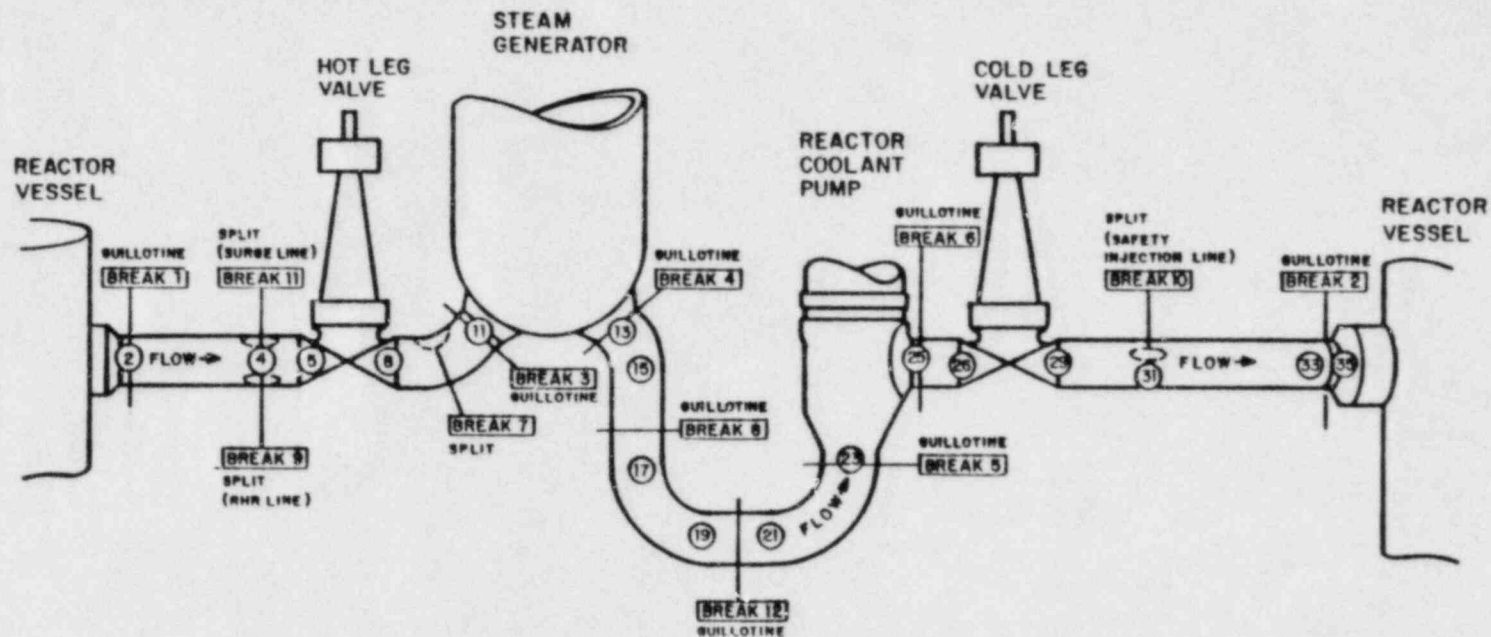
FIGURE Q480.37-19
 FORCES ON REACTOR COOLANT
 PUMP DUE TO UNIT PRESSURES
 BETWEEN ELEVATIONS 3'-8"
 & 17'-6" (NODES 2-5) OR
 28'-6" & 48'-4" (NODES 14-17)
 MILLSTONE NUCLEAR POWER STATION
 UNIT 3
 FINAL SAFETY ANALYSIS REPORT



SECTION 1-1

NODE 23 IS THE CONTAINMENT

FIGURE Q480.37-20
ELEVATION VIEW (SECTION 1-1)
OF THE STEAM GENERATOR
CUBICLE 1A
MILLSTONE NUCLEAR POWER STATION
UNIT 3
FINAL SAFETY ANALYSIS REPORT



(n) NODE No. (1-LOOP MODEL)

FIGURE Q480.37-21
POSTULATED BREAK LOCATIONS
IN SG CUBICLE (WCAP-8082)
MILLSTONE NUCLEAR POWER STATION
UNIT 3
FINAL SAFETY ANALYSIS REPORT

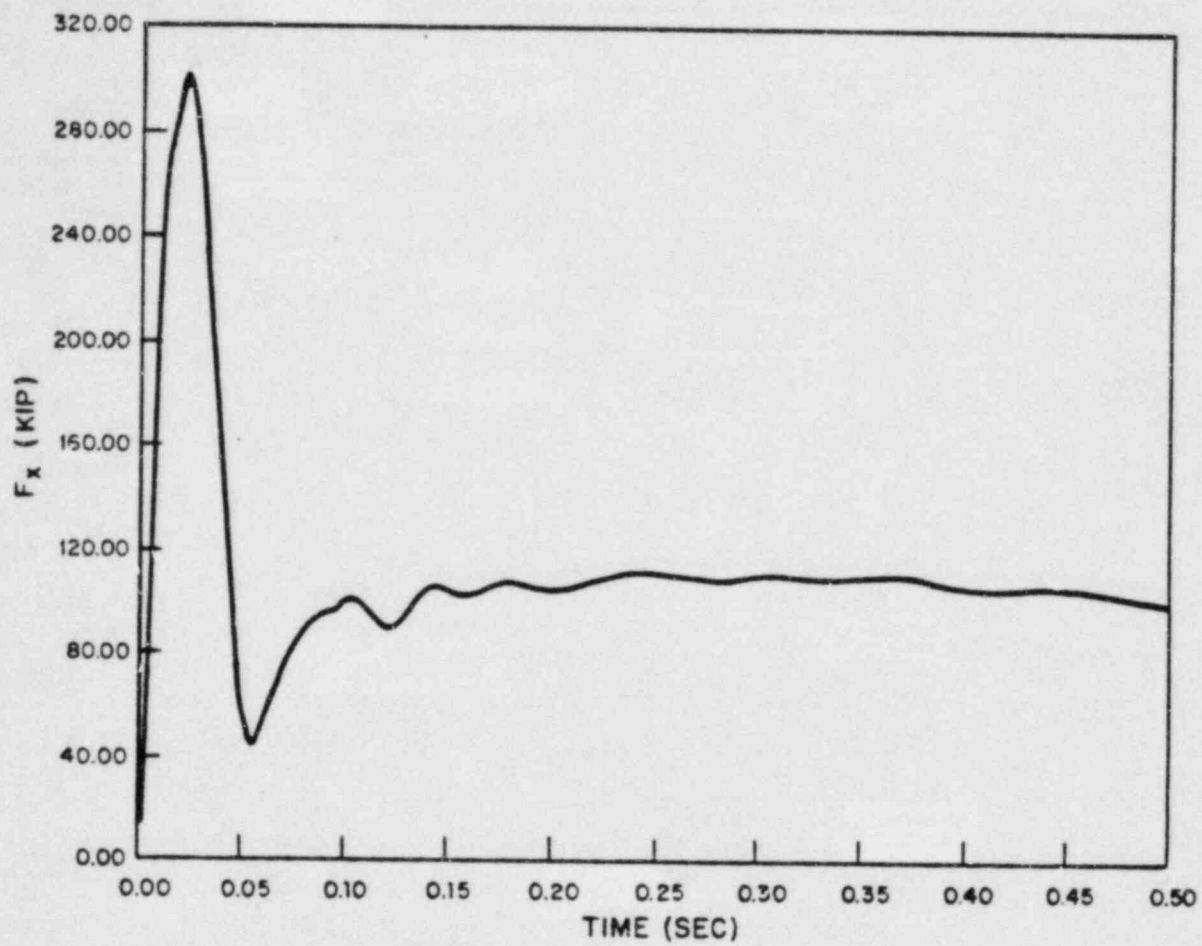


FIGURE Q480.37-22
NET FORCE IN GLOBAL X
DIRECTION ON SG - BREAK 7
MILLSTONE NUCLEAR POWER STATION
UNIT 3
FINAL SAFETY ANALYSIS REPORT

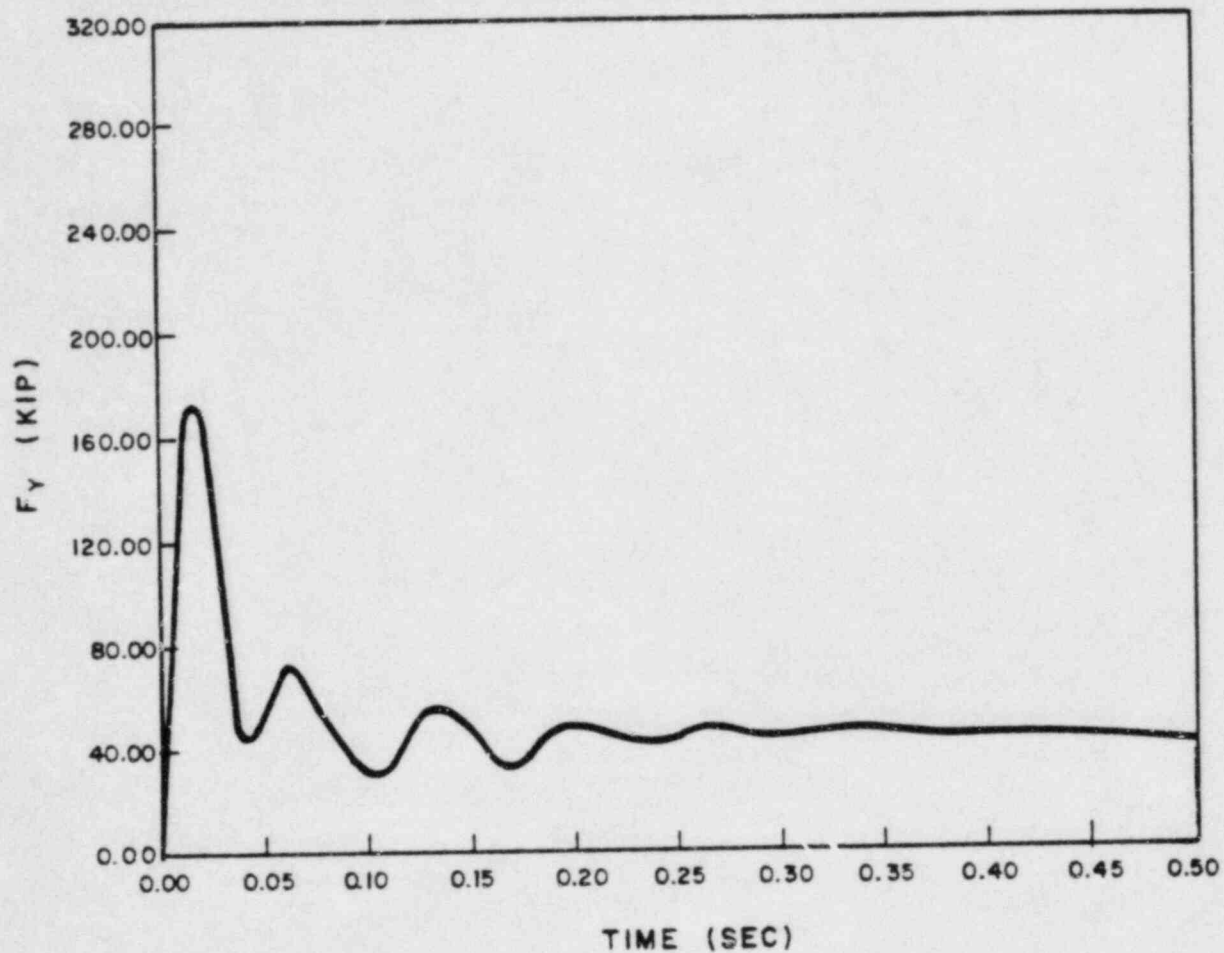


FIGURE Q480.37-23
NET FORCE IN GLOBAL Y
DIRECTION ON SG-BREAK 7
MILLSTONE NUCLEAR POWER STATION
UNIT 3
FINAL SAFETY ANALYSIS REPORT

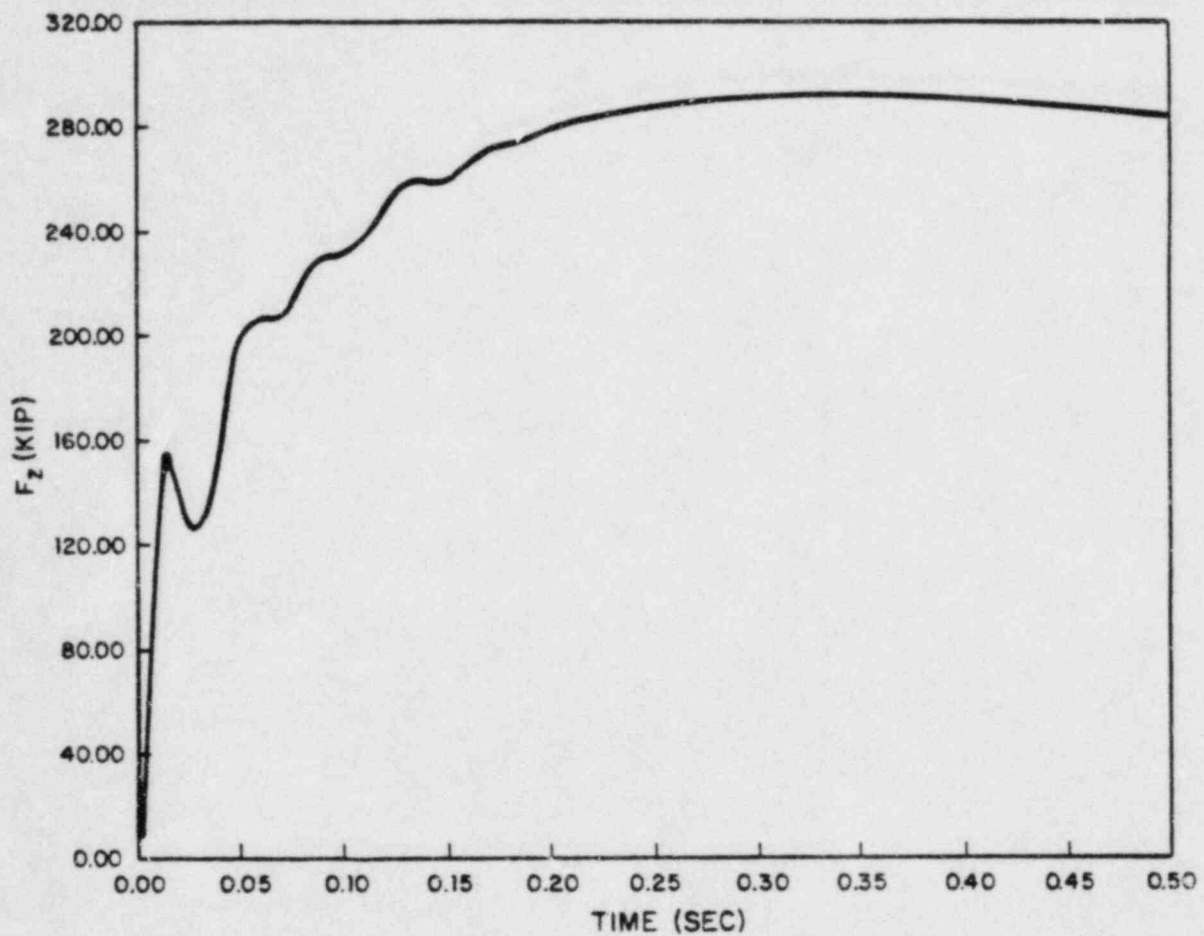


FIGURE Q480.37-24
NET FORCE IN GLOBAL Z
DIRECTION ON SG-BREAK 7
MILLSTONE NUCLEAR POWER STATION
UNIT 3
FINAL SAFETY ANALYSIS REPORT

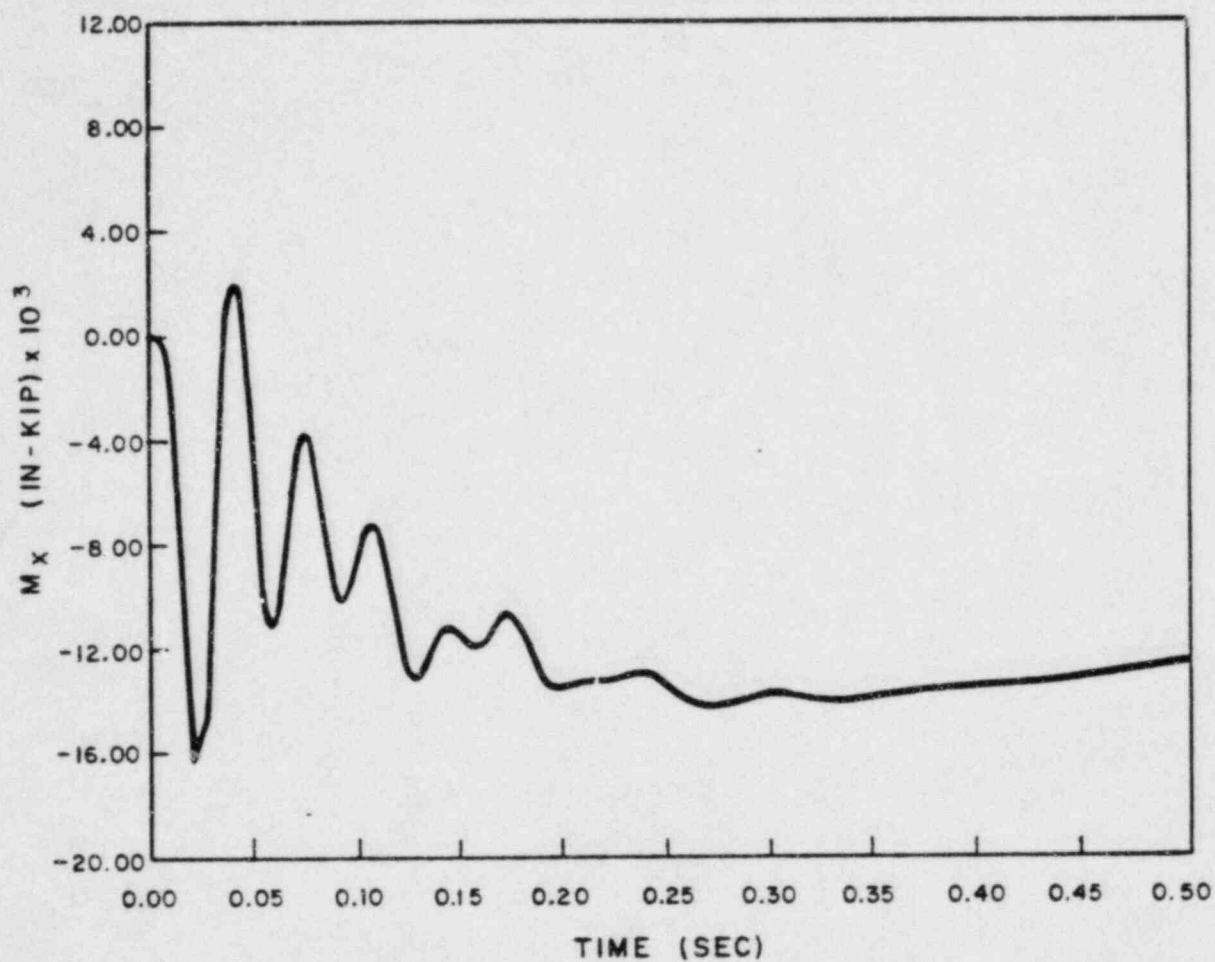


FIGURE Q480.37-25
NET MOMENT ABOUT GLOBAL X
AXIS AT SG NODE 12 - BREAK 7
MILLSTONE NUCLEAR POWER STATION
UNIT 3
FINAL SAFETY ANALYSIS REPORT

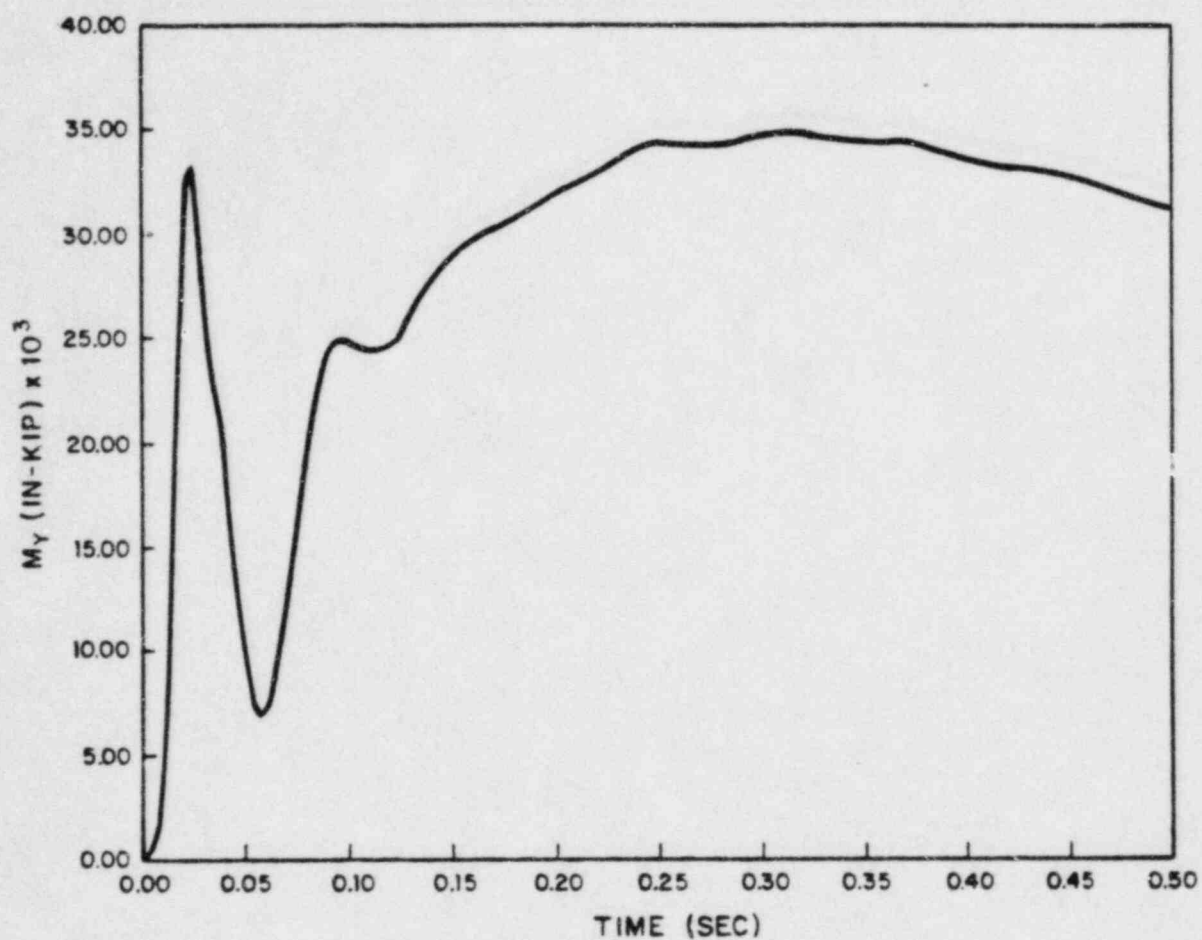


FIGURE Q480.37-26
NET MOMENT ABOUT GLOBAL Y
AXIS AT SG NODE 12-BREAK 7
MILLSTONE NUCLEAR POWER STATION
UNIT 3
FINAL SAFETY ANALYSIS REPORT

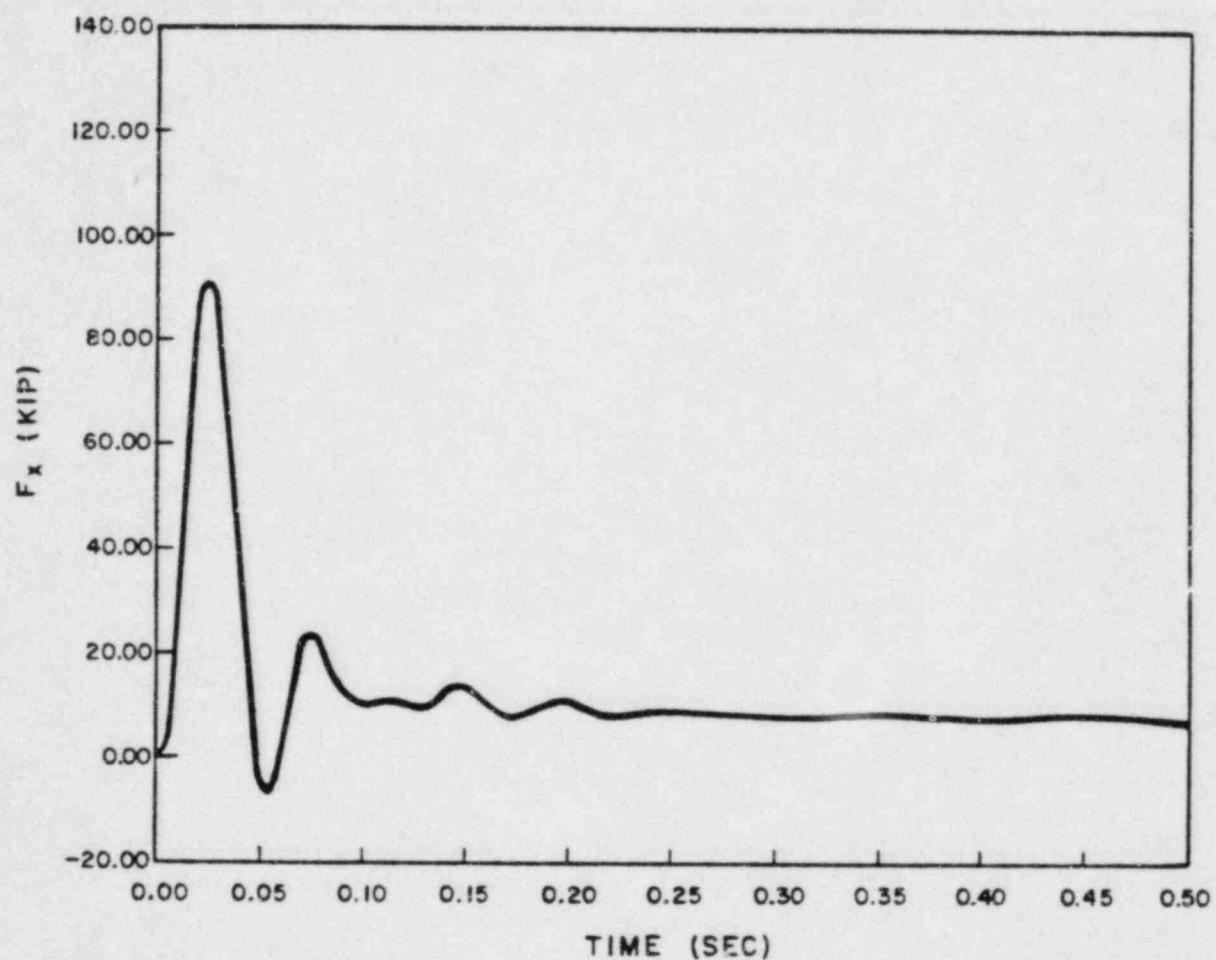


FIGURE Q480.37-27
NET FORCE IN GLOBAL X
DIRECTION ON RCP - BREAK 7
MILLSTONE NUCLEAR POWER STATION
UNIT 3
FINAL SAFETY ANALYSIS REPORT

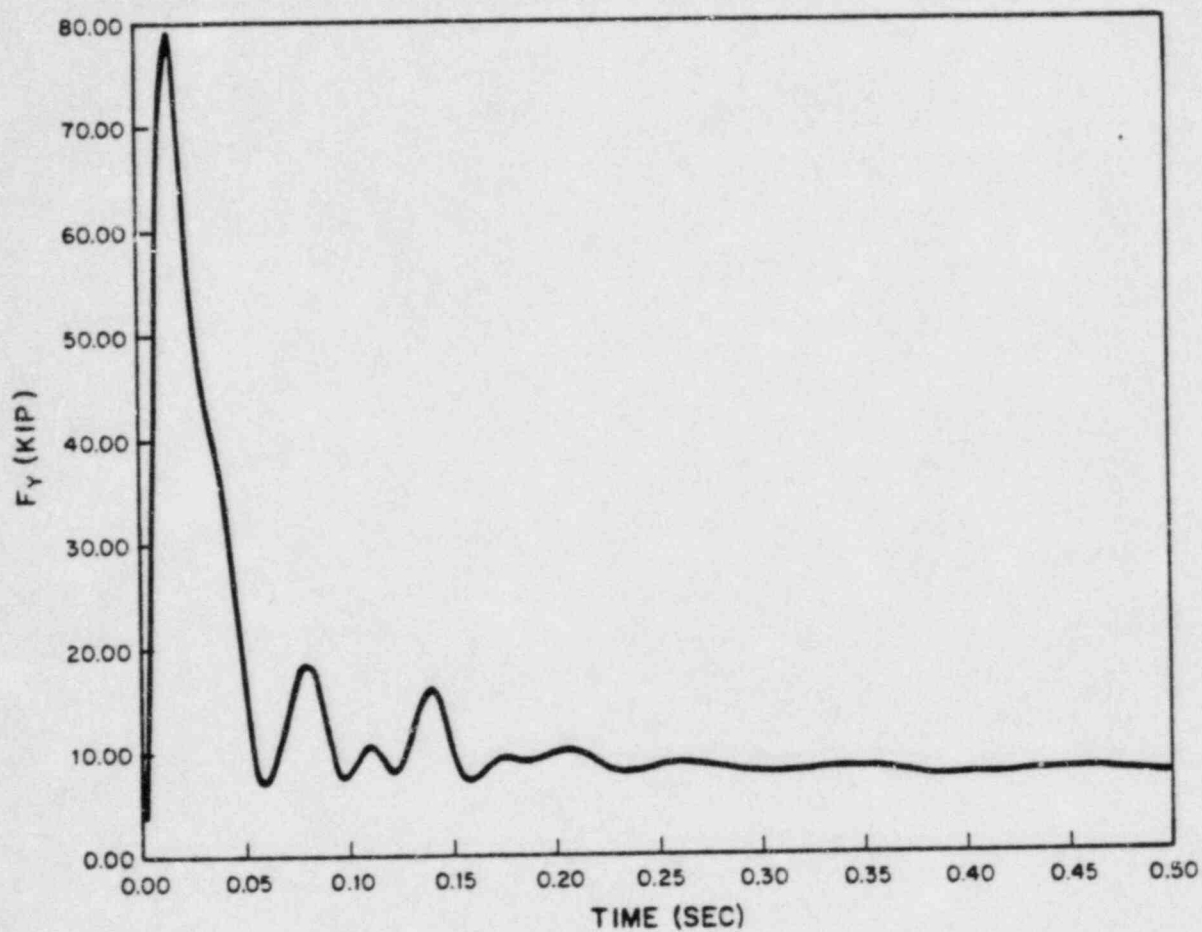


FIGURE Q480.37-28
NET FORCE IN GLOBAL Y
DIRECTION ON RCP-BREAK 7
MILLSTONE NUCLEAR POWER STATION
UNIT 3
FINAL SAFETY ANALYSIS REPORT

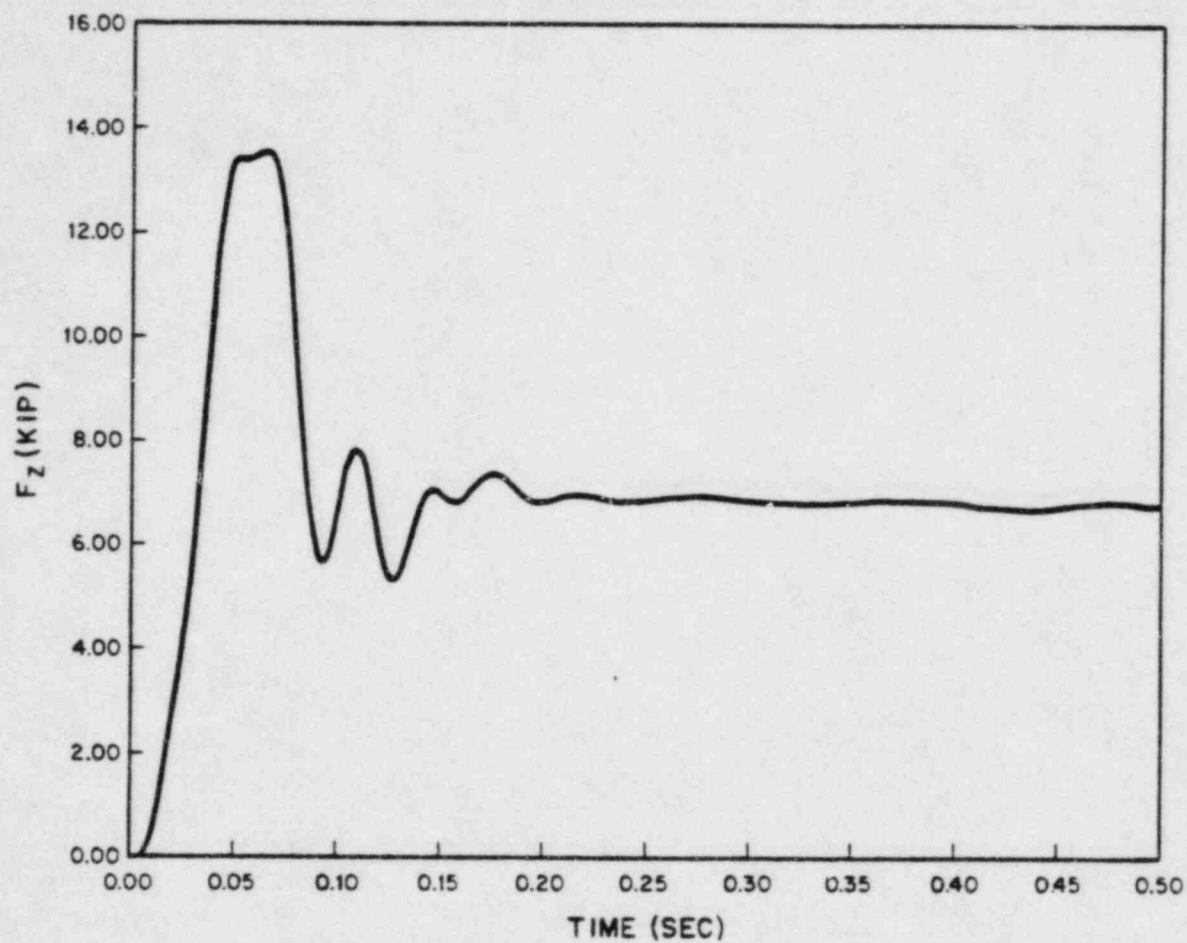


FIGURE Q480.37 - 29
NET FORCE IN GLOBAL Z
DIRECTION ON RCP - BREAK 7
MILLSTONE NUCLEAR POWER STATION
UNIT 3
FINAL SAFETY ANALYSIS REPORT

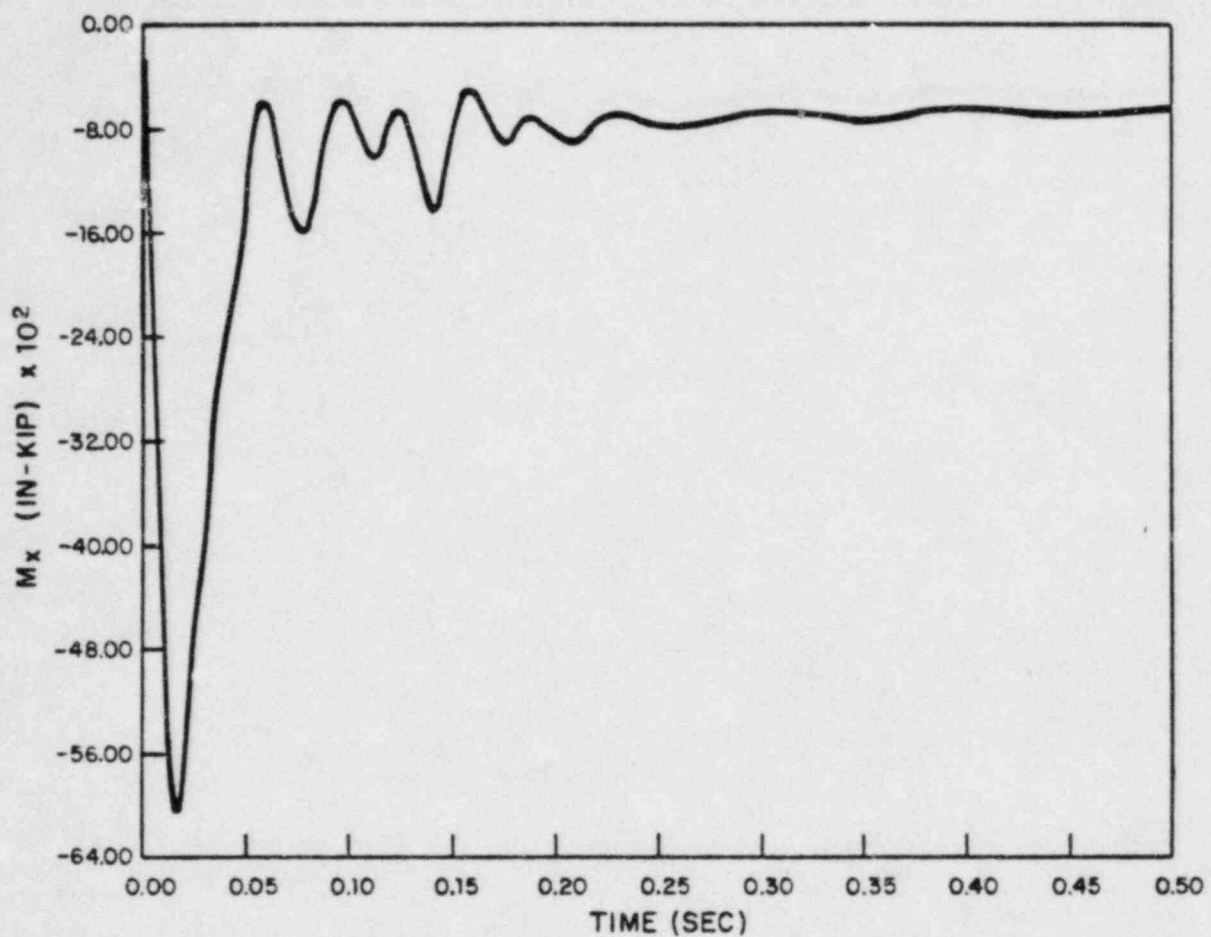


FIGURE Q480.37-30
NET MOMENT ABOUT GLOBAL X
AXIS AT RCP NODE 24- BREAK 7
MILLSTONE NUCLEAR POWER STATION
UNIT 3
FINAL SAFETY ANALYSIS REPORT

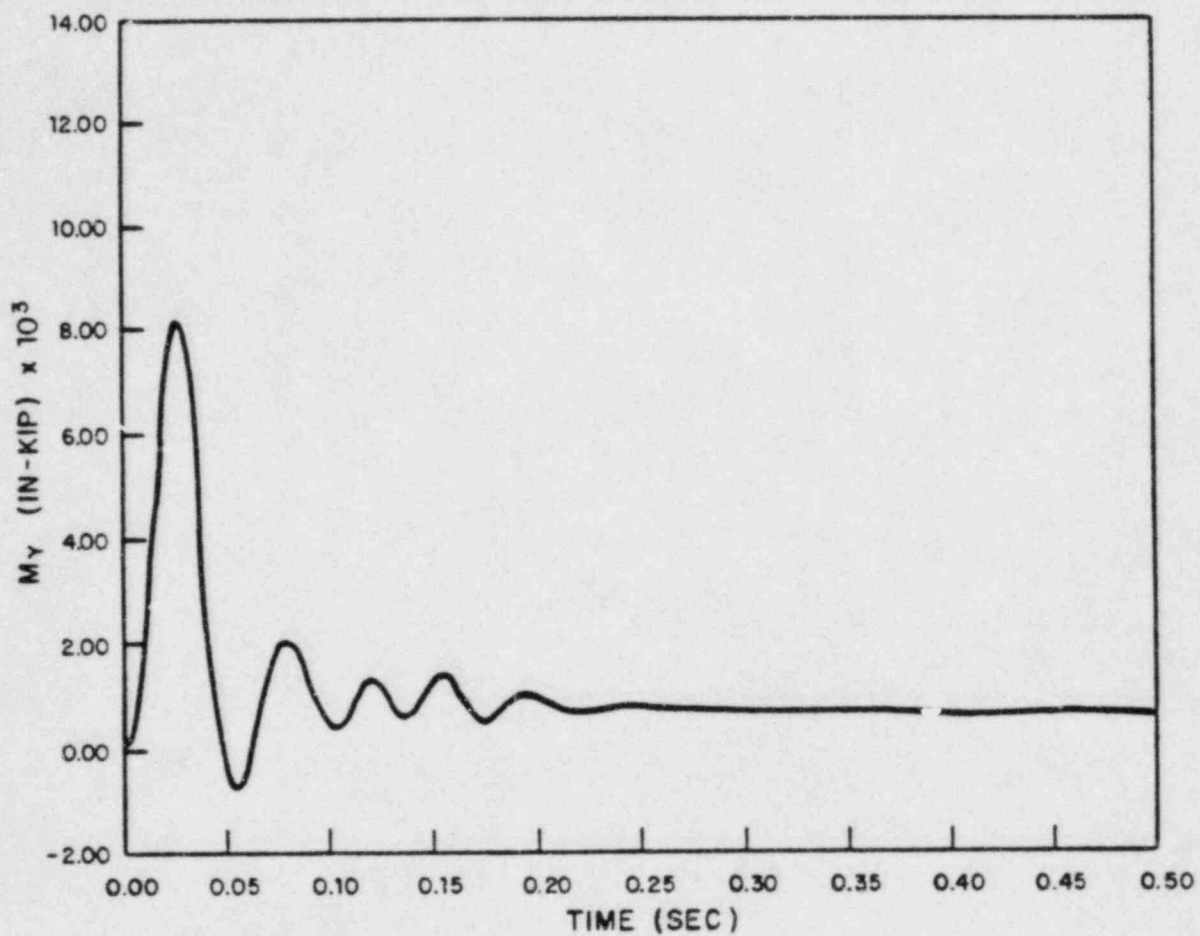


FIGURE Q480.37-31
NET MOMENT ABOUT GLOBAL Y
AXIS AT RCP NODE 24-BREAK 7
MILLSTONE NUCLEAR POWER STATION
UNIT 3
FINAL SAFETY ANALYSIS REPORT

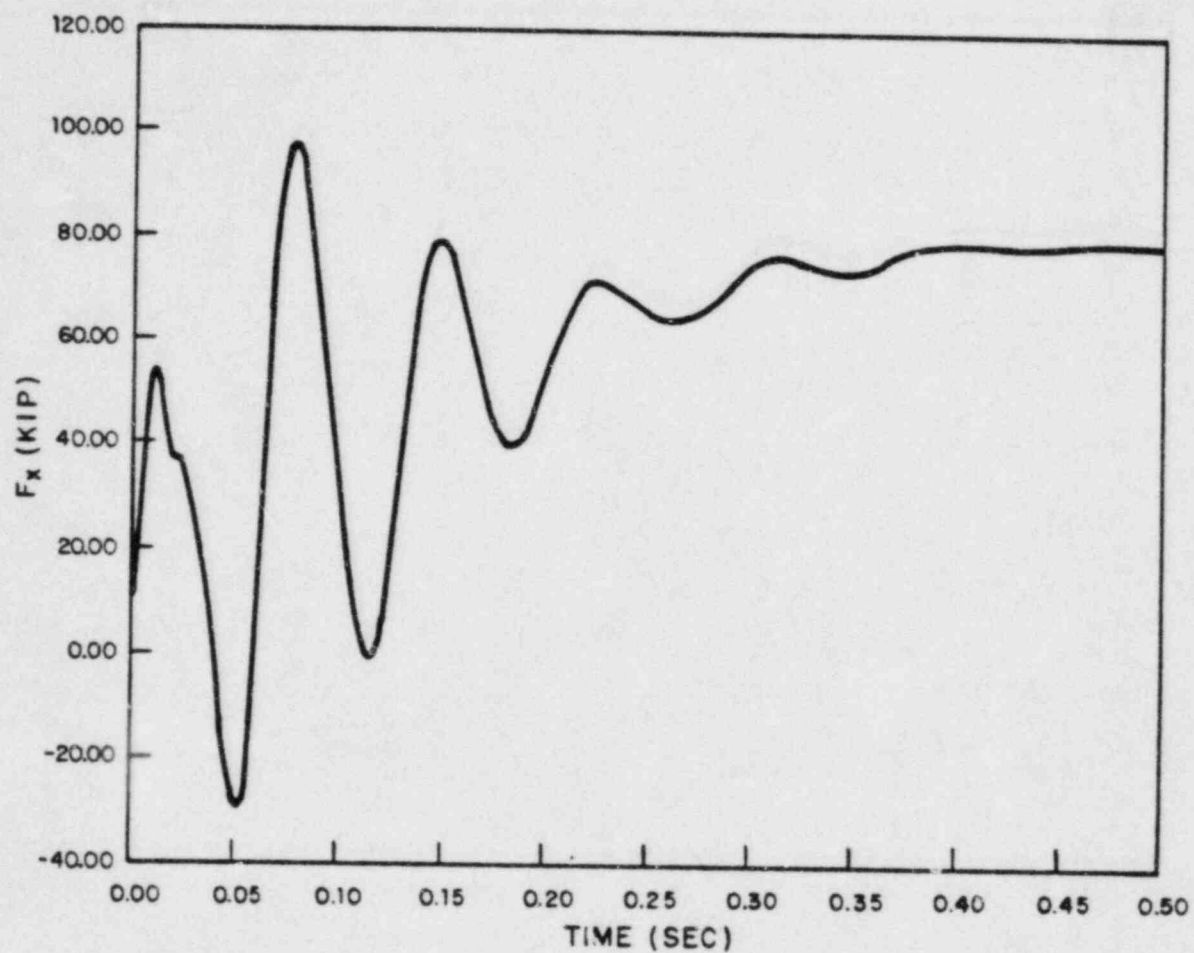


FIGURE Q480.37-32
NET FORCE IN GLOBAL X
DIRECTION ON SG - BREAK 4
MILLSTONE NUCLEAR POWER STATION
UNIT 3
FINAL SAFETY ANALYSIS REPORT

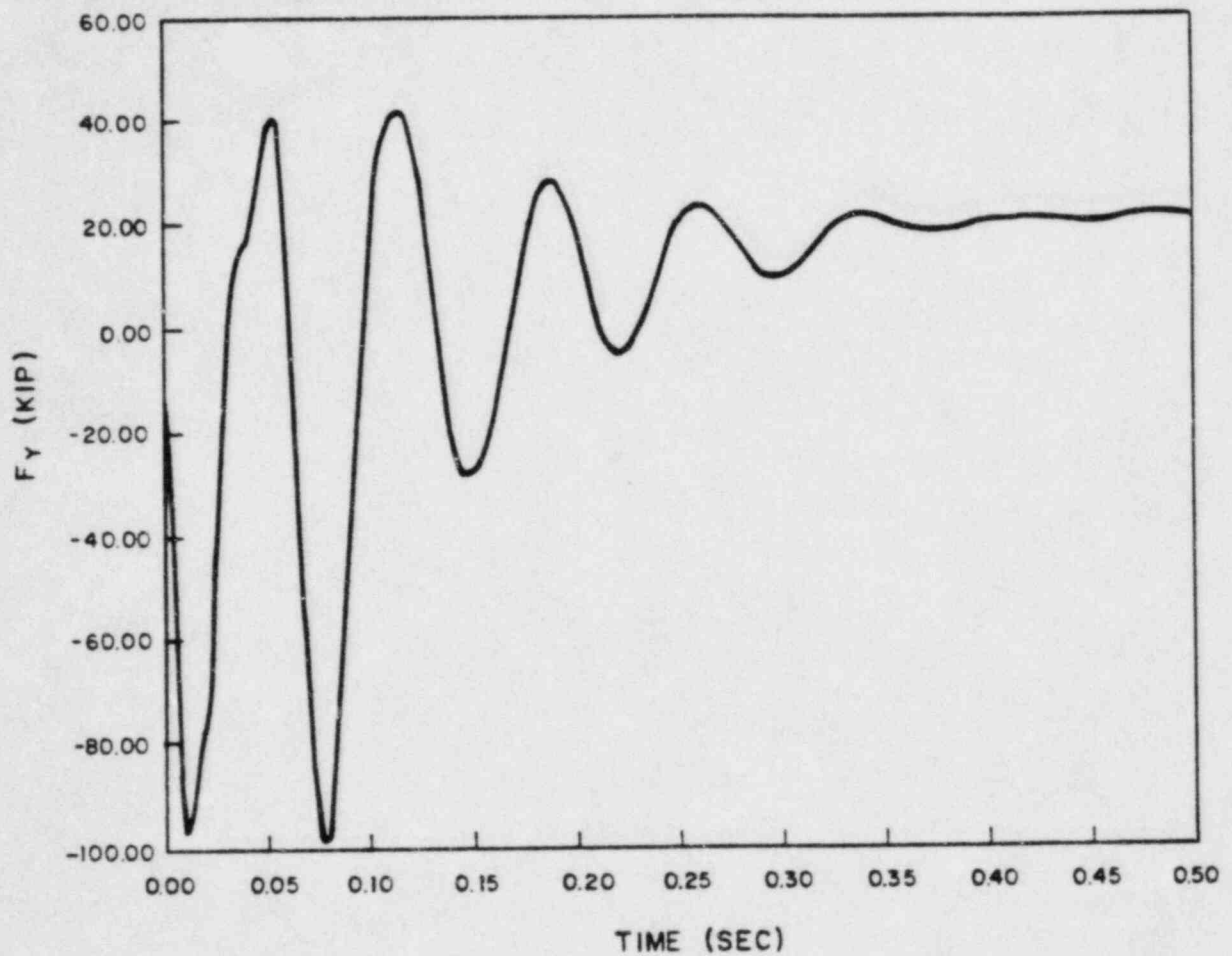


FIGURE Q480.37-33
NET FORCE IN GLOBAL Y
DIRECTION ON SG - BREAK 4
MILLSTONE NUCLEAR POWER STATION
UNIT 3
FINAL SAFETY ANALYSIS REPORT

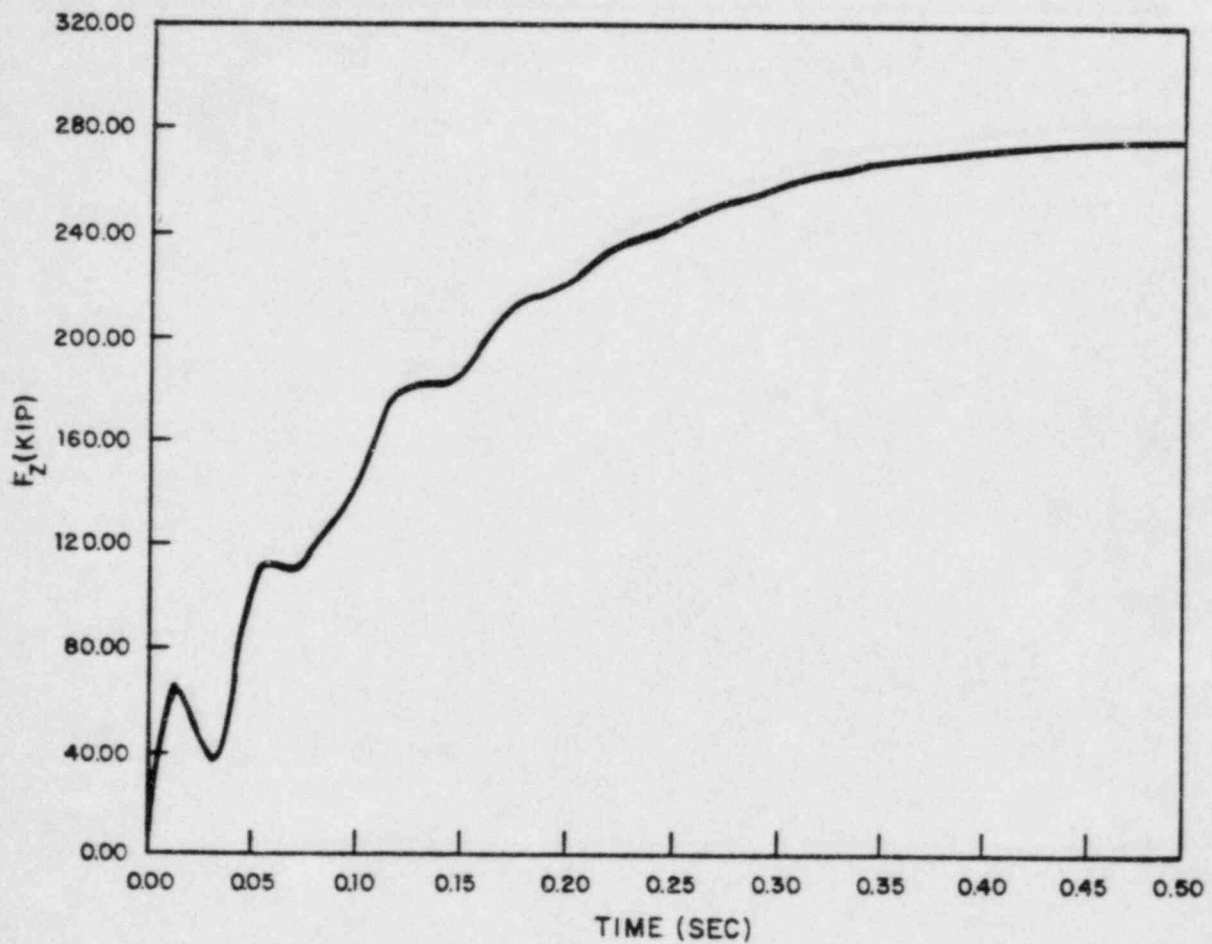


FIGURE Q480.37-34
NET FORCE IN GLOBAL Z
DIRECTION ON SG-BREAK 4
MILLSTONE NUCLEAR POWER STATION
UNIT 3
FINAL SAFETY ANALYSIS REPORT

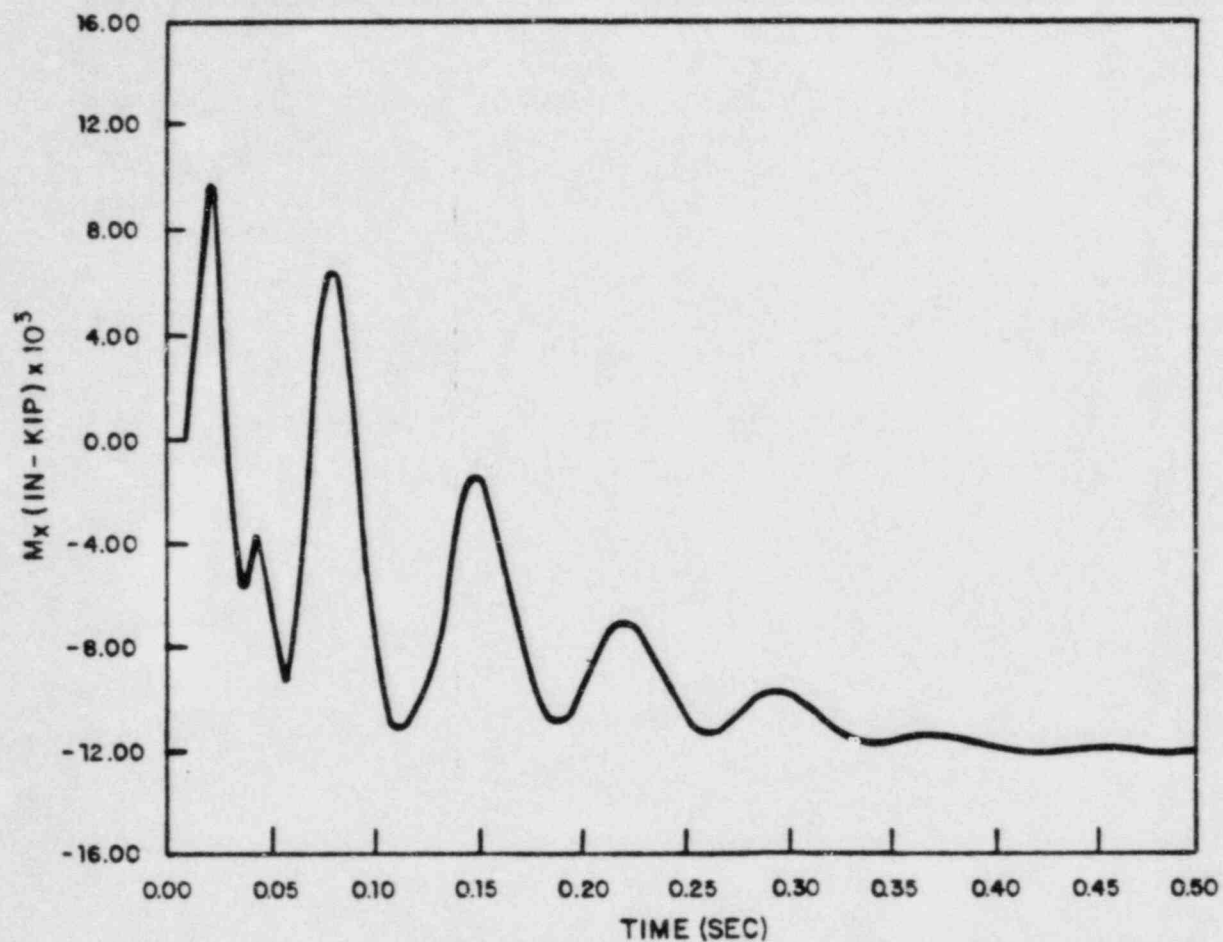


FIGURE Q480.37-35
NET MOMENT ABOUT GLOBAL X
AXIS AT SG NODE 12 - BREAK 4
MILLSTONE NUCLEAR POWER STATION
UNIT 3
FINAL SAFETY ANALYSIS REPORT

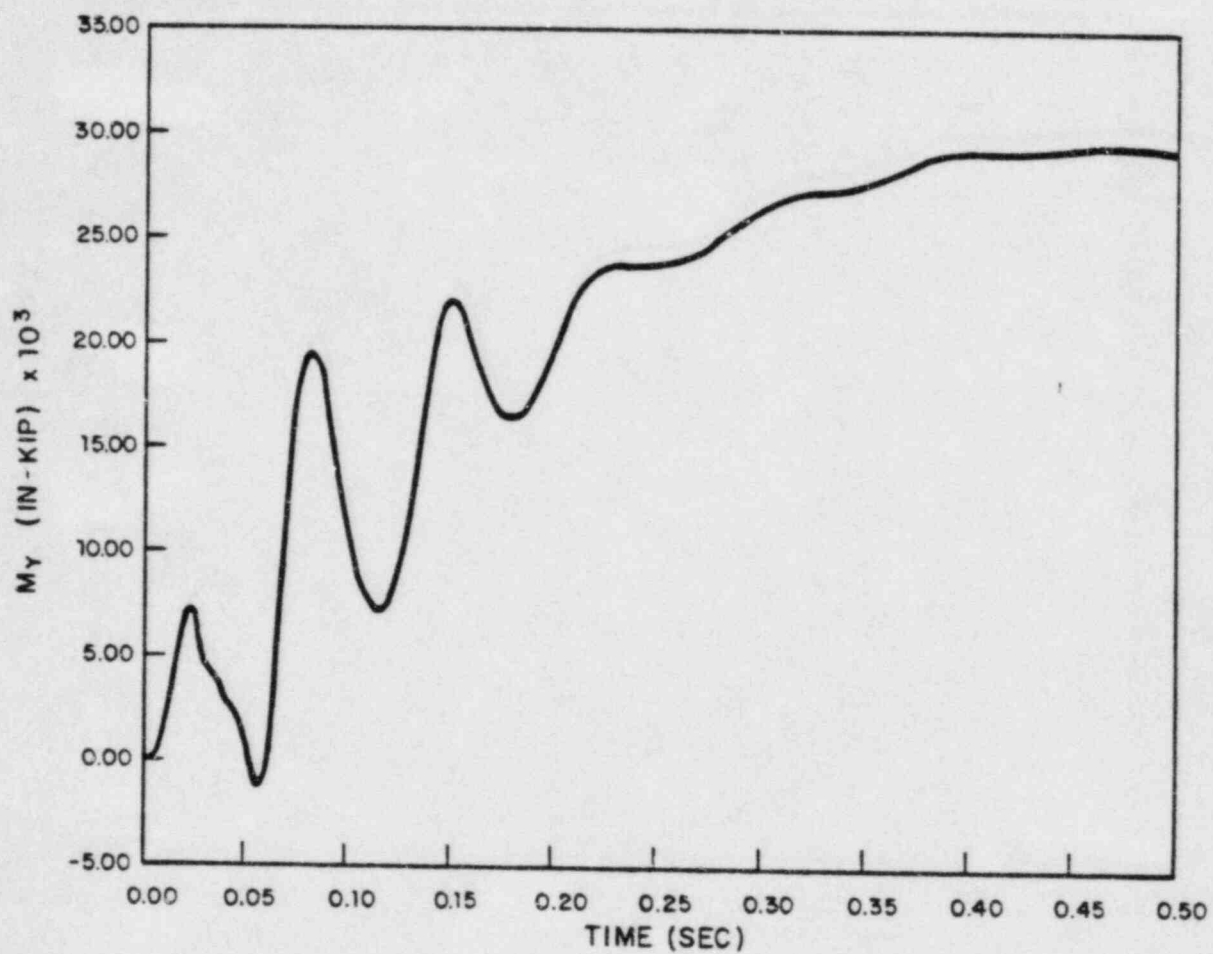


FIGURE Q480.37-36
NET MOMENT ABOUT GLOBAL Y
AXIS AT SG NODE 12-BREAK 4
MILLSTONE NUCLEAR POWER STATION
UNIT 3
FINAL SAFETY ANALYSIS REPORT

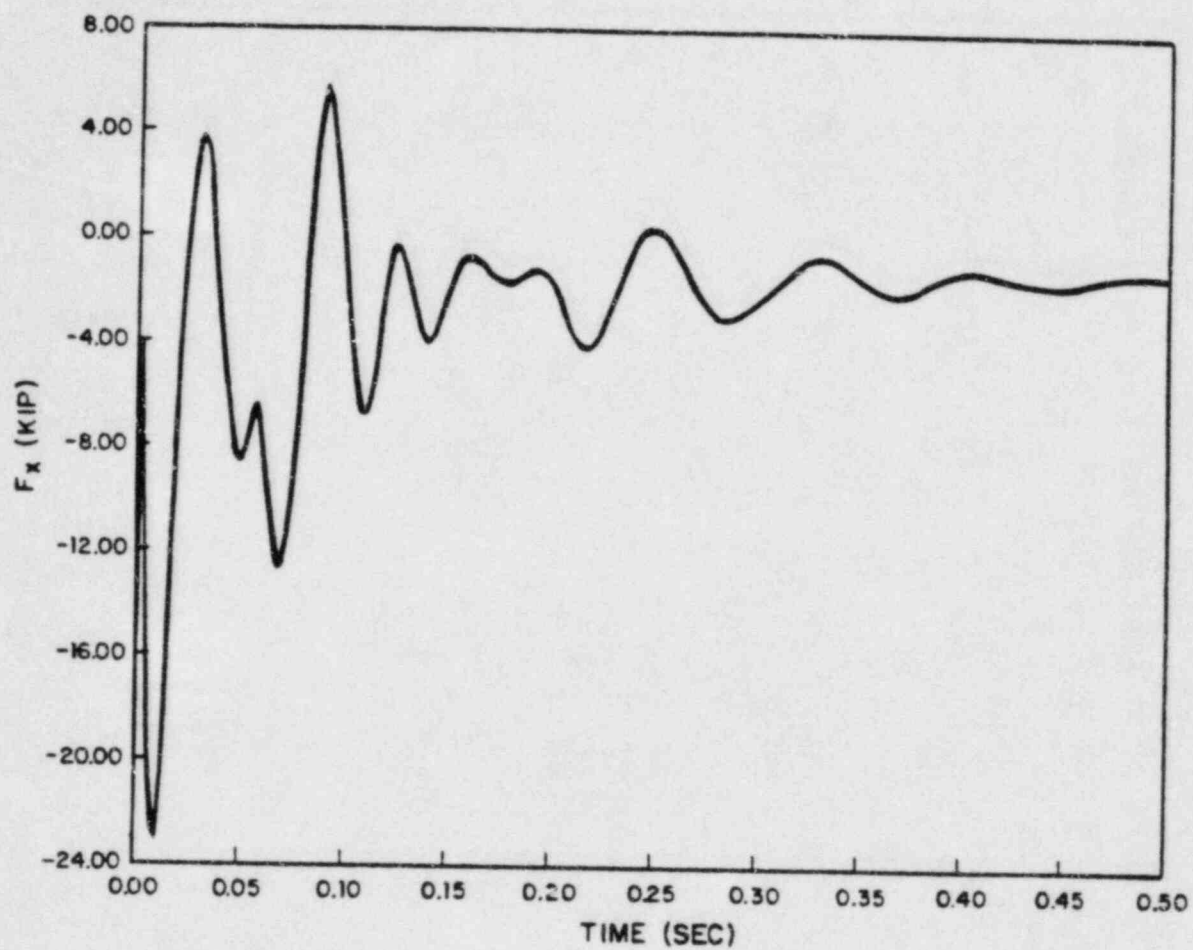


FIGURE Q480.37-37
NET FORCE IN GLOBAL X
DIRECTION ON RCP - BREAK 4
MILLSTONE NUCLEAR POWER STATION
UNIT 3
FINAL SAFETY ANALYSIS REPORT

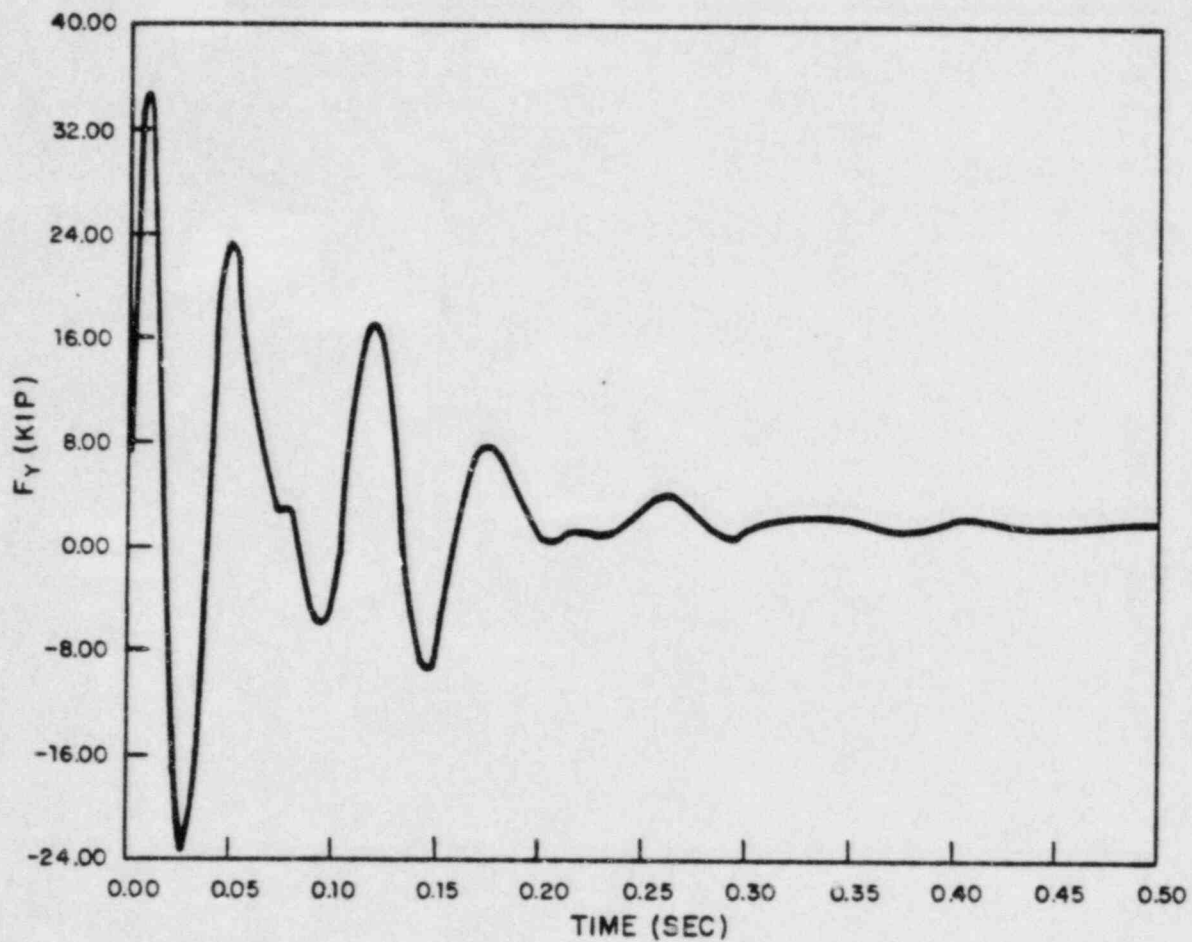


FIGURE Q480.37-38
NET FORCE IN GLOBAL Y
DIRECTION ON RCP-BREAK 4
MILLSTONE NUCLEAR POWER STATION
UNIT 3
FINAL SAFETY ANALYSIS REPORT

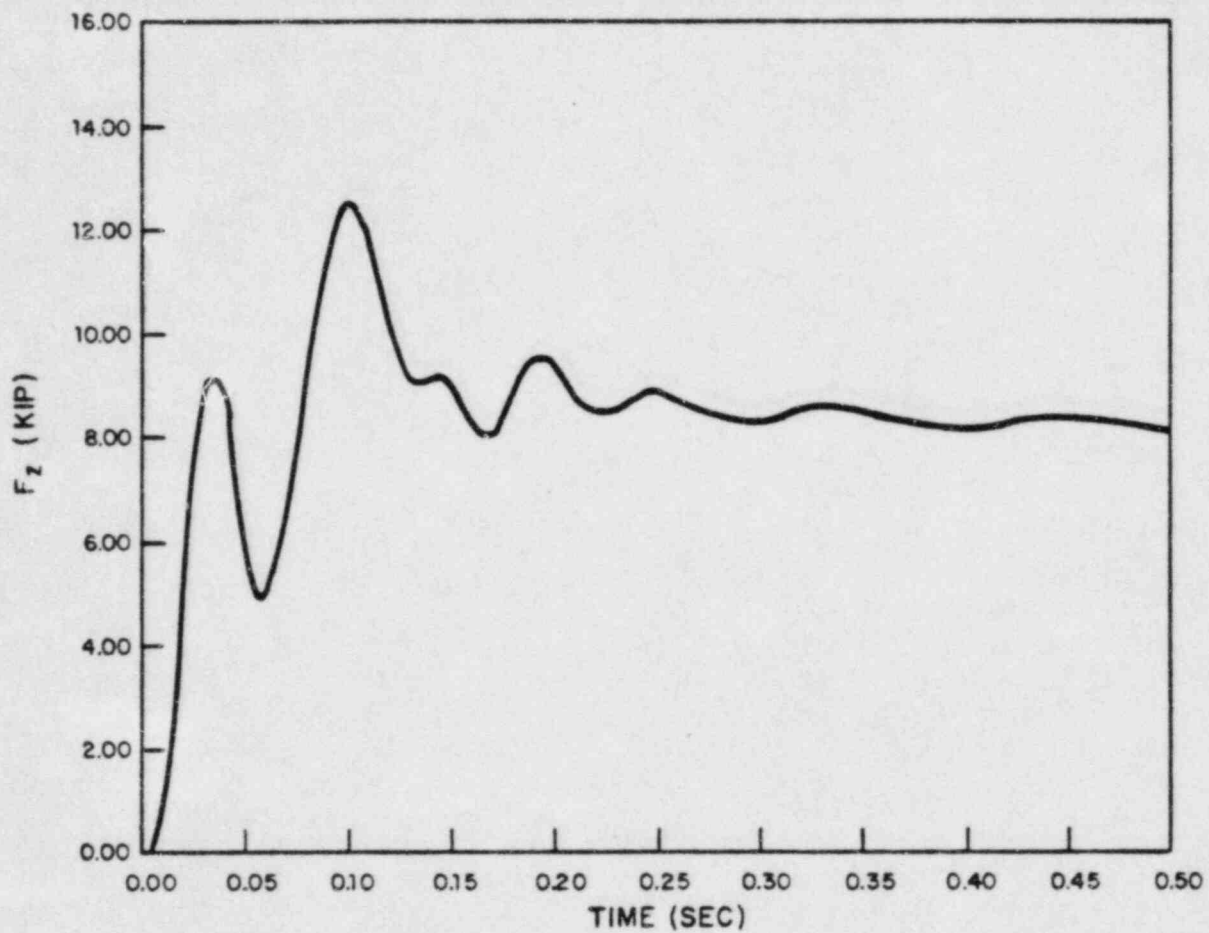


FIGURE Q480.37-39
NET FORCE IN GLOBAL Z
DIRECTION ON RCP-BREAK 4
MILLSTONE NUCLEAR POWER STATION
UNIT 3
FINAL SAFETY ANALYSIS REPORT

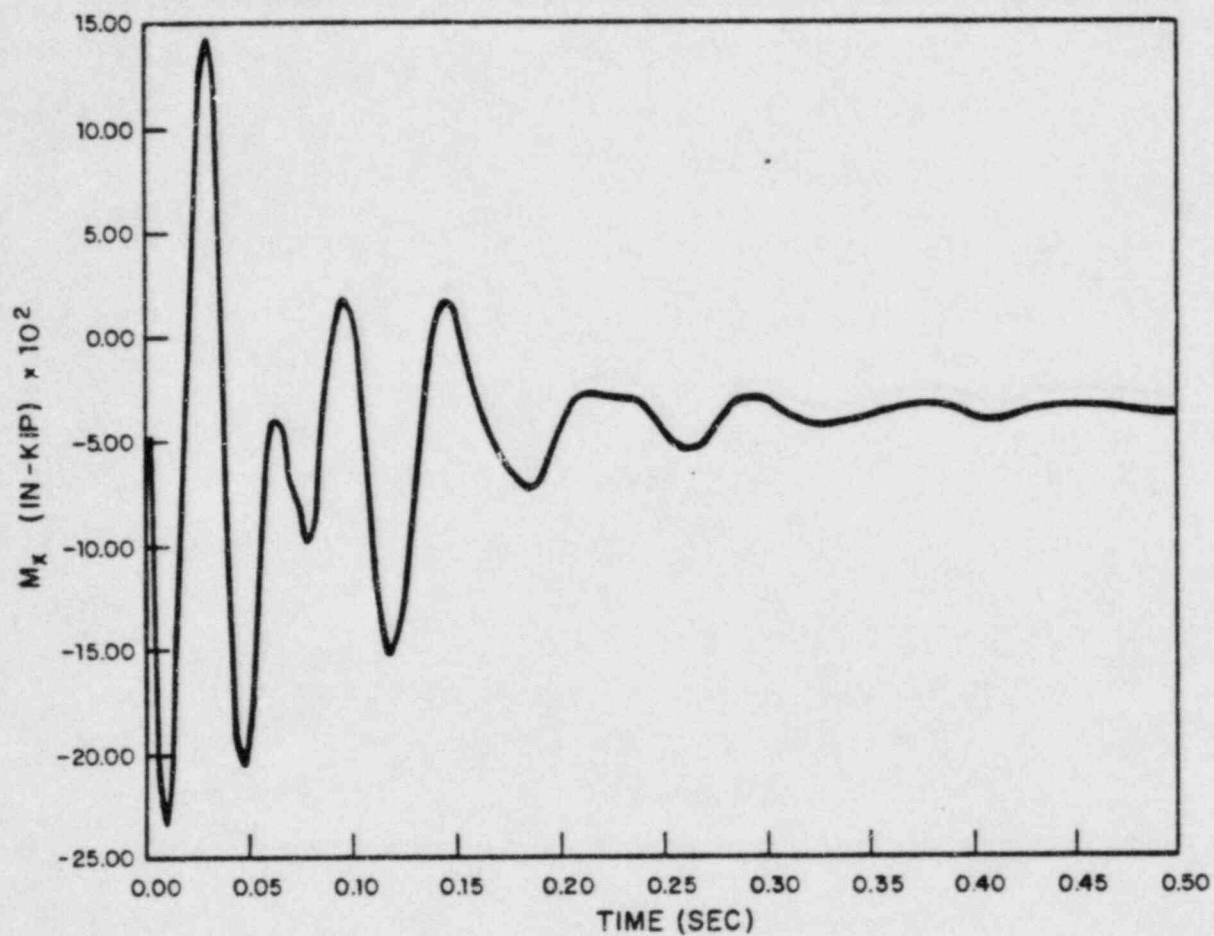


FIGURE Q480.37-40
NET MOMENT ABOUT GLOBAL X
AXIS AT RCP NODE 24-BREAK 4
MILLSTONE NUCLEAR POWER STATION
UNIT 3
FINAL SAFETY ANALYSIS REPORT

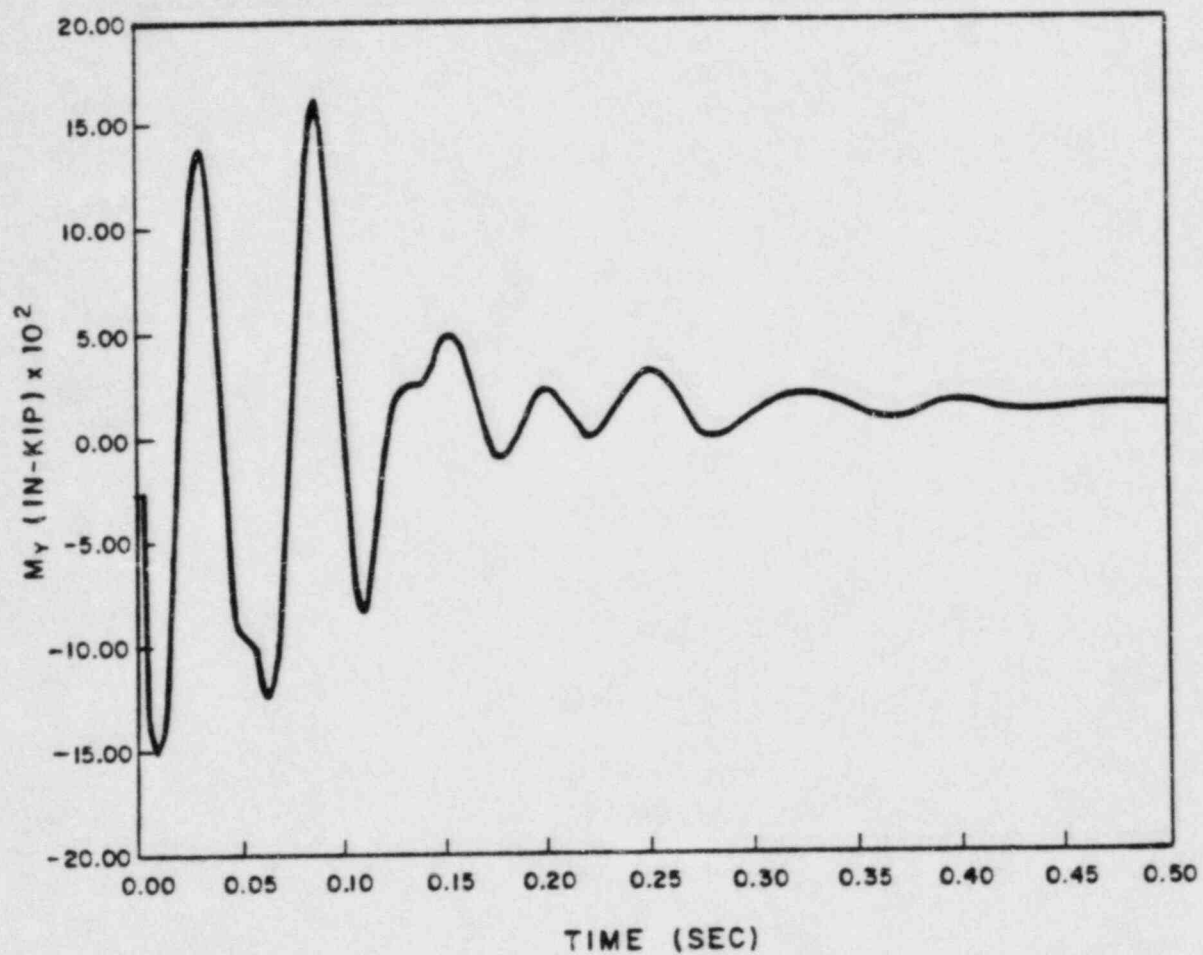


FIGURE Q480.37-41
NET MOMENT ABOUT GLOBAL Y
AXIS AT RCP NODE 24-BREAK 4
MILLSTONE NUCLEAR POWER STATION
UNIT 3
FINAL SAFETY ANALYSIS REPORT

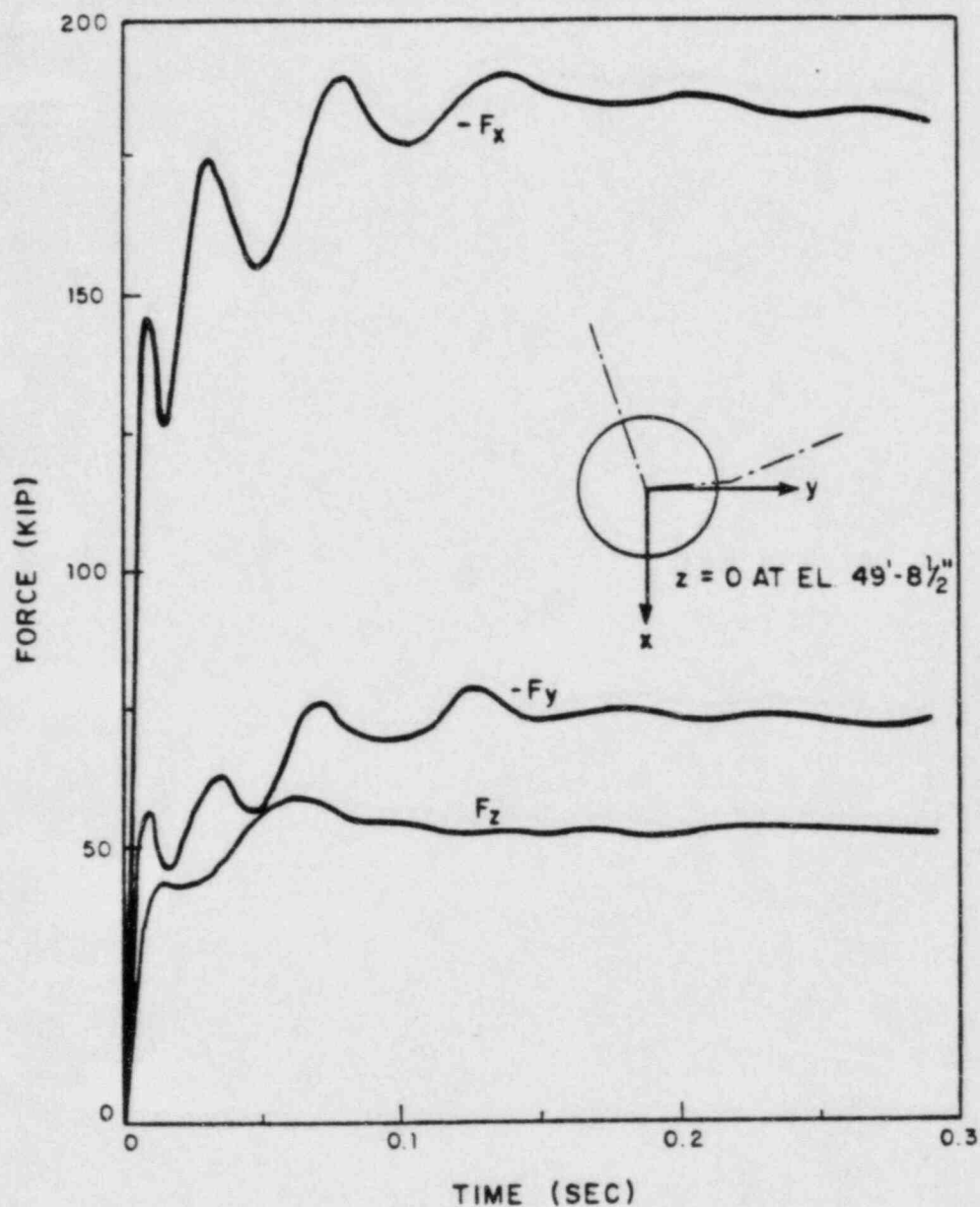


FIGURE Q480.37-42
 NET FORCES ON SG-FEEDWATER
 LINE BREAK (CUBICLE B)
 MILLSTONE NUCLEAR POWER STATION
 UNIT 3
 FINAL SAFETY ANALYSIS REPORT

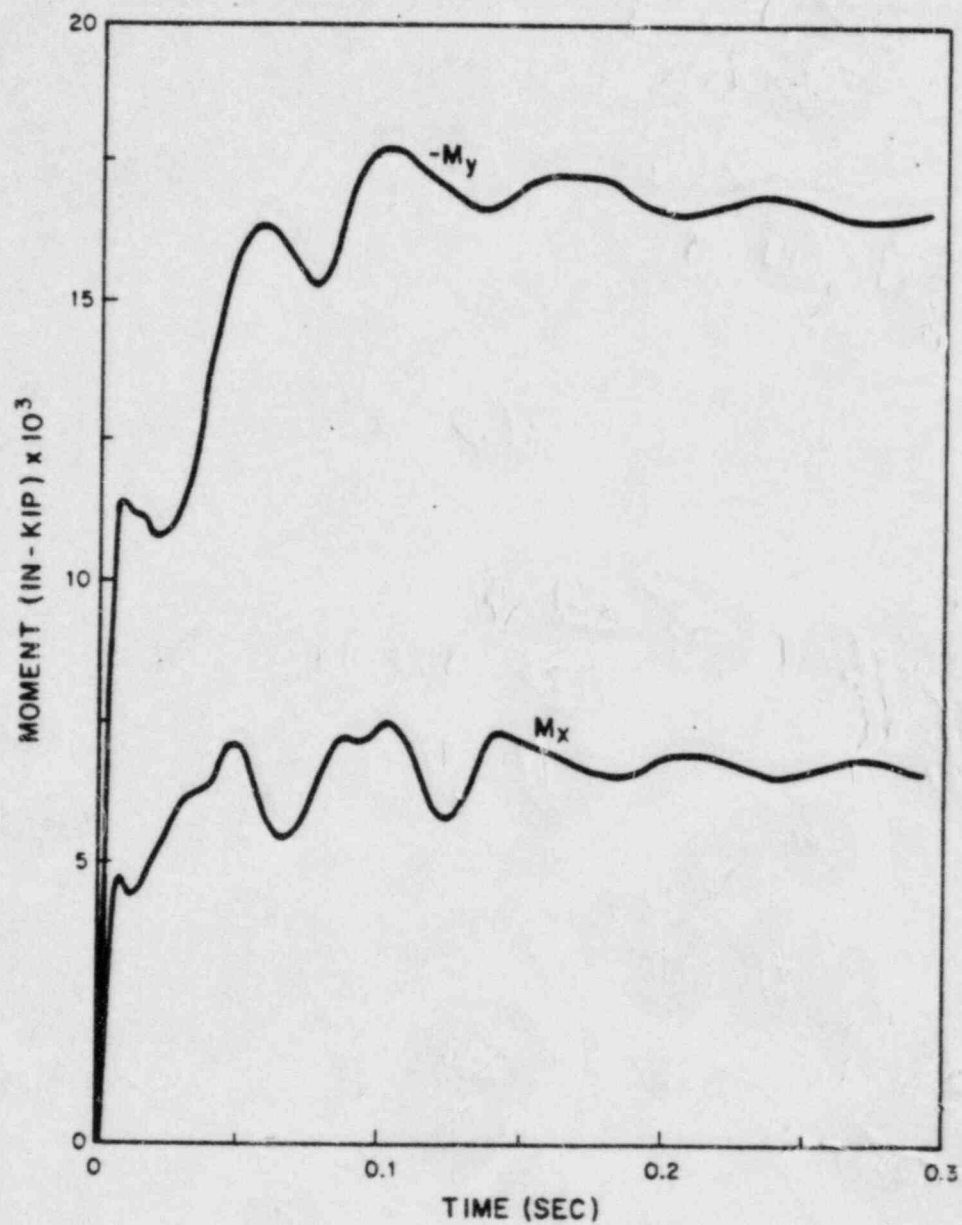


FIGURE Q480.37-43
NET MOMENTS ON SG-
FEEDWATER LINE BREAK
MILLSTONE NUCLEAR POWER STATION
UNIT 3
FINAL SAFETY ANALYSIS REPORT

336°F. For this accident, the peak calculated containment liner is 1.10
236.3°F. The liner temperature shown is the inside surface 1.11
temperature.

The qualification of safety related equipment inside the containment 1.12
to the pressure and temperature resulting from a steam line break is 1.13
discussed in Section 3.11.

A chronology of events for the limiting containment pressure and 1.14
temperature cases is given in Tables 6.2-24 and 6.2-25, respectively. 1.15

6.2.1.1.3.8 Feedwater Pipe Break Results 1.17

The feedwater pipe break is not as severe as the main steam pipe 1.18
break, since the break effluent is at a lower specific enthalpy. The 1.21
feedwater pipe break analysis is, therefore, not analyzed.

6.2.1.2 Containment Subcompartments 1.24

6.2.1.2.1 Design Basis 1.25

The containment subcompartments are designed in accordance with 1.26
General Design Criteria 4 and 50.

Break locations and types (Section 3.6.2) are chosen as follows for 1.28
the various subcompartments:

1. Upper pressurizer cubicle - Spray line doubled ended rupture 1.30
(DER) in the upper pressurizer cubicle is the largest break 1.31
that can occur in the upper pressurizer cubicle.
Section 6.2.1.2.3 describes the break types. 1.32

2. Lower pressurizer cubicle - Surge line DER in the lower 1.33
pressurizer cubicle. This is the largest break which can 1.34
occur within the pressurizer cubicle.

3. Lower steam generator subcompartments - Reactor coolant 1.35
system (RCS) 707 sq in. hot leg intrados split break in the 1.36
lower steam generator subcompartment. This is the largest 1.37
area break which can occur in the steam generator
subcompartment.

4. Upper steam generator subcompartments - A feedwater line 1.38
DER. 480.37

5. Upper reactor cavity - RCS 100 sq in. cold leg limited 1.39
displacement break inside the upper reactor cavity. This 1.40
break area exceeds the maximum which can occur inside the
upper reactor cavity.

Additional smaller breaks used for the major component support 1.42
evaluation are identified in the discussion of the results in 1.43
Section 6.2.1.2.3. 480.37

A full power condition with hot leg equal to 616.4°F and cold leg equal to 555.9°F yields the maximum mass and energy release rates. 1.44
1.45

The RCS mass and energy release rates are computed by SATAN V Program (Section 6.2.1.5.1). For subcompartment analysis, 110 percent of the SATAN V mass and energy release rates is used. 1.46
1.47

The initial containment conditions selected to maximize the resultant differential pressure within the subcompartments are: 1.48
1.49

1. Maximum temperature 120°F 1.51
2. Minimum air partial pressure 9.00 psia 1.52
3. Minimum relative humidity 50 percent 1.53 | 10

Subcompartment nodalization schemes are chosen to provide a conservative load and moment on a given component and structure. All vent flow paths used in the analysis are unobstructed by moveable objects throughout the transient. These flow path areas are conservatively calculated. Nominal reductions to the net vent areas are typically made to account for building tolerances and blockages that may occur from insulation displaced from the ruptured pipe. Insulation and associated materials are the only moveable obstructions to flow. Vent areas in the steam generator and pressurizer subcompartments are relatively large, and accordingly, the likelihood of significant blockage by displaced insulation is remote. Vent areas local to the break location in the upper reactor cavity subcompartment are, in general, significantly smaller than in other subcompartments and are, therefore, more susceptible to blockage. According to the Subcompartment Analysis Procedures (Gido 1979), it is conservative to assume blockage of some vent areas local to the break. However, it is unlikely that the blockage will sustain itself because the high local pressures would immediately dislodge the debris. 1.55
1.57
1.58
1.59
1.60
2.1
2.2
2.3 480.37
2.4
2.6
2.7
2.8
2.9
2.10

The flows through all flow paths with the nodalized subcompartment model are based on a homogeneous mixture in thermal equilibrium with the assumption of 100 percent liquid carryover (Section 6.2.1.2.3.3). 2.11
2.12

The subcompartment design differential pressure is equal to or greater than the calculated differential pressure in that subcompartment (Table 6.2-26). Multinode schemes providing a conservative load and moment on a given component and structure are considered in the subcompartment design. 2.13
2.14
2.15
2.16

6.2.1.2.2 Design Features 2.18

Figures 3.8-59 and 3.8-60 provide detailed plan and section drawings of the containment subcompartments. They show the arrangement of structures and components within the containment. Views of the subcompartment are shown on Figures 6.2-17 and 6.2-18, 6.2-19 through 6.2-22, and 6.2-23 for the upper and lower pressurizer cubicle, the most limiting steam generator subcompartment, and the upper reactor 2.19 | 10
2.21
2.22
2.25 | 10

cavity. Schematic nodalization models of the upper and lower
 pressurizer cubicle, the most limiting steam generator
 subcompartment, and the upper reactor cavity are given on
 Figures 6.2-24, 6.2-25, and 6.2-23, respectively. The corresponding
 subcompartment vent path and nodal descriptions are given in
 Tables 6.2-27 through 6.2-30.

6.2.1.2.3 Design Evaluation 2.30

Conditions considered in the subcompartment analyses are the
 development of pressure gradients across the walls, major equipment,
 and supports. The resulting asymmetric pressures are used to
 calculate loads and moments applied to the equipment and its
 supports. The maximum differential pressure across the walls is used
 as the design basis for the subcompartment structures.

The volume of the subcompartment is divided into a series of nodes
 with as many connecting vents as there are significant flow
 resistances. A model that provides a conservative load and moment on
 the given component and structure is used.

Break Type Definitions and Areas 2.41

Two types of breaks are used to analyze containment subcompartments.
 The first is a guillotine break. A guillotine break, which results
 in a break flow area of two pipe cross sections, is called a double-
 ended rupture (DER). In some subcompartments, pipe restraints limit
 the displacement of the two broken ends of the pipe so that the break
 flow area is less than two pipe cross-sectional areas. This type
 break is called a limited displacement rupture (LDR). The special
 case of a LDR of one pipe cross-sectional area is called a single
 ended rupture (SER).

The second type of break is a longitudinal split which is equivalent
 to a hole in the wall of the pipe. A split which results in a break
 flow area of one pipe cross section is called a single ended split
 (SES).

The containment subcompartment analysis results describe all breaks
 analyzed within a particular subcompartment. Pipe restraints are
 provided to limit the break areas to those analyzed. Break areas are
 determined by the NSSS vendor.

A DER is considered in the analyses for the pressurizer cubicle and
 upper steam generator subcompartment. Breaks with less than two
 cross-sectional flow areas are used in the analysis for the reactor
 cavity and steam generator subcompartment. The analytical model used
 for predicting the mass and energy release rates for the primary
 coolant system breaks is given in WCAP-8264-P-A (1975) and
 WCAP-8312-A, Revision 2 (1975).

The mass and energy releases for the feedwater line full DER
 (Table 6.2-36A) were determined by a manual calculation using the
 frictionless Moody correlation for a saturated liquid. The initial

480.37

480.37

temperature and pressure of the feedwater were taken at 102 percent reactor power with valves wide open (Figure 10.1-3). These conditions produce the limiting releases for this break. As the reactor power decreases, the pressure and temperature of the steam generator inventory increases slightly. However, the pressure and temperature of the feedwater line inventory decreases significantly. Accordingly, the total calculated release is maximum at the 102 percent reactor power level.

480.37

Vent Loss Coefficient

The vent loss coefficients used in the subcompartment analyses depend on the geometry of the particular vent. The basis for the coefficients is the Handbook of Hydraulic Resistance (Idelchik 1960). Tables 6.2-27, thru 6.2-30 give the values of the loss coefficients utilized in subcompartment analyses.

Subcompartment Analytical Model

1. Functional Description of THREED Code

The THREED computer program is used to calculate the transient conditions of pressure, temperature, and humidity in various subcompartments following a postulated rupture in a moderate or high energy pipeline. The results obtained from such an analysis are used to calculate loads on structures and to define environmental conditions for equipment qualification.

The THREED computer program is similar to RELAP4 (Aerojet Nuclear Company 1976; Moore and Rettig 1974) and will give the same results as RELAP4 if similar options are chosen. THREED performs subcompartment analyses with capabilities and options extended beyond those available in RELAP4. A significant improvement in THREED is that the homogeneous equilibrium mode (HEM) has been extended to include two-phase, two-component flow which is encountered in subcompartment analysis.

The current THREED computer program was put into use in October 1978, and has been used in the design of Beaver Valley Power Station Unit 2, River Bend Station, and Nine Mile Point Nuclear Station Unit 2.

480.8

2. Description of the Model

The THREED computer code can be viewed as a numerical integrator for the macroscopic form of the basic field equations describing the conservation of mass, energy, and momentum. The conservation equations, along with the equation of state for the fluid, give a complete solution to the fluid flow phenomena. THREED solves a stream tube form of the field equations based on the assumptions of one-dimensional, homogeneous, thermal-equilibrium flow.

Although THREED does not prohibit the use of 3.55
multidimensional flow paths, the flow paths are modeled to 3.58
approximate a one-dimensional equation. Subcompartments are
modeled in THREED as a hydraulic network which consists of a 3.59
series of interconnecting user defined nodes (mass and 3.60
energy control volumes). Nodes are connected by internal
junctions (momentum control volumes) with the internodal
flow rates being determined by the solution of the momentum 4.1
equation. An internal junction control volume is defined as 4.2
the composite volume between the centers of adjacent nodes.
This inconsistency in control volumes (different control 4.3
volume for momentum than for mass and energy) is illustrated
on Figure 6.2-26. This "staggered mesh" approximation is 4.5
necessary for purposes of solving the equations.

Fill junctions are dissimilar to internal junctions in that 4.6
they have no initial node and their flow rate is dependent
only on the junction area and time. These junctions are 4.8
used to simulate flow originating external to the network
(blowdown). Mathematically, they are treated as boundary 4.9
conditions.

THREED numerically solves finite difference equations which 4.10
account for mass and energy flows into and out of a node.
Figure 6.2-27 summarizes the computational approach used in 4.11
THREED.

The fluid conservation equations used by THREED can be 4.12
obtained by integrating the stream tube equations over a
fixed volume, V . The mass and energy equations are 4.14
developed for the generalized i node, while the momentum
equation is developed for the generalized j internal 4.15
junction connecting nodes K and L . Neglecting kinetic 4.16
energy affects the resulting equations as follows:

| | |
|--|----------------------|
| 7. Incompressible form of the momentum equation. | 1.9 |
| 8. Kinetic energy effects are neglected. | 1.10 |
| 9. For the choked flow models, the static properties in the nodes are considered to be stagnation properties. | 1.11 |
| 10. Valves open/close instantaneously. | 1.12 |
| <u>Containment Subcompartment Analysis Results</u> | 1.15 |
| 1. Pressurizer Cubicle | 1.16 |
| The pressurizer cubicle is analyzed according to the nodalization diagram of Figure 6.2-24. | 1.18 |
| A spray line DER in the upper cubicle and a surge line DER in the lower cubicle are considered for the pressurizer cubicle analysis. The pressurizer is supported from the floor at elevation 51 ft-4 in. which defines the boundary between the upper and lower cubicles. | 1.20 1.22 1.23 |
| The mass and energy release for a spray line DER are given in Table 6.2-31 and for a surge line DER in Table 6.2-32. | 1.24 1.25 |
| Pressurizer cubicle subcompartment nodal volumes, vent areas, K-factors, and inertias for the THREED analysis are listed in Table 6.2-27. | 1.26 1.27 |
| The pressure response for the pressurizer cubicle (maximum pressure differential) is shown on Figures 6.2-28 and 6.2-29 for both the spray line and surge line DER, respectively. | 1.28 1.29 |
| The peak calculated differential pressures between contiguous nodes for the pressurizer cubicle are given in Table 6.2-33. The time of peak differential pressure is given with the peak calculated differential pressure. | 1.30 1.32 |
| 2. Steam Generator Compartment | 1.35 |
| The nodalization schematic used in the steam generator compartment analysis is shown on Figure 6.2-25. Seven postulated breaks are considered for the steam generator analysis. They are as follows. | 1.37 1.39 1.40 |
| 1. Steam generator inlet nozzle with a 196.6 sq in. LDR (Break 3). | 1.42 |
| 2. Pressurizer surge line with a 196.6 sq in. LDR (Break 11). | 1.43 |
| 3. Residual heat removal line with 196.6 sq in. LDR (Break 9). | 1.44 |

| | | | |
|----|--|------|--------|
| 4. | RCS hot leg intrados split break with 707 sq in. opening (Break 7). | 1.45 | |
| 5. | Feedwater line 477.6 sq in. DER. | 1.46 | |
| 6. | Steam generator outlet nozzle LDR with 500 sq in. opening (Break 4). | 1.47 | 480.37 |
| 7. | Pump suction loop closure weld LDR with 500 sq in. opening (Break 12). | 1.48 | |
| | Refer to Figure Q480.37-21 which shows the locations of the various breaks. | 1.50 | |
| | The steam generator cubicle subcompartments (cubicles A and B) nodal volumes, vent areas, K-factors, and inertias for the THREED analysis are listed in Tables 6.2-28 and 6.2-29. | 1.51 | |
| | Cubicle B was used for analysis of breaks that can occur in either cubicle. This is conservative because the K-factors and inertia values are larger and the node volumes and vent areas in cubicle B are smaller. | 1.52 | |
| | | 1.53 | |
| | | 1.54 | |
| | | 1.55 | |
| | The peak nodal pressures and time at which it occurred for each of the above-listed breaks are shown in Table 6.2-34. | 1.56 | |
| | Tables 6.2-35, 6.2-36, 6.2-36A, and 6.2-36B give the mass and energy release rates for the 196.6 sq in. LDR, the 707 sq in. intrados split break, the 477.6 sq in. feedwater line DER, and the 500 sq in. outlet nozzle LDR, respectively. | 1.57 | |
| | | 1.58 | |
| | | 1.59 | |
| | | 1.60 | 480.37 |
| | Figures 6.2-30 through 6.2-34D show the pressure response for the steam generator cubicle (maximum pressure differential across the steam generator and the cubicle walls for each break). | 2.1 | |
| | | 2.2 | |
| | The main steam line is not routed through any portion of the compartment and is not considered in the analysis. | 2.3 | |
| | | 2.4 | |
| | Tables 6.2-37 through 6.2-40 and 6.2-26 list the peak calculated differential pressures between contiguous nodes of each of the above-listed breaks. The time of peak differential pressure is given with the peak calculated differential pressure. | 2.5 | 10 |
| | | 2.9 | |
| 3. | Upper Reactor Cavity | 2.12 | |
| | The design of the neutron shield tank and the reactor vessel insulation prevent venting downward below the upper reactor cavity. Thus, the reactor cavity analysis considers pressurization of the upper cavity and the refueling cavity which is directly above the upper reactor cavity. | 2.14 | |
| | | 2.15 | |
| | | 2.17 | |
| | | 2.18 | |
| | The upper reactor cavity and the refueling cavity is analyzed according to the nodalization schematic shown on | 2.19 | |

Figure 6.2-23. The minimum number of nodes required to predict the peak local pressure is determined by performing a nodalization sensitivity study. Since the reactor cavity is symmetrical, only one-half of the cavity was analyzed.

The design nodal configuration for the reactor cavity employs a vertical plane through each reactor vessel nozzle centerline. Thus, the number of circumferential nodes is equal to the number of reactor vessel nozzles. A horizontal plane is also passed through the centerline of the nozzle where the break is assumed and the centerline of two nozzles on both sides of this nozzle. Thus, the total number of nodes inside the reactor cavity is 12. Based on symmetry, six nodes were analyzed plus four nodes in the refueling cavity and the remainder of the containment for a total of 11 nodes with this configuration. All node boundaries inside the upper reactor cavity are placed at the minimum flow area available for internodal flow. This results in the most conservative configuration for reactor cavity pressurization calculations.

Table 6.2-30 lists the node, volumes, vent areas, K-factors, and inertias used for the THREED analysis.

Table 6.2-41 gives the resultant peak calculated differential pressures. The time of peak differential pressure is given with the peak calculated differential pressure. Table 6.2-42 gives the mass and energy releases for the cold leg LDR (100 sq in. area).

Table 6.2-43 summarizes the subcompartment differential pressures (design and maximum calculated).

4. Reactor Cavity Nodalization Sensitivity Study

A total of six different nodal configurations were analyzed inside the reactor cavity. The different configurations consist of 1, 4, 8, 16, 24, and 48 node models. The remainder of the containment is represented by an additional node in these analyses. A 100 sq in. pump discharge LDR is postulated in the nodalization study.

The 1 node model considers the entire upper reactor cavity pressurization to be uniform.

The nodes in the 4 node model are bounded by vertical planes through the centerline of the broken pipe and every second pipe from the broken pipe. The resultant differential pressure is higher than the one node model. In the 8 node model, the nodes are bounded by vertical planes through the centerline of every pipe.

In the 16 node model, the nodes are bounded by vertical and horizontal planes through the centerline of every pipe. In

models with a large number of nodes (16 node model and larger), several of the nodes located relatively far from the break were combined into a single node. This did not influence the results significantly since these nodes would have nearly equal pressure if kept separate. This model results in a higher calculated differential pressure than any of the other models using lesser nodes. The results indicate that the peak differential pressure is nearly constant for all models with sixteen or more nodes, so the 16-node model was used as the limiting model.

In the 24 node model, the nodes are bounded by vertical and horizontal planes through the centerline of every pipe plus a horizontal plane 4 ft-1/2 in. above the pipe centerline. The resultant differential pressure is essentially equal to that calculated using the 16 node model.

5. Primary Shield Wall Pipe Penetrations 3.5

There are no breaks postulated inside the primary shield wall pipe penetrations. The penetrations are conservatively designed to withstand with maximum design pressure within the upper reactor cavity.

6.2.1.3 Mass and Energy Release Analyses for Postulated Loss-of-Coolant Accidents 3.12

This analysis presents the mass and energy releases to the containment subsequent to a hypothetical loss-of-coolant accident (LOCA). The release rates are calculated for pipe failure at three distinct locations:

1. Hot leg (between vessel and steam generator) 3.19
2. Pump suction (between steam generator and pump) 3.20
3. Cold leg (between pump and vessel) 3.21

During the reflood phase, these breaks have the following different characteristics. For a cold leg pipe break, all of the fluid which leaves the core must vent through a steam generator and becomes superheated. However, relative to breaks at the other locations, the core flooding rate (and therefore the rate of fluid leaving the core) is low, because all the core vent paths include the resistance of the reactor coolant pump. For a hot leg pipe break, the vent path resistance is relatively low, which results in a high core flooding rate, but the majority of the fluid which exits the core bypasses the steam generators in venting to the containment. The pump suction break combines the effects of the relatively high core flooding rate, as in the hot leg break, and steam generator heat addition, as in the cold leg break. As a result, the pump suction breaks yield the highest energy flow rates during the post-blowdown period.

The spectrum of breaks analyzed includes the largest cold and hot leg breaks, reactor inlet and outlet, respectively, and a range of pump suction breaks from the largest (10.48 sq ft) to a 3.0 sq ft break. Because of the phenomena of reflood as discussed above, the pump suction break location is the worst case for long term containment depressurization. This conclusion is supported by studies of smaller hot leg breaks which have been shown on similar plants to be less severe than the double-ended hot leg. Cold leg breaks, however, are lower both in the blowdown peak and in the reflood pressure rise. Thus, an analysis of smaller pump suction breaks is representative of the spectrum of break sizes. The hot leg break is the worst case for containment pressure.

The LOCA transient is typically divided into four phases:

1. Blowdown - which includes the period from accident occurrence (when the reactor is at steady state operation) to the time when the total break flow stops.
2. Refill - the period of time when the lower plenum is being filled by accumulator and safety injection water. (This phase is conservatively neglected in computing mass and energy releases for containment evaluations.)
3. Reflood - begins when the water from the lower plenum enters the core and ends when the core is completely quenched.
4. Post-Reflood - describes the period following the reflood transient. For the pump suction and cold leg breaks, a two-phase mixture exits the core, passes through the hot legs, and is superheated in the steam generators. After the broken loop steam generator cools, the break flow becomes two phase.

6.2.1.3.1 Mass and Energy Release Data

Blowdown Mass and Energy Release Data

Tables 6.2-7, 6.2-12, 6.2-18, 6.2-45, and 6.2-46 present the calculated mass and energy releases for the blowdown phase of the various breaks analyzed.

The mass and energy releases for the hot leg double-ended break, given in Table 6.2-7, terminate 25.2 seconds after the postulated accident. Since safety injection does not become effective until about the time blowdown terminates, these releases apply for both maximum and minimum safety injection.

Reflood Mass and Energy Release Data

Tables 6.2-13, 6.2-19, 6.2-47, 6.2-48, and 6.2-49 present the calculated mass and energy releases for the reflood phase of the various breaks analyzed along with the corresponding safety injection assumption (maximum or minimum). The release data for the 3.0 sq ft

pump suction split and the cold leg double-ended rupture also include the dry steam post-reflood mass and energy release data. 4.25

Two Phase Post-Reflood Mass and Energy Release Data 4.28

Tables 6.2-50 and 6.2-20 present the two phase (froth) mass and energy release data for a double-ended pump suction break using maximum and minimum safety injection assumptions, respectively. The data was generated using an assumed 3,600 second containment depressurization transient. 4.30 4.33 4.34

A sensitivity analysis was performed utilizing the release data presented in Tables 6.2-50 and 6.2-20 and a second set of release data generated with an assumed 1,800-second containment depressurization transient. The data presented produced the worst case for containment depressurization (Section 6.2.1.1). 4.35 4.36 4.37

Table 6.2-14 presents the post-reflood mass and energy release data for 0.6 double-ended pump suction break using minimum safety injection. 4.38 4.39

leak-rate test described in Section 6.2.6.1 adequately demonstrates the leak tightness of the containment. 1.10
1.11

An evaluation of in-leakage following a LOCA shows the containment pressure to be effectively subatmospheric at -0.5 psig 30 days following the accident. The inleakage analysis is based on the maximum specified out-leakage rate of 0.9 percent per day at approximately 45 psig adjusted to the pressure differences determined to be present following a LOCA. 1.12
1.13
1.14
1.15 480.22

The maximum in-leakage rate to the subatmospheric containment during normal operation is approximately 14 scfm at 9.5 psia, the lowest normal operating containment pressure. This corresponds to the out-leakage rate of 0.9 percent per day at 45 psig adjusted for the pressure differential and other important flow parameters. 1.16
1.17
1.18
1.19

The containment structure enclosure will be evacuated by the supplementary leak collection and release system (SLCRS) to slightly negative pressure immediately following the design bases accident initiation of the engineered safety features actuation system (ESFAS). This will ensure all leakage from the primary containment (0.9 percent per day) is passed through the high-efficiency particulate air (99-percent efficient) filters of the SLCRS prior to release from the containment structure enclosure, engineered safety feature building, main steam valve building, hydrogen recombiner building or auxiliary building which are all connected to the SLCRS. 1.20
1.21
1.22
1.23
1.25
1.26
1.28

This filtration will ensure the reduction of primary leakage from 0.9 percent per day to less than 0.1 percent per day released to the environment. The SLCRS will be tested prior to loading fuel to verify that a slightly negative pressure can be obtained and maintained following an ESFAS actuation in the areas mentioned above. This test will be conducted again at each refueling or at intervals not to exceed 18 months. Some leakage through piping systems may bypass the secondary containment. This leakage is limited to the design leak rates through these piping systems. The bypass leakage penetrations, identified in Table 6.2-65, are tested in accordance with Section 6.2.6.3, and the combination of their leakage rates is compared with the maximum allowable rate (9 scfh). When the actual leakage rate approaches this limit, corrective action will be taken. 1.29
1.30
1.31
1.32
1.33
1.34
1.35
1.36
1.38
1.39

6.2.7 References for Section 6.2 1.41

Aerojet Nuclear Company, 1976. RELAP4/MOD5: A Computer Program for Transient Thermal Hydraulic Analysis of Nuclear Reactors and Related Systems. User's Manual Vol I-III, Report ANCR-NUREG-1335. Aerojet Nuclear Company. 1.43
1.45

American Nuclear Society (ANS) 1978. Decay Heat Power in Light Water Reactors. ANS Standard, June 1, 1978, Revised September 1978. 1.48
1.49

Atomics International Division Rockwell International. Test Procedure - Hydrogen Analyzer Systems, No. N019DTP120003. 1.51

| | | |
|--|-----------------------------|--------|
| Baer, Robert L. (Office of Reactor Regulation Division of Project Management, (USNRC) 1978. Letter to Mr. Gordan Pinsky (Owens-Corning Fiberglass Corporation). | 1.52 1.53 | |
| Bloom, G.R., et al. Hydrogen Distribution in a Containment with a High Velocity Hydrogen-Steam Source. Presented at the Second International Workshop on the Impact of Hydrogen on Water Reactor Safety, Albuquerque, New Mexico, October 3-7, 1982. | 1.54 1.55 1.56 | 480.19 |
| Brocard, D.N. Buoyancy, Transport and Head Loss of Fibrous Reactor Insulation. NUREG/CR-2982, U.S. Nuclear Regulatory Commission. Prepared by Alden Research Laboratory, Worcester Polytechnic Institute, Holden, Massachusetts. November 1982. | 1.57 1.58 1.59 2.1 | 480.18 |
| CONTEMPT - A Computer Program for Predicting the Containment Pressure-Temperature Response to a Loss-of-Coolant Accident (LOCA), IDO-17220 1967. | 2.2 2.3 | |
| Crank, J. The Mathematics of Diffusion. Oxford University Press, 1956, pp 186-199. | 2.5 | 480.11 |
| Gido, R.G. Liner-Concrete Heat Transfer Study for Nuclear Power Plant Containments, Los Alamos Scientific Laboratory, LA-7089-MS Informal Report NRC-4, issued January 1978. | 2.6 2.7 | |
| Gido, R.G. Subcompartment Analysis Procedures. Los Alamos Scientific Laboratory. NUREC/CK-1199, LA-8169-MS, Informal Report R-4. December 1979. | 2.9 2.10 2.11 | 480.37 |
| Hanover, Stephen H. (Chairman Advisory Committee of Reactor Safeguards) 1969. Letter to Hon. Glenn T. Seaborg (Chairman USAEC) Report on Brunswick Steam Electric Plant. | 2.12 2.13 | |
| Hanover, Stephen H. (Chairman Advisory Committee of Reactor Safeguards) 1969. Letter to Hon. Glenn T. Seaborg (Chairman USAEC) Report on Edwin I. Hatch Nuclear Plant. | 2.14 2.15 | |
| Hilliard, R.K., et al. 1970. Removal of Iodine and Particles from Containment Atmosphere by Sprays. Battelle-Northwest, Richland, Wash. BNWL-1244. | 2.17 2.18 | |
| Hilliard, R.K. and Coleman, L.F. Natural Transport Effects on Fission Product Behavior in the Containment Systems Experiment. BNWL-1457, Battelle Pacific Northwest Laboratories, Richland, Washington. December 1970. | 2.20 2.21 2.22 | 480.19 |
| IDCOR Program Report, Technical Report 12.2, Hydrogen Distribution in Reactor Containment Building. September 1983. | 2.23 2.24 | |
| Idel'chik, I.E. 1960. Handbook of Hydraulic Resistance, Published pursuant to an agreement with the U.S. Atomic Energy Commission and the National Science Foundation, Washington, D.C. | 2.26 2.27 | |

| | |
|---|----------------------|
| Knudsen, J.G. and Hilliard, R.K. 1969. Fission Product Transport by Natural Processes in Containment Vessels. Battelle-Northwest, Richland, Wash. BNWL-943. | 2.29 2.30 |
| LOCTIC - A Computer Code to Determine the Pressure and Temperature Response of Dry Containments to a Loss-of-Coolant Accident, SWND-1, (SWECC), 1971. Letter from W.J.L. Kennedy to P.A. Morris et al. | 2.31 2.32 2.33 |
| Los Alamos Scientific Laboratory Reactor Safety and Technology Quarterly Progress Report, 1976. LA-NUREG-6447-PR, p 53. | 2.34 2.35 |
| McAdams, W.H. 1954. Heat Transmission, Third Edition, p 44. | 2.37 |
| Moody, L.J. 1965. Maximum Flow Rate of a Single Component, Two-Phase Mixture. Journal of Heat Transfer Transactions, ASME Vol. 87, p 134-142. | 2.39 2.40 |
| Moore, K.V. and Rettig, W.H. 1974. RELAP4 - A Computer Program for Thermal Hydraulic Analysis. Report ANCR-1127 Aerojet Nuclear Company. | 2.42 2.43 |
| Norberg, J.A. et al 1969. Simulated Design Basis Accident Tests of the Carolinas Virginia Tube Reactor Containment - Preliminary Results, IN-1324. Idaho Nuclear Corporation. | 2.45 2.47 |
| NS-TMA-2075. 1979. A letter from T.M. Anderson, Westinghouse, to J.F. Stolz, 1979. Westinghouse LOCA Mass and Energy Release Model for Containment Design - March 1979 Version. | 2.50 2.51 |
| Nystrom, J.B. Experimental Evaluation of a Reactor Containment Sump, MNPS-3, Alden Research Laboratory, Report No. 114-82/M10XXF, October 1982. | 2.52 2.53 |
| ORNL - TM 2412. Parsly, L.F. 1970 Design Considerations of Reactor Containment Spray Systems - Part VI, the Heating of Spray Drops in Air/Steam Atmosphere. | 2.55 2.56 |
| Sandia National Laboratory and General Physics Corporation. NUREG/CR-2726, SAND 82-1137, R3, Light Water Reactor Hydrogen Manual. June 1983. | 2.57 2.58 2.59 |
| Schmidt, R.C., et al 1970. Simulated Design Basis Accident Tests of the Carolinas Virginia Tube Reactor Containment - Final Report. UC-80, Idaho Nuclear Corporation. | 3.1 3.2 |
| Slaughterbeck, D.C. 1970. A Review of Heat Transfer Coefficients for Condensing Steam in a Containment Building Following a Loss-of-Coolant Accident. Interim Task Report, Subtask 4.2.2.1, Idaho Nuclear Corp. | 3.4 3.6 |
| Spray Engineering Company. Spray Analysis on SPRACo Model 1713A Nozzles. Nashua, New Hampshire. | 3.8 3.9 |

MNPS-3 FSAR

| | |
|---|----------------------|
| Uchida, H.; Oyama, A.; and Togo, Y. 1964. Evaluation of Post-Incident Cooling Systems of Light-Water Power Reactors. Proceedings of the Third International Conference on the Peaceful Uses of Atomic Energy held in Geneva. Vol. 13, New York: United Nations 93-104, (A/CONF 28/P/436). | 3.11 3.12 3.13 |
| USAEC, Division of Reactor Licensing 1970. Safety Evaluation Report for Virginia Electric and Power Company, North Anna Power Station Units 1 and 2. Docket 50-338 and 50-339. | 3.15 3.16 |
| USAEC, Directorate of Licensing 1972a. Safety Evaluation Report for Virginia Electric and Power Company, North Anna Power Station Units 3 and 4. Dockets 50-404 and 405. | 3.18 3.19 |
| USAEC, Division of Reactor Licensing 1972b. Safety Evaluation Report for Virginia Electric Power Company, Surry Power Station Units 1 and 2. Docket 50-280 and 50-281. | 3.21 3.22 |
| USAEC, Division of Reactor Licensing 1972c. Safety Evaluation Report for Maine Yankee Atomic Power Station. Docket 50-309. | 3.24 3.25 |
| USAEC, Directorate of Licensing 1974a. Safety Evaluation Report Supplement No. 2 for the Cleveland Electric Illuminating Company, Duquesne Light Company, Ohio Edison Company, Pennsylvania Power Company, and Toledo Edison Company, Beaver Valley Power Station Unit 2. Docket 50-412. | 3.27 3.28 3.29 |
| USAEC 1974b. Evaluation of LOCA Hydrodynamics. Regulatory Staff: Technical Review. | 3.32 |
| USAEC, Directorate of Licensing 1974c. Safety Evaluation Report for the Duquesne Light Company, Toledo Edison Company, Pennsylvania Power Company, Beaver Valley Power Station Unit 1. Docket 50-334. | 3.34 3.36 |
| WCAP-6174, 1974. Bordelon, F.M. et al. SATAN-VI Program: Comprehensive Space-Time Dependent Analysis of Loss-of-Coolant. | 3.39 |
| WCAP-8170, 1974. Collier, G. et al. 1974. Computational Model for Core Reflooding After a Loss-of-Coolant Accident (WREFLOOD Code). | 3.42 |
| WCAP-8264-P-A (Proprietary) and WCAP-8312-A (Non-proprietary), Revision 2, Westinghouse Corp. 1975. Westinghouse Mass Energy Release for Containment Design. | 3.43 3.44 |
| WCAP-8339, 1974. Burdelon, F.M.; Massie, H.W.; Zordum, J.A. Westinghouse Emergency Core Cooling System Evaluation Model - Summary. | 3.46 |
| WCAP-8859. Land, R.E. TRANFLO Steam Generator Code Description. | 3.48 |
| WCAP-8860. Land, R.E. Mass and Energy Release Following a Steam Line Rupture. | 3.50 |
| WCAP-9220, 1978. Westinghouse ECCS Evaluation Model. | 3.52 |

08/07/84

MNPS-3 FSAR

246

1.7

TABLE 6.2-34

STEAM GENERATOR CUBICLE PEAK PRESSURES

| Node (No.) | Steam Generator Inlet Nozzle | | Pressurizer Surge Line | | Residual Heat Removal Line | | RCS Hot Leg Intrados Split | | Feedwater Line | |
|---------------|---------------------------------|---------------|---------------------------|---------------|-------------------------------|---------------|-------------------------------|---------------|--------------------|---------------|
| | Pressure (psia) | Time (sec) | Pressure (psia) | Time (sec) | Pressure (psia) | Time (sec) | Pressure (psia) | Time (sec) | Pressure (psia) | Time (sec) |
| 1 | 13.79 | 0.064 | 14.07 | 0.062 | 13.80 | 0.046 | 26.78 | 0.501 | 10.64 | 0.501 |
| 2 | 13.59 | 0.044 | 13.76 | 0.072 | 13.53 | 0.052 | 26.65 | 0.501 | 10.64 | 0.501 |
| 3 | 13.71 | 0.066 | 14.30 | 0.066 | 13.58 | 0.068 | 26.64 | 0.501 | 10.64 | 0.501 |
| 4 | 14.42 | 0.030 | 15.12 | 0.026 | 15.35 | 0.024 | 26.83 | 0.501 | 10.63 | 0.501 |
| 5 | 13.62 | 0.086 | 14.03 | 0.072 | 16.25 | 0.010 | 26.84 | 0.501 | 10.63 | 0.501 |
| 6 | 13.94 | 0.094 | 13.85 | 0.028 | 14.54 | 0.020 | 26.88 | 0.501 | 10.63 | 0.501 |
| 7 | 14.21 | 0.048 | 14.86 | 0.052 | 13.83 | 0.058 | 26.78 | 0.501 | 10.64 | 0.501 |
| 8 | 14.66 | 0.054 | 14.40 | 0.054 | 13.30 | 0.070 | 26.62 | 0.501 | 10.64 | 0.501 |
| 9 | 14.07 | 0.056 | 14.59 | 0.094 | 14.48 | 0.068 | 26.64 | 0.501 | 10.64 | 0.501 |
| 10 | 14.70 | 0.070 | 16.78 | 0.016 | 16.19 | 0.026 | 27.24 | 0.501 | 10.63 | 0.501 |
| 11 | 15.42 | 0.012 | 18.36 | 0.010 | 13.63 | 0.088 | 27.67 | 0.501 | 10.63 | 0.501 |
| 12 | 17.77 | 0.010 | 13.75 | 0.046 | 14.50 | 0.054 | 29.29 | 0.014 | 10.64 | 0.501 |
| 13 | 12.76 | 0.146 | 13.18 | 0.062 | 13.22 | 0.058 | 25.26 | 0.501 | 10.72 | 0.031 |
| 14 | 12.95 | 0.102 | 13.07 | 0.102 | 13.07 | 0.056 | 25.25 | 0.501 | 10.66 | 0.501 |
| 15 | 12.99 | 0.106 | 13.14 | 0.094 | 13.24 | 0.070 | 25.14 | 0.501 | 10.65 | 0.501 |
| 16 | 13.65 | 0.030 | 13.70 | 0.086 | 13.51 | 0.082 | 25.48 | 0.501 | 10.65 | 0.501 |
| 17 | 13.00 | 0.074 | 13.40 | 0.076 | 13.67 | 0.078 | 25.50 | 0.501 | 10.65 | 0.501 |
| 18 | 13.37 | 0.020 | 13.22 | 0.030 | 13.20 | 0.064 | 25.52 | 0.501 | 10.65 | 0.501 |
| 19 | 10.77 | 0.501 | 10.98 | 0.601 | 11.65 | 1.001 | 13.31 | 0.501 | 16.66 | 0.010 |
| 20 | 10.77 | 0.501 | 10.98 | 0.601 | 11.65 | 1.001 | 13.31 | 0.501 | 16.67 | 0.010 |
| 21 | 11.25 | 0.501 | 11.53 | 0.601 | 12.06 | 1.001 | 17.17 | 0.501 | 11.37 | 0.013 |
| 22 | 11.24 | 0.501 | 11.52 | 0.601 | 12.06 | 1.001 | 17.16 | 0.501 | 11.51 | 0.013 |
| 23 | 10.56 | 0.501 | 10.74 | 0.601 | 11.47 | 1.001 | 11.89 | 0.501 | 10.46 | 0.501 |
| 24 | 11.80 | 0.064 | 12.12 | 0.114 | 12.38 | 1.001 | 23.37 | 0.501 | 14.77 | 0.010 |
| 25 | 11.92 | 0.104 | 12.06 | 0.074 | 12.37 | 1.001 | 23.34 | 0.501 | 14.36 | 0.010 |
| 26 | 12.29 | 0.026 | 12.34 | 0.074 | 12.42 | 1.001 | 23.46 | 0.501 | 11.41 | 0.016 |
| 27 | 12.19 | 0.096 | 12.32 | 0.032 | 12.43 | 1.001 | 23.48 | 0.501 | 12.17 | 0.017 |
| 28 | 13.16 | 0.090 | 13.43 | 0.032 | 13.51 | 0.096 | 25.88 | 0.501 | 10.61 | 0.501 |

TABLE 6.2-34 (Cont)

| Node (No.) | Steam Generator Outlet Nozzle | | Steam Generator Pump Suction Loop Closure Weld | | |
|---------------|-------------------------------|---------------|---|---------------|------|
| | Pressure (psia) | Time (sec) | Pressure (psia) | Time (sec) | |
| 1 | 26.32 | 0.630 | 26.59 | 0.628 | 2.2 |
| 2 | 26.69 | 0.618 | 26.93 | 0.608 | 2.3 |
| 3 | 26.67 | 0.622 | 26.82 | 0.622 | 2.4 |
| 4 | 26.32 | 0.622 | 26.82 | 0.626 | 2.5 |
| 5 | 26.33 | 0.642 | 26.90 | 0.640 | 2.7 |
| 6 | 26.30 | 0.642 | 26.58 | 0.626 | 2.8 |
| 7 | 26.33 | 0.652 | 26.59 | 0.632 | 2.9 |
| 8 | 26.79 | 0.608 | 26.76 | 0.610 | 2.10 |
| 9 | 26.67 | 0.612 | 26.78 | 0.618 | 2.11 |
| 10 | 26.67 | 0.614 | 26.39 | 0.632 | 2.13 |
| 11 | 26.93 | 0.606 | 26.35 | 0.636 | 2.14 |
| 12 | 26.24 | 0.648 | 26.37 | 0.636 | 2.15 |
| 13 | 24.84 | 0.632 | 24.74 | 0.618 | 2.16 |
| 14 | 24.84 | 0.616 | 24.74 | 0.650 | 2.17 |
| 15 | 24.72 | 0.622 | 24.61 | 0.612 | 2.19 |
| 16 | 24.92 | 0.620 | 24.77 | 0.608 | 2.20 |
| 17 | 24.94 | 0.632 | 24.79 | 0.636 | 2.21 |
| 18 | 24.94 | 0.628 | 24.80 | 0.618 | 2.22 |
| 19 | 13.91 | 0.751 | 13.89 | 0.751 | 2.23 |
| 20 | 13.91 | 0.751 | 13.89 | 0.751 | 2.25 |
| 21 | 17.17 | 0.751 | 17.11 | 0.751 | 2.26 |
| 22 | 17.17 | 0.751 | 17.11 | 0.751 | 2.27 |
| 23 | 12.65 | 0.751 | 12.64 | 0.751 | 2.28 |
| 24 | 23.90 | 0.642 | 22.89 | 0.630 | 2.29 |
| 25 | 22.97 | 0.660 | 22.86 | 0.644 | 2.31 |
| 26 | 23.03 | 0.642 | 22.90 | 0.616 | 2.32 |
| 27 | 23.05 | 0.638 | 22.92 | 0.614 | 2.33 |
| 28 | 25.40 | 0.640 | 25.87 | 0.630 | 2.34 |

480.37

TABLE 6.2-36 (Cont)

| <u>Time</u> <u>(sec)</u> | <u>Mass</u> <u>(lb/sec)</u> | <u>Energy</u> <u>(Btu/sec)</u> | <u>Average</u> <u>Enthalpy</u> <u>(Btu/lb)</u> | |
|-----------------------------|--------------------------------|-----------------------------------|--|------|
| 2.10001 | 36,858.204 | 24,656,318 | 668.95 | 1.19 |
| 2.30009 | 36,048.665 | 24,068,766 | 667.67 | 1.20 |
| 2.50025 | 35,210.472 | 23,501,169 | 667.45 | 1.21 |
| 2.70019 | 34,537.213 | 23,028,338 | 666.77 | 1.22 |
| 3.00027 | 36,798.127 | 24,517,748 | 666.28 | 1.23 |

480.37

TABLE 6.2-36A

1.10

MASS AND ENERGY RELEASE RATES FOR A FEEDWATER
LINE FULL DER IN THE STEAM GENERATOR CUBICLE

1.12

1.13

| Time (sec) | Mass Flow | Mass Flow | Energy | Energy | Total | Total | 1.16 |
|---------------|-----------|----------------|----------|----------------|-----------|-----------|------|
| | SG Side | Piping Side | SG Side | Piping Side | Mass Flow | Energy | |
| | (lb/sec) | (lb/sec) | (Btu/lb) | (Btu/lb) | (lb/sec) | (Btu/sec) | 1.17 |
| | | | | | | | 1.18 |
| | | | | | | | 1.19 |
| 0.0 | 13101. | 8623. | 7.048E6 | 3.622E6 | 21724. | 10.67E6 | 1.21 |
| 2.0 | 13101. | 8623. | 7.048E6 | 3.622E6 | 21724. | 10.67E6 | 1.22 |

TABLE 6.2-36B

MASS AND ENERGY RELEASE RATES FOR A 500 SQUARE
INCH COLD LEG LDR IN THE STEAM GENERATOR CUBICLE

| Time (sec) | Mass (lb/sec) | Energy (Btu/sec) | Average Enthalpy (Btu/lb) | |
|---------------|------------------|---------------------|---------------------------------|------|
| 0.0 | 0.0 | 0.0 | 0.00 | 1.25 |
| 0.0300 | 2.7553554E4 | 1.5365431E7 | 557.62 | 1.26 |
| 0.00762 | 3.5126475E4 | 1.9615838E7 | 558.44 | 1.27 |
| 0.01101 | 3.5272477E4 | 1.9668454E7 | 557.61 | 1.29 |
| 0.01504 | 4.0481375E4 | 1.8815784E7 | 557.54 | 1.30 |
| 0.01901 | 3.5526048E4 | 1.9804758E7 | 557.47 | 1.31 |
| 0.02302 | 3.4149137E4 | 1.9031251E7 | 557.30 | 1.32 |
| 0.02704 | 3.2223069E4 | 1.7947655E7 | 557.00 | 1.33 |
| 0.03105 | 3.1357026E4 | 1.7463354E7 | 556.92 | 1.35 |
| 0.03500 | 3.1173067E4 | 1.7360838E7 | 556.90 | 1.36 |
| 0.03901 | 3.1572734E4 | 1.7587118E7 | 556.87 | 1.37 |
| 0.04301 | 3.2089701E4 | 1.7872020E7 | 556.94 | 1.38 |
| 0.04701 | 3.2943141E4 | 1.8348849E7 | 556.99 | 1.39 |
| 0.05101 | 3.2957101E4 | 1.8356301E7 | 556.97 | 1.41 |
| 0.05501 | 3.3752582E4 | 1.8800311E7 | 557.06 | 1.42 |
| 0.05902 | 4.3581443E4 | 2.4295982E7 | 557.48 | 1.43 |
| 0.06303 | 4.6559619E4 | 2.5966536E7 | 557.71 | 1.44 |
| 0.06703 | 5.0176752E4 | 2.7997336E7 | 557.97 | 1.45 |
| 0.07102 | 5.1474565E4 | 2.8126708E7 | 558.08 | 1.47 |
| 0.07504 | 5.5649593E4 | 3.1082255E7 | 558.47 | 1.48 |
| 0.07906 | 5.5871919E4 | 3.1176204E7 | 558.01 | 1.49 |
| 0.08302 | 5.4253849E4 | 3.0266530E7 | 557.87 | 1.50 |
| 0.08707 | 5.2995360E4 | 2.9556141E7 | 557.71 | 1.51 |
| 0.09109 | 5.2667082E4 | 2.9373640E7 | 557.72 | 1.53 |
| 0.09506 | 5.1601936E4 | 2.8767941E7 | 557.50 | 1.54 |
| 0.09905 | 4.9847279E4 | 2.7788070E7 | 557.46 | 1.55 |
| 0.11501 | 5.1517896E4 | 2.8730435E7 | 557.68 | 1.57 |
| 0.13502 | 5.4052551E4 | 3.0150688E7 | 557.90 | 1.59 |
| 0.15505 | 5.1675352E4 | 2.8820766E7 | 557.73 | 1.60 |
| 0.17501 | 5.2674332E4 | 2.9387760E7 | 557.91 | 2.1 |
| 0.19510 | 5.2804854E4 | 2.9465270E7 | 558.00 | 2.2 |
| 0.23013 | 5.2756783E4 | 2.9445480E7 | 558.14 | 2.3 |
| 0.27008 | 5.2125022E4 | 2.9105085E7 | 558.37 | 2.5 |
| 0.31003 | 5.2666673E4 | 2.9427243E7 | 558.75 | 2.6 |
| 0.35007 | 5.2049310E4 | 2.9097595E7 | 559.04 | 2.7 |

TABLE 6.2-36B (Cont)

| <u>Time</u> <u>(sec)</u> | <u>Mass</u> <u>(lb/sec)</u> | <u>Energy</u> <u>(Btu/sec)</u> | <u>Average</u> <u>Enthalpy</u> <u>(Btu/lb)</u> | |
|-----------------------------|--------------------------------|-----------------------------------|--|------|
| 0.39030 | 5.1629608E4 | 2.8883611E7 | 559.44 | 2.11 |
| 0.43075 | 5.1939759E4 | 2.9081424E7 | 559.91 | 2.12 |
| 0.47007 | 5.1562917E4 | 2.8895244E7 | 560.39 | 2.13 |
| 0.51007 | 5.1387973E4 | 2.8827092E7 | 560.97 | 2.14 |
| 0.55001 | 5.1343287E4 | 2.8833112E7 | 561.58 | 2.15 |
| 0.59013 | 5.0769706E4 | 2.8544503E7 | 562.23 | 2.17 |
| 0.63001 | 5.0486202E4 | 2.8420679E7 | 562.94 | 2.18 |
| 0.67003 | 5.0033919E4 | 2.8201396E7 | 563.65 | 2.19 |
| 0.71008 | 4.9638937E4 | 2.8017887E7 | 564.43 | 2.20 |
| 0.75010 | 4.9336961E4 | 2.7886235E7 | 565.22 | 2.21 |
| 0.79004 | 4.8769620E4 | 2.7603714E7 | 568.00 | 2.23 |
| 0.83007 | 4.8204470E4 | 2.7322395E7 | 566.80 | 2.24 |
| 0.87003 | 4.7848952E4 | 2.7158782E7 | 567.59 | 2.25 |
| 0.91006 | 4.7389542E4 | 2.6935723E7 | 568.39 | 2.26 |
| 0.95011 | 4.6948187E4 | 2.6721463E7 | 569.17 | 2.27 |
| 0.99002 | 4.6504795E4 | 2.6503781E7 | 569.92 | 2.29 |
| 1.00012 | 4.6372995E4 | 2.6437194E7 | 570.10 | 2.30 |

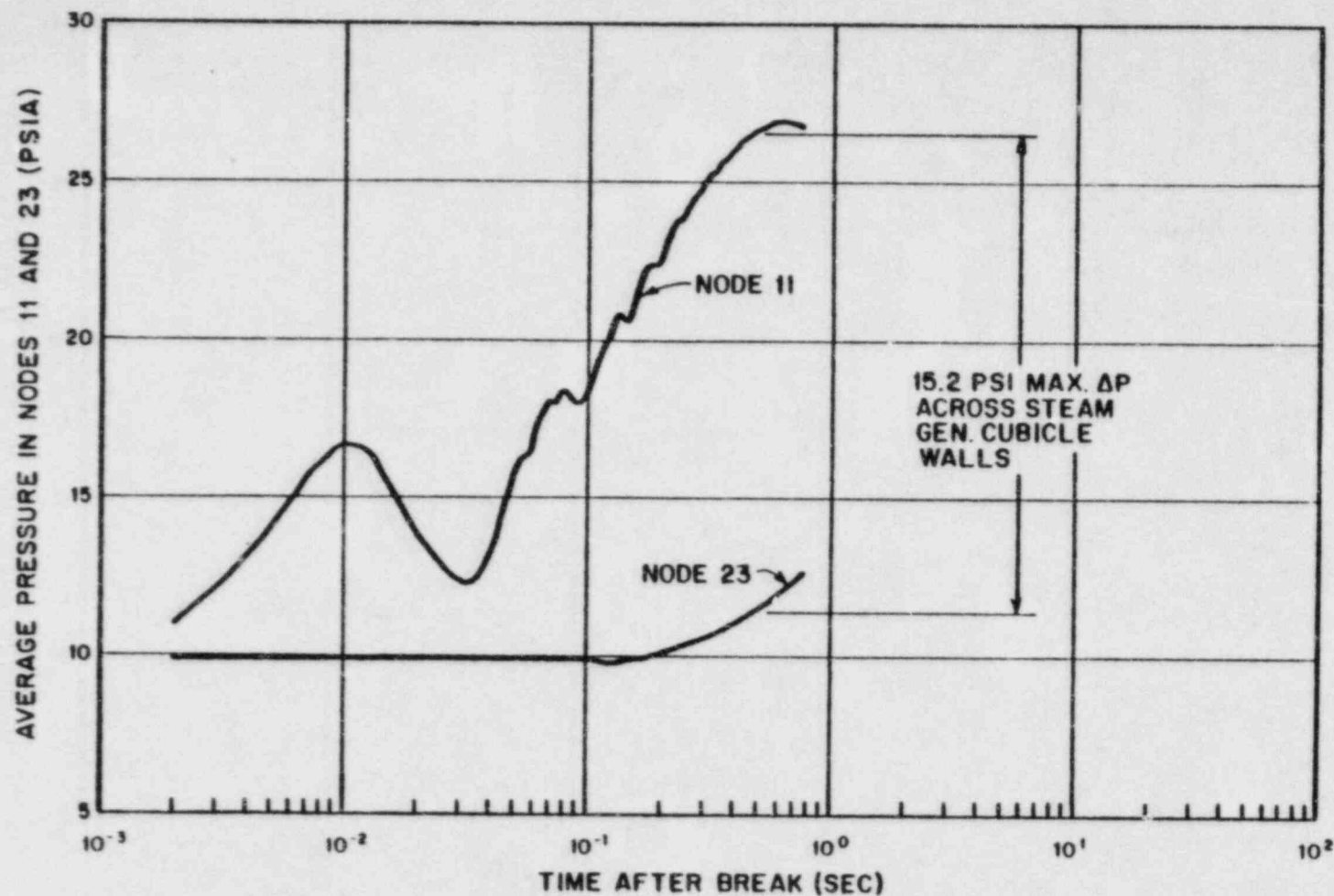
TABLE 6.2-37A
STEAM GENERATOR CUBICLE PEAK DIFFERENTIAL PRESSURES,
STEAM GENERATOR OUTLET NOZZLE LDR

| Vent Path (No.) | Vent Path Connecting Nodes From | Vent Path Connecting Nodes To | Pressure (psid) | Time (sec) | Vent Path (No.) | Vent Path Connecting Nodes From | Vent Path Connecting Nodes To | Pressure (psid) | Time (sec) | Vent Path (No.) | Vent Path Connecting Nodes From | Vent Path Connecting Nodes To | Pressure (psid) | Time (sec) |
|-----------------|---------------------------------|-------------------------------|-----------------|------------|-----------------|---------------------------------|-------------------------------|-----------------|------------|-----------------|---------------------------------|-------------------------------|-----------------|------------|
| 1 | 1 | 2 | -3.64 | 0.082 | 36 | 16 | 17 | 1.28 | 0.029 | 1.14 | 1.15 | 1.16 | 1.8 | 1.10 |
| 2 | 2 | 3 | -2.18 | 0.033 | 37 | 17 | 18 | 1.55 | 0.080 | 1.18 | 1.19 | 1.20 | 1.11 | 1.11 |
| 3 | 3 | 4 | 3.11 | 0.034 | 38 | 14 | 17 | -0.84 | 0.041 | 1.19 | 1.20 | 1.21 | | |
| 4 | 4 | 5 | 1.62 | 0.028 | 39 | 13 | 18 | 1.21 | 0.047 | 1.21 | 1.22 | 1.23 | | |
| 5 | 5 | 6 | 1.72 | 0.018 | 40 | 13 | 23 | 13.06 | 0.488 | 1.24 | 1.25 | 1.26 | | |
| 6 | 2 | 5 | 2.26 | 0.027 | 41 | 13 | 24 | 1.86 | 0.566 | 1.27 | 1.28 | 1.29 | | |
| 7 | 1 | 6 | 2.02 | 0.042 | 42 | 14 | 23 | 13.03 | 0.472 | 1.30 | 1.31 | 1.32 | | |
| 8 | 1 | 7 | 3.15 | 0.036 | 43 | 14 | 25 | 1.88 | 0.615 | 1.33 | 1.34 | 1.35 | | |
| 9 | 1 | 23 | 14.58 | 0.479 | 44 | 15 | 23 | 12.91 | 0.476 | 1.36 | 1.37 | 1.38 | | |
| 10 | 2 | 8 | -5.75 | 0.010 | 45 | 17 | 25 | 2.01 | 0.079 | 1.39 | 1.40 | 1.41 | | |
| 11 | 3 | 9 | 4.67 | 0.033 | 46 | 16 | 23 | 13.12 | 0.476 | 1.42 | 1.43 | 1.44 | | |
| 12 | 3 | 23 | 14.93 | 0.471 | 47 | 16 | 23 | 13.12 | 0.476 | 1.45 | 1.46 | 1.47 | | |
| 13 | 4 | 10 | -4.59 | 0.015 | 48 | 17 | 26 | 1.93 | 0.079 | 1.48 | 1.49 | 1.50 | | |
| 14 | 4 | 28 | 2.23 | 0.025 | 49 | 17 | 23 | 13.13 | 0.486 | 1.51 | 1.52 | 1.53 | | |
| 15 | 5 | 11 | -6.28 | 0.009 | 50 | 17 | 23 | 13.13 | 0.486 | 1.54 | 1.55 | 1.56 | | |
| 16 | 5 | 28 | 2.01 | 0.019 | 51 | 18 | 27 | 1.90 | 0.562 | 1.57 | 1.58 | 1.59 | | |
| 17 | 6 | 12 | 2.87 | 0.032 | 52 | 18 | 23 | 13.15 | 0.481 | 1.60 | 1.61 | 1.62 | | |
| 18 | 6 | 28 | 1.60 | 0.058 | 53 | 19 | 20 | -0.28 | 0.070 | 1.63 | 1.64 | 1.65 | | |
| 19 | 7 | 8 | -5.85 | 0.010 | 54 | 20 | 21 | -3.75 | 0.474 | 1.66 | 1.67 | 1.68 | | |
| 20 | 8 | 9 | 4.65 | 0.009 | 55 | 21 | 22 | 0.31 | 0.079 | 1.69 | 1.70 | 1.71 | | |
| 21 | 9 | 10 | -1.32 | 0.123 | 56 | 19 | 22 | -3.75 | 0.474 | 1.72 | 1.73 | 1.74 | | |
| 22 | 10 | 11 | -5.12 | 0.008 | 57 | 19 | 23 | 1.37 | 0.489 | 1.75 | 1.76 | 1.77 | | |
| 23 | 11 | 12 | 5.80 | 0.009 | 58 | 20 | 23 | 1.37 | 0.503 | 1.78 | 1.79 | 1.80 | | |
| 24 | 8 | 11 | -0.95 | 0.007 | 59 | 21 | 23 | 5.12 | 0.480 | 1.81 | 1.82 | 1.83 | | |
| 25 | 7 | 12 | 1.47 | 0.048 | 60 | 22 | 23 | 5.12 | 0.479 | 1.84 | 1.85 | 1.86 | | |
| 26 | 7 | 13 | 3.07 | 0.051 | 61 | 24 | 25 | -1.55 | 0.081 | 1.87 | 1.88 | 1.89 | | |
| 27 | 8 | 14 | 6.06 | 0.011 | 62 | 25 | 26 | -0.77 | 0.040 | 1.90 | 1.91 | 1.92 | | |
| 28 | 9 | 15 | 4.93 | 0.019 | 63 | 26 | 27 | 1.14 | 0.086 | 1.93 | 1.94 | 1.95 | | |
| 29 | 14 | 23 | 13.03 | 0.472 | 64 | 27 | 24 | 0.79 | 0.033 | 1.96 | 1.97 | 1.98 | | |
| 30 | 10 | 16 | 4.88 | 0.017 | 65 | 24 | 19 | 9.84 | 0.488 | 1.99 | 2.00 | 2.01 | | |
| 31 | 11 | 17 | 6.52 | 0.010 | 66 | 25 | 20 | 9.80 | 0.472 | 2.02 | 2.03 | 2.04 | | |
| 32 | 12 | 18 | 2.93 | 0.053 | 67 | 26 | 21 | 6.13 | 0.561 | 2.05 | 2.06 | 2.07 | | |
| 33 | 13 | 14 | -2.04 | 0.023 | 68 | 27 | 22 | 6.17 | 0.568 | 2.08 | 2.09 | 2.10 | | |
| 34 | 14 | 15 | 1.38 | 0.049 | 69 | 28 | 23 | 13.63 | 0.479 | 2.11 | 2.12 | 2.13 | | |
| 35 | 15 | 16 | -1.11 | 0.084 | | | | | | | | | | |

TABLE 6.2-37B

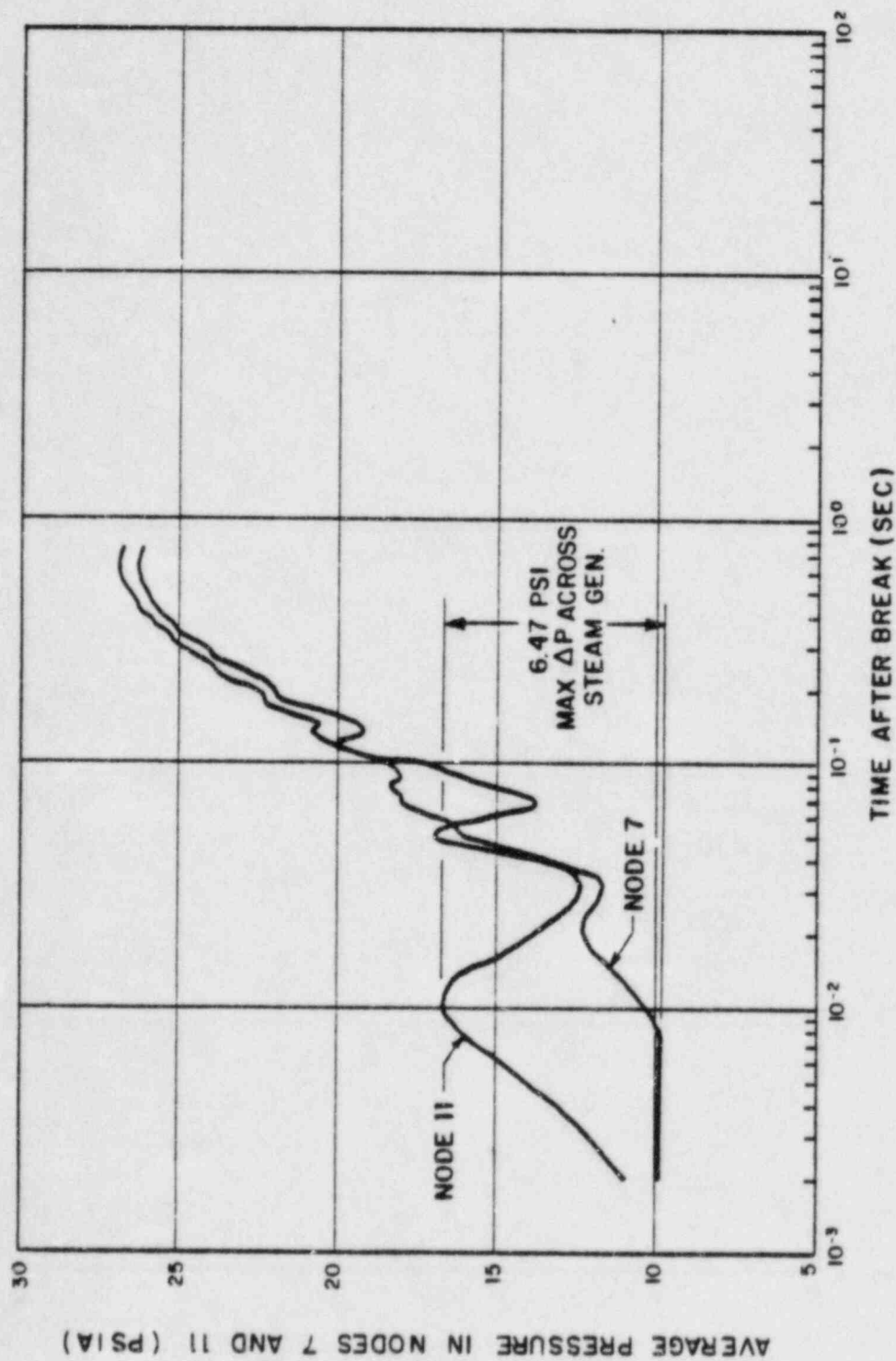
STEAM GENERATOR CUBICLE PEAK DIFFERENTIAL PRESSURES,
PUMP SUCTION LOOP CLOSURE WELD LDR

| Vent Path (no.) | Vent Path Connecting Nodes From To | Pressure (psid) | Time (sec) | Vent Path (no.) | Vent Path Connecting Nodes From To | Pressure (psid) | Time (sec) |
|--------------------|--|--------------------|---------------|--------------------|--|--------------------|---------------|
| 1 | 1 | -5.94 | 0.013 | 35 | 15 | -0.92 | 0.056 |
| 2 | 2 | 4.65 | 0.010 | 36 | 16 | -0.41 | 0.113 |
| 3 | 3 | 2.51 | 0.073 | 37 | 17 | -0.64 | 0.056 |
| 4 | 4 | -4.30 | 0.009 | 38 | 14 | -0.73 | 0.052 |
| 5 | 5 | 4.49 | 0.009 | 39 | 13 | -0.52 | 0.094 |
| 6 | 2 | 2.34 | 0.019 | 40 | 13 | 12.97 | 0.491 |
| 7 | 1 | 1.91 | 0.038 | 41 | 13 | 1.86 | 0.568 |
| 8 | 1 | 1.71 | 0.021 | 42 | 14 | 12.93 | 0.505 |
| 9 | 1 | 14.86 | 0.476 | 43 | 14 | 1.89 | 0.584 |
| 10 | 2 | 5.20 | 0.011 | 44 | 15 | 12.79 | 0.512 |
| 11 | 3 | 3.31 | 0.018 | 45 | 17 | 2.11 | 0.114 |
| 12 | 3 | 15.09 | 0.445 | 46 | 16 | 12.97 | 0.489 |
| 13 | 4 | 2.55 | 0.018 | 47 | 16 | 12.97 | 0.489 |
| 14 | 4 | 2.18 | 0.022 | 48 | 17 | 1.89 | 0.581 |
| 15 | 5 | 4.51 | 0.009 | 49 | 17 | 12.99 | 0.490 |
| 16 | 5 | 4.26 | 0.009 | 50 | 17 | 12.99 | 0.490 |
| 17 | 6 | 2.61 | 0.019 | 51 | 18 | 1.88 | 0.559 |
| 18 | 6 | 1.36 | 0.053 | 52 | 18 | 13.02 | 0.486 |
| 19 | 7 | -3.17 | 0.021 | 53 | 19 | 0.23 | 0.049 |
| 20 | 8 | -3.60 | 0.032 | 54 | 20 | -3.68 | 0.489 |
| 21 | 9 | 3.04 | 0.034 | 55 | 21 | -0.20 | 0.068 |
| 22 | 10 | 2.64 | 0.028 | 56 | 19 | -3.67 | 0.486 |
| 23 | 11 | 1.70 | 0.017 | 57 | 19 | 1.36 | 0.496 |
| 24 | 8 | 1.76 | 0.026 | 58 | 20 | 1.36 | 0.504 |
| 25 | 7 | 1.98 | 0.040 | 59 | 21 | 5.03 | 0.492 |
| 26 | 7 | 4.12 | 0.035 | 60 | 22 | 5.03 | 0.489 |
| 27 | 8 | 4.03 | 0.023 | 61 | 24 | 1.22 | 0.118 |
| 28 | 9 | 6.97 | 0.030 | 62 | 25 | -0.61 | 0.058 |
| 29 | 14 | 12.93 | 0.505 | 63 | 26 | -0.73 | 0.052 |
| 30 | 10 | 4.76 | 0.027 | 64 | 27 | -0.44 | 0.065 |
| 31 | 11 | 2.59 | 0.023 | 65 | 24 | 9.76 | 0.492 |
| 32 | 12 | 3.22 | 0.029 | 66 | 25 | 9.70 | 0.499 |
| 33 | 13 | -1.46 | 0.085 | 67 | 26 | 6.08 | 0.551 |
| 34 | 14 | 0.64 | 0.035 | 68 | 27 | 6.13 | 0.487 |
| | 15 | | | 69 | 28 | 14.14 | 0.466 |



NOTE
STEAM GENERATOR OUTLET NOZZLE
LDR IN NODES 8 AND 11.

FIGURE 6.2.-34 A
PRESSURE RESPONSE
STEAM GENERATOR CUBICLE
MILLSTONE NUCLEAR POWER STATION
UNIT 3
FINAL SAFETY ANALYSIS REPORT



NOTE:
STEAM GENERATOR OUTLET NOZZLE
LDR IN NODES 8 AND 11

FIGURE 6.2-34B
PRESSURE RESPONSE
STEAM GENERATOR CUBICLE
MILLSTONE NUCLEAR POWER STATION
UNIT 3
FINAL SAFETY ANALYSIS REPORT

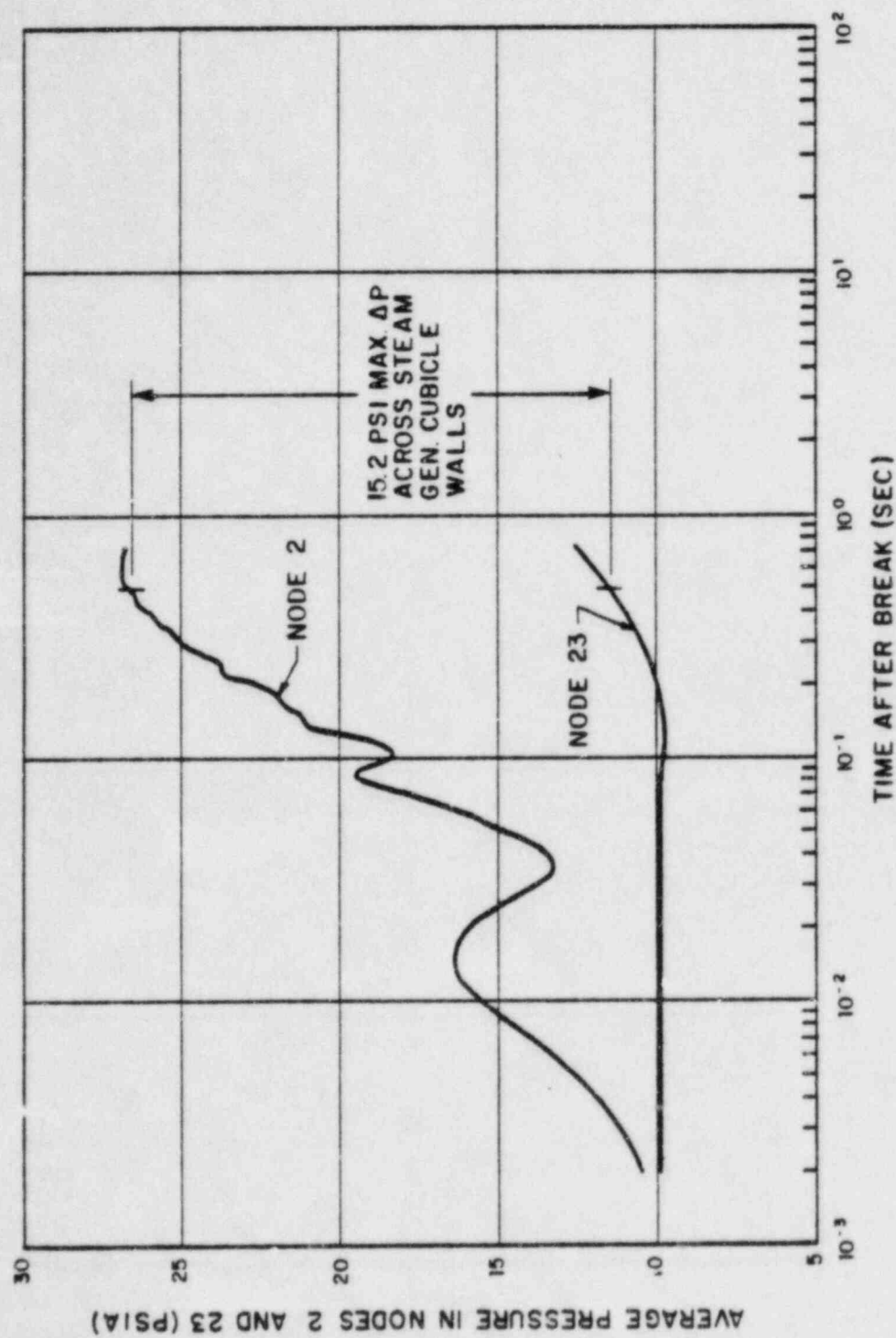
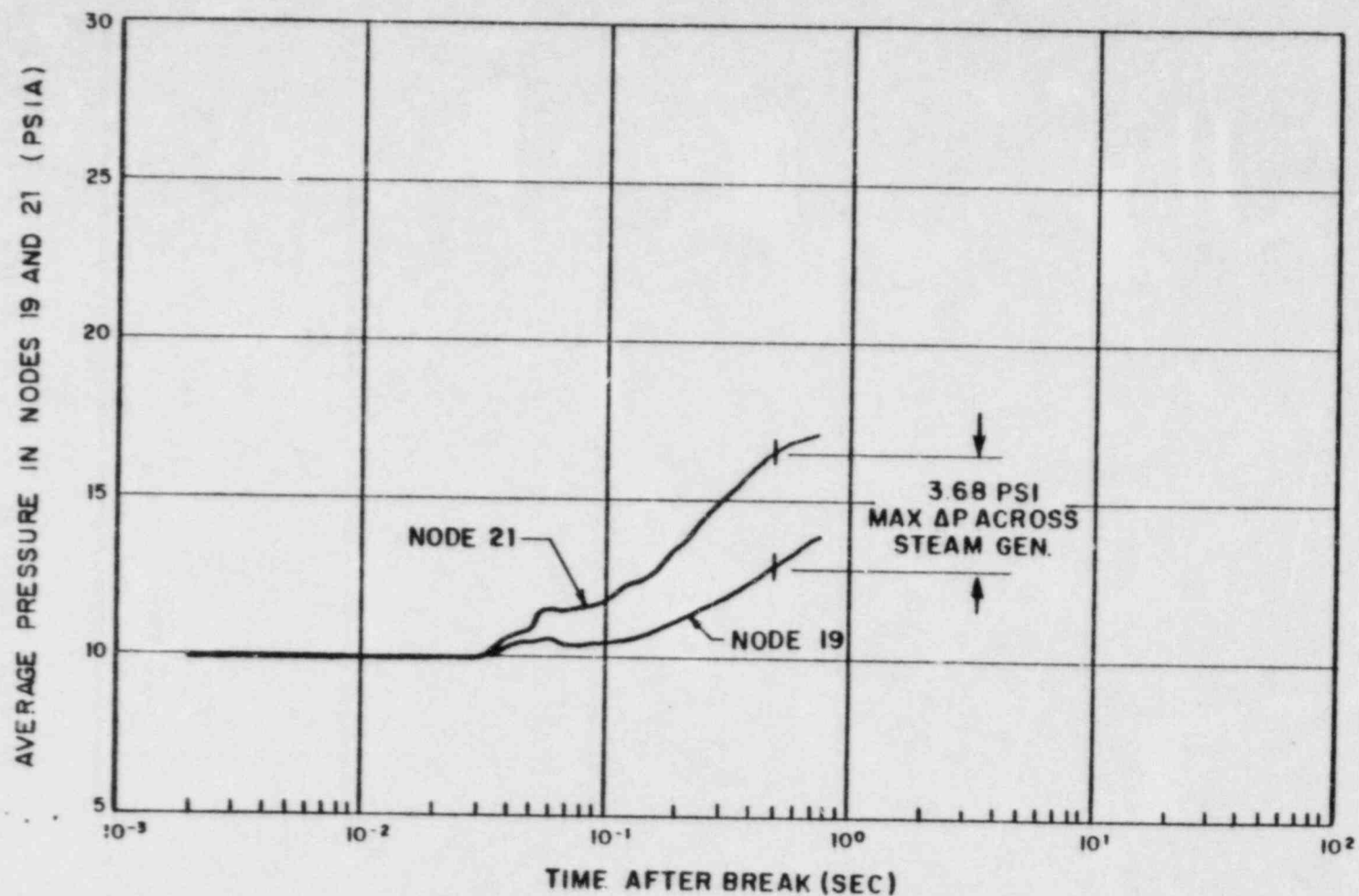


FIGURE 6.2-34C
PRESSURE RESPONSE
STEAM GENERATOR CUBICLE
MILLSTONE NUCLEAR POWER STATION
UNIT 3
FINAL SAFETY ANALYSIS REPORT

NOTE
STEAM GENERATOR PUMP SUCTION LOOP
CLOSURE WELD LDR IN NODES 2 AND 5.



NOTE

STEAM GENERATOR PUMP SUCTION LOOP
CLOSURE WELD LDR IN NODES 2 AND 5.

FIGURE 6.2-34D
PRESSURE RESPONSE
STEAM GENERATOR CUBICLE
MILLSTONE NUCLEAR POWER STATION
UNIT 3
FINAL SAFETY ANALYSIS REPORT